Theoretical and Experimental Study of AM and FM Molecular Communications

Final Year Project

by

Ivan Pérez Laka

Universitat Politècnica de Catalunya

New Jersey Institute of Technology

Advisor: Raquel Pérez Castillejos

Acknowledgment

I would like to take the opportunity to thank to all the people who have helped me during the development of this project. During this time I have grown as researcher but especially I have grown as person.

First of all, I would like to thank my family for their support during all these years of degree and because of understand my decision to travel so far from the beginning. Without them none of this would have been possible. I would also like to mention all the colleagues that I have been meeting during my period in UPC with who I spent a great time.

Especial gratitude to my advisor Raquel Pérez Castillejos, who always had time to help me and who after one year became a very good friend. Her support has been really helpful to carry out this project. I would also like to thank to all the people of the The Tissue Models Lab group of NJIT who helped me when I needed. They form a fantastic group and I will always remember the awesome time that we spent together; Anil B. Shrirao, Isabel Burdallo, Neha Jain and Olga Ordeig, part of this thesis has been possible thanks to you.

For their financial support I would like to thank *Fundación Vodafone España*, *Generalitat de Cataluña*, *Universitat Politècnica de Catalunya* and *Obra Social Bancaja*.

Finally I want to thank to *Escola Tècnica Superior d'Enginyeria de Telecumincació de Barcelona (ETSETB)* and *New Jersey Institute of Technology* for their institutional support and for give me the opportunity to do this unforgettable journey.

Thanks to all of you.

Table of Contents

1 MOTIVATIONS AND OBJECTIVES

Molecular communications are defined as those that use molecules as information carriers between transmitter and receiver. This type of communications is the one used by biological cells either in intra-cell communications or in inter-cell communications. In recent years there has been a growing interest by this type of communications driven by the development of nanotechnologies. Molecular communications is essential to communicate nodes and devices in networks at nanometric scale.

Molecular communications are a new investigation field with applications in biomedicine and in the development of technology at nano-level. For example a new treatment in the cure for cancer, specifically the metastases of it, is based on angiogenesis processes [1], which are based basically on molecular communications. Likewise, the future of the technology goes through the miniaturization of devices beyond the current micrometric scale. The next step is the nanotechnology, and a communication system that controls all devices of these sizes is needed. The current communication technologies such as electromagnetism or optics cannot be used on these scales; however molecular communications are intrinsically designed to this kind of sizes.

One of the motivations of this work is the interdisciplinary nature of molecular communications that includes fields such as biology, chemistry, microfluidics, electronics or telecommunications. Cellular communications are a perfect example of how molecular communication systems work, so that a study of them is essential for understanding these systems. The encoding and decoding information is done by chemical reactions that must be understood on order to characterize and optimize communication processes. The fabrication of devices for the practical study of these systems is based on microelectronic fabrication technologies as well as in microfluidic technologies. They allow the monitorization of the evolution of biocellular parameters needed in the study of communications. Finally telecommunications provide a background for understanding all bio-chemical processes from a perspective of information theory that can be applied in different situations such as networks with nanometric sizes.

It has been demonstrated that cells are able to encode the information transmitted using modulations in amplitude (AM) or in frequency (FM) [2] using molecules as information carriers. This type of molecular modulations allows the use of the same communications channel to transmit different communications at the same time and

provides a better noise immunity. The application of molecular modulations is essential in the development of technologies at nanometric scale.

Although this is a field currently being investigated, actually a general model for molecular communications that describes this communication process is still needed.

The purpose of this project is getting a mathematical model that describes molecular communications based on diffusion processes of particles. With this model the behavior of this type of communications will be studied according to the physical parameters that determine it.

Also, this model will be used to study the modulation processes, either amplitude or frequency modulation and will establish a criterion for which decide under what situations biological cells decide to encode the information using one form or the other.

This report is structured in seven sections. Firstly, in Chapter 2, the basic fundamentals of bio-cell communications, molecular communication systems and a briefly introduction of microfluidics are presented in order to clarify some concepts of systems that are based on molecular communications. The concepts defined in this section are fundamental to understand the next sections.

Once this new scenario has been presented, in Chapter 3, the mathematical model for molecular communication systems is calculated and analyzed. The behavior of these systems is discussed and the stability issues that the model has are studied.

Since molecular communications are based on diffusion processes in Chapter 4, a microfluidic device, whose operating principle is the diffusion of particles, is presented, the **T-SENSOR**. In this section a T-Sensor is designed, fabricated and characterized in order to study the diffusion experimentally.

The goal of Chapters 5 and 6 is getting a simulator able to predict the behavior of communications between transmitter and receiver using molecular communications. This simulator solves the issues that the mathematical model presented in Chapter 3 has. Chapter 5 is based in the programming of a T-Sensor simulator. This device is based on the same principles as molecular communications. The simulator presented in this chapter is validated using the experimental results got in Chapter 4.

Chapter 6 presents the molecular communications simulator and compares the results using this simulator and the results using the mathematical model. The criterion of decision for amplitude and frequency modulations is determined. This simulator is obtained from the T-Sensor simulator with a previous modification that is also presented in this chapter.

Finally the conclusions of this work are stated in Chapter 7

2 BACKGROUND INFORMATION

In this section the basic concepts necessary to understand how molecular communications work is presented. The chapter is divided in three different sections. An overview of cell communications is explained in the first one that provides a biological perspective of molecular communications. The second section presents a point of view more technological, explaining the new field of nanonetworks that are strongly dependent on molecular communications. Finally in the last section it is presented a briefly explanation about microfluidics, a science that will be needed in further chapters because of its intrinsic features for diffusion of particles.

2.1 Cell Communications Fundamentals

2.1.1 Basic concept of cell communication

Unicellular organisms have been present in the earth since long before multicellular organisms. The complexity of the mechanisms needed for the interaction in multicellular organisms is probably one of the reasons of their slow evolution. The cells have to be able to communicate with one other in a complex ways if they want to control their own behavior for the benefit of the unique organism.

The extracellular signal molecules are the fundamental piece in these communications. They are produced by cells which want to communicate with their neighbors or with cells further away. And also, an elaborate system of proteins that each cell contains enables it to react to a particular set of these signals in a specific way. Some of these proteins are the cell-surface receptor proteins, which bind the signal molecule; or the intracellular signaling proteins that distribute the signal to different parts in the cell. This distribution takes place through different intracellular signaling pathways, and at the end of each one there are target proteins, which react when the pathway is active changing the cell's behavior.

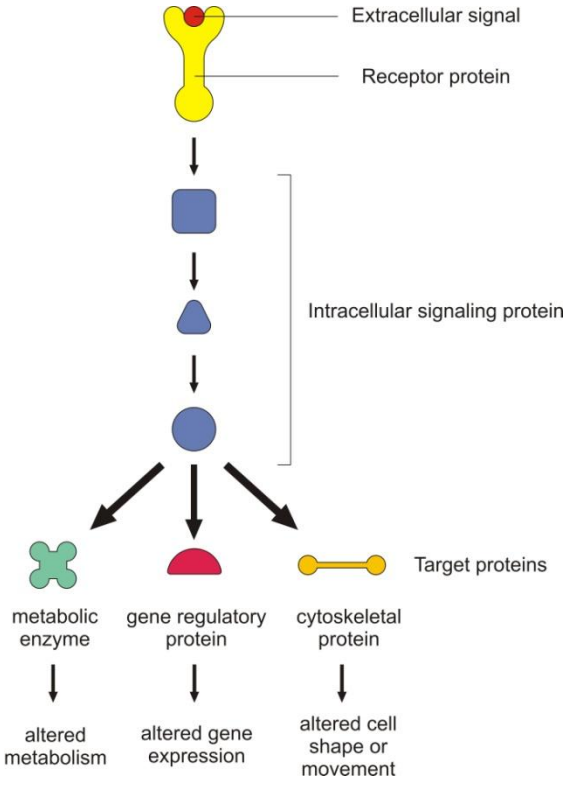

Fig. 2.1 Intracellular signaling pathway activated by extracellular signal.

Some unicellular organisms are able to communicate by secreting a few kinds of small peptides, but in higher multicellular organism communicate using hundreds of kinds of molecules. In most of the cases the signaling cell secretes the molecules to the

extracellular space by exocytosis (process by which a cell directs the contents of secretory vesicles out of the cell membrane). In other cases the molecules are released by diffusion through the plasma membrane, and in some others they are exposed to the extracellular space while remaining tightly bound to the signaling cell's surface.

The target cell detects the signal by means of receptors [3], a protein which binds specifically the signal molecule and this binding starts the reaction in the target cell. The extracellular signal molecules usually act at very low concentration and the receptor that detects them bind them with high affinity. In most cases this receptor proteins are on the target cell surface. The signal molecules (ligand) which are hydrophilic and then are unable to cross the plasma membrane directly, bind to cell-surface receptors, which in turn generate one or more signals inside the target cell that alter the behavior of the cell. Some small signal molecules can diffuse across the plasma membrane and bind to receptors inside the cell. This requires that the signal molecules be hydrophobic and sufficiently insoluble in aqueous solutions.

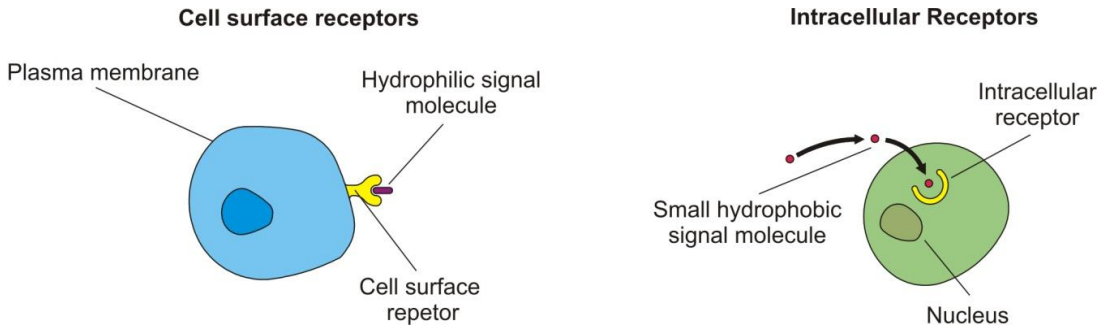

Fig. 2.2 The binding of extracellular signal molecules to either cell surface receptors (on the left) or intracellular receptors (on the right).

2.1.2 Forms of intercellular signaling

Cells have different ways to communicate [3]. In multicellular organism, the most "public" style of communication is the endocrine signaling. The signal molecules (called hormones in animal's cells) are secreted into the blood stream, which carries the information to the whole body. The cells that produce hormones are called endocrine cells. For example, part of the pancreas is an endocrine gland that produces the hormone insulin, which regulates glucose uptake in cells all over the body.

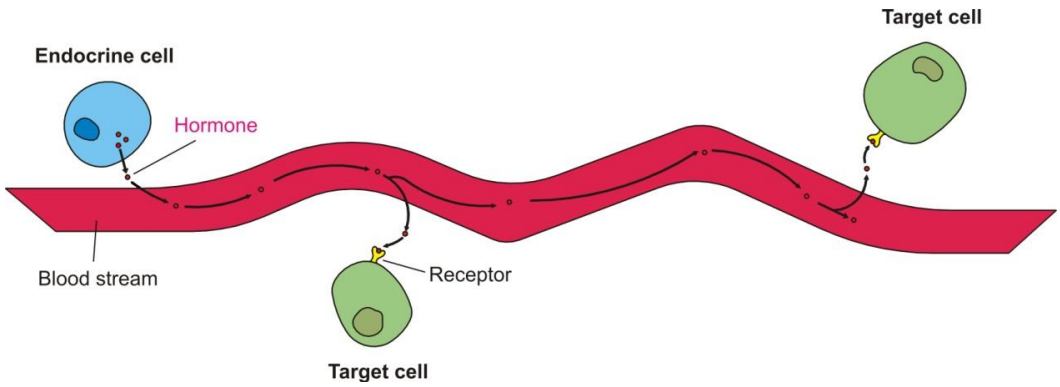

Fig. 2.3 Endocrine signaling.

The process known as paracrine signaling is less public than the endocrine signaling. In this case, signal molecules are secreted. The molecules secreted diffuse locally through the extracellular medium, affecting only cells in the immediate environment of the signaling cell. Thus they act as local mediators on nearby cells. The regulation of the inflammation process at the side on an infection is controlled using this kind of signaling.

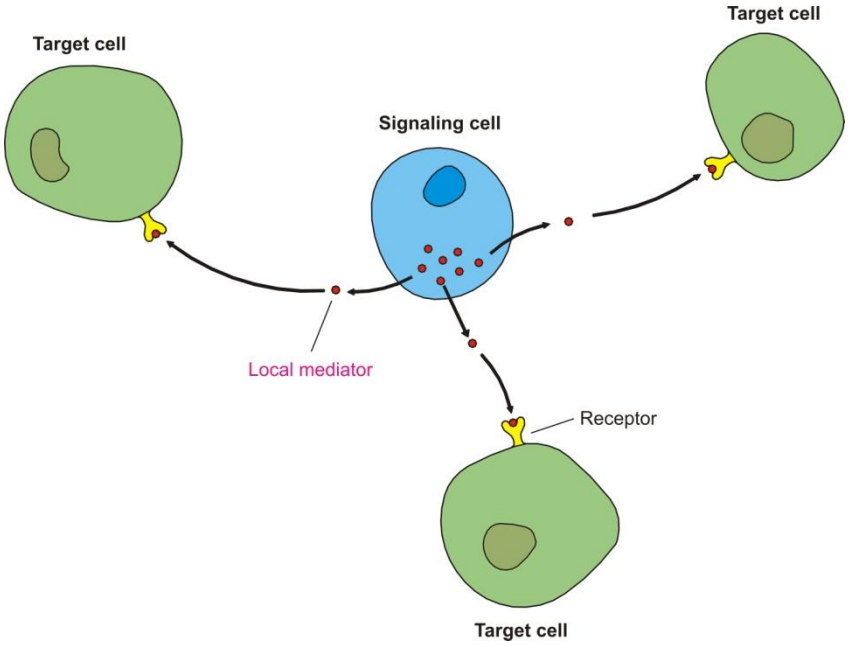

Fig. 2.4 Paracrine signaling.

The neuronal signaling is a sophisticated communication processes what such as happen in the endocrine signaling the message can be delivered across long distances. In this case, however, the message is delivered quickly to a specific target cell instead of broadcasted to the whole body. The specific cells called neurons, send electrical impulses rapidly along its axon (long part in the body of the neurons), and then, when the impulse reaches the end of the axon, it causes the secretion of a chemical signal

called neurotransmitter. This signal is secreted at specialized cell junctions called chemical synapse, which ensures that the neurotransmitter is delivered specifically to the postsynaptic target cell. The neurotransmitter diffuses across the gap between the axon-terminal membrane and the membrane of the target cell in less than 1 msec.

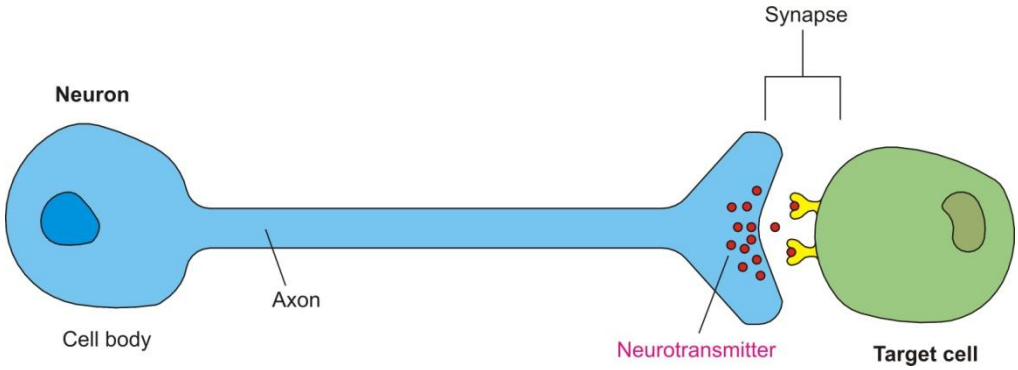

Fig. 2.5 Neuronal signaling.

Finally, when the cells are in physical contact it is not required the secretion of molecules to the extracellular medium. The message is delivered when the signal molecules are attached in the plasma membrane of the signaling cell, and they binds to a receptor embedded in the plasma membrane of the target cell. This process is called contact-dependent signaling and is important during development and in immune responses.

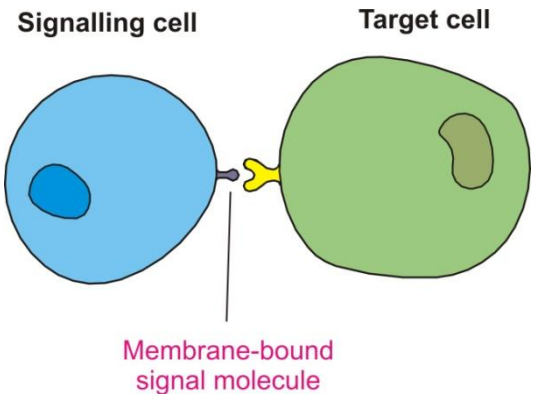

Fig. 2.6 Contact-dependent signaling.

2.1.3 Each cell responds to a specific extracellular signal molecules

In a multicellular organism the cells are exposed to a hundreds of different signals in its environment. These signals can be bound to the surface of a neighbor cell or they can be soluble in the extracellular fluid. Each cell must detect selectively some signals or ignoring others, according to their specialization function. A cell responds to a signal molecule if it has the specific receptor for that signal, otherwise the cell will ignore the presence of those molecules in the medium and will not react.

The cells restrict the amount of molecules that they can detect by producing a limited set of receptors out of the thousands that are possible. But even with this limited set of receptors, those signals are able to control the cell's behavior in a complex way. One signal binding to one receptor can cause many different effects in the target cell such as the movement of the cell or the alteration of the cell's shape. At the same time the cell's receptors can bind more than one molecule, and these signals, by acting together, can produce reactions that are more than the combination of the effects caused of each signals by their own. The intracellular transmission systems for the different signals interact, so the presence of one signal changes the reaction to another [3]. A cell may be programmed to respond to one combination of signals by differentiating, to another combination by multiplying, and to by doing a specialized task such as secretion or contraction. Even, most of the cells need the detection of a combination of signals simply to survive. In absence of these signals, the cells kill themselves; a process called apoptosis or programmed cell death.

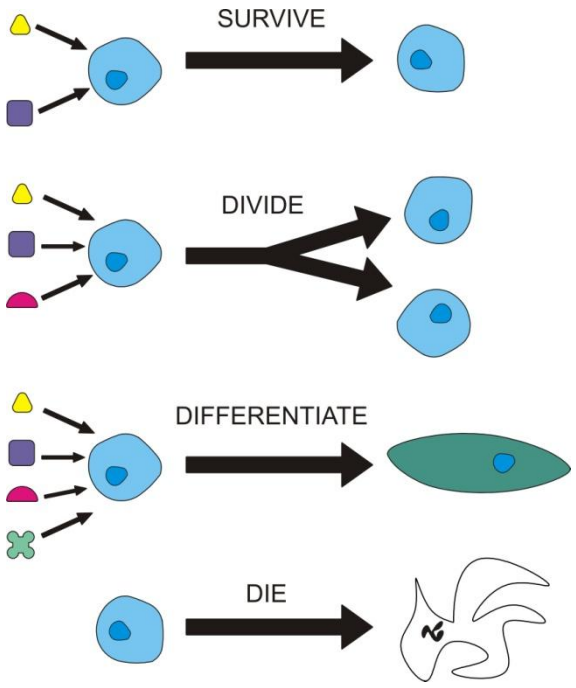

Fig. 2.7 Cell's dependence on multiple extracellular signals.

A cell can respond in many different ways to its environment. It depends on the set of receptor proteins the cell possesses, which determines the different set of signals that it is able to detect. And also it depends on the intracellular process, which understands the signals that it receives. Thus, a single molecule often has different effects on different targets cells. For example the neurotransmitter acetylcholine is detected by the skeletal muscle cells, they begin to contract. But when the heart muscle is exposed to the same neurotransmitter the rate and force of its contractions decrease. This happens because the acetylcholine receptor proteins on the heart muscle cell are different from those on the skeletal muscle cells. But these differences in the receptors are not the only reason

this success. It is perfectly possible that the same signal molecules binds to the same receptor proteins in two different types of target cell, and yet produce a very different responses. The receptor protein in the salivary gland is similar to the receptor protein presents in the heart muscle cells, but in this case, the gland secretes components of saliva instead of decrease the contraction.

2.1.4 Intracellular signal pathways

When a signal molecule binds with a receptor protein the signal reception begins. The receptor does the first transduction; it receives an external signal and generates a new intracellular response [4]. This is the first step in a chain in which the message passes from one intracellular signal to another, activating and generating the next intracellular signal, until arrive to a metabolic enzyme which execute some action, or to a gen regulatory protein, or to a cytoskeletal protein, changing the cell's configuration. This final result is called the response of the cell. These signaling cascades in the intracellular signaling have some important functions as:

- They are the responsible in the transduction of the signal into a molecular form appropriate to be transmitted through the cell.
- They relay the signal from the point where it is received to the point where the response will be produced.
- The signaling cascades can distribute the signal in order to affect different process at the same time. At any step in the pathway the signal can be relayed to other targets creating complex responses.
- The signal received can be amplified by the signaling cascades. With this few extracellular signal molecules are enough to start the intracellular response.
- All the steps in this cascade are susceptible to be modulated so the effects of the signal can be adapted to the conditions either inside or outside the cell.

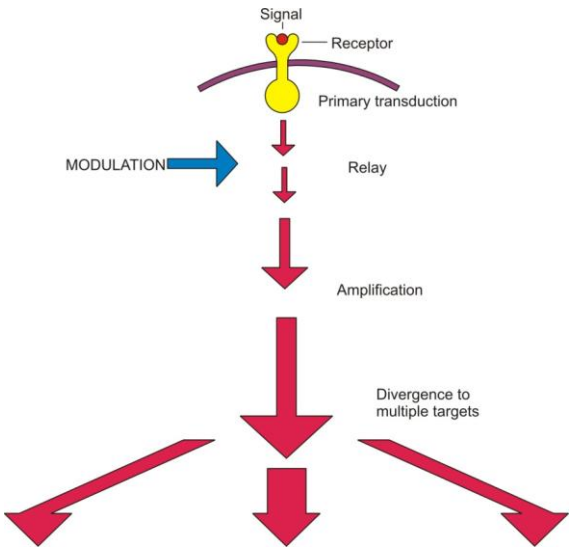

Fig. 2.8 Cellular signaling cascades.

Signaling pathways are usually long and with a lot of branches. Therefore, many intracellular parts are affected by the information received by the receptors at the cell surfaces. In these cases the molecules are too large or too hydrophilic to cross the plasma membrane of the target cell. Because of this they have to bind on the receptors at the cell surface to relay the message across the membrane. But it is also true that some signal pathways are more direct. This happens when the molecules are small enough and hydrophobic enough, they are able to cross the plasma membrane directly; Fig. 2.2.

2.1.4.1 Many intracellular signaling acts as molecular switches

One of the keys in the intracellular signal pathways lies in how fast an extracellular signal molecule evokes a response inside the cell. Some cellular responses are smoothly graded in simple proportion to the concentration of the molecule. This happens when the molecules bind to a single molecule receptor and the intracellular target reacts independently to each binding. As the concentration of molecules increases, the concentration of activated receptors increases proportionally, as does the number of complexes bound to specific intracellular targets. The response of the cell is then linear and gradual. Otherwise, in many cases, the responses to extracellular signal molecules begin more abruptly as the concentration of the molecules increases. Sometimes even occur almost as molecular switches, being undetectable below a threshold concentration and then reaching a maximum as soon as this concentration is exceeded. There are several reasons why this may happen; when an intracellular signaling molecule activates one enzyme and, at the same time, inhibits the enzyme which catalyzes the opposite reaction the responses become sharper. In other cases it is require more than one intracellular complex bind to some target macromolecule to induce a response. When this happen the responses become sharper as soon as the number of cooperative molecules increases, and as the number is getting larger responses like all-or-none type can be achieved.

All-or-none threshold responses usually depend on positive feedback mechanism; nerve and muscle cells generate all-or-none action potential in reaction to neurotransmitters.

These chemical switches can be in the active or inactive state. Once one of the steps in the pathway is activated it can turn on some other steps, and this activation can persist in an active state until some other process switches them off again.

2.1.4.2 Memory in cells. The cells can remember the effect of some signals

The effect of an extracellular signal on a target cell can persist well after the signal has disappeared [3]. The positive feedback process is one type of mechanism that represents this kind of persistence. If this system has been switched on by increasing the concentration above a threshold this system remains activated even after the disappearance of the signal; instead of reflecting the real level of signal, thus the

response system displays memory. Some of these changes can even persist for the rest of the life of the organism. They usually depend on self-activating memory mechanisms that operate in the last steps in the signaling pathway, at the level of gene transcription. For example, the signals that determine if a cell has to become a muscle cell turn on a series of muscle-specific gene regulatory proteins which produce many other muscle cell proteins. In this way, the decision to become a cell muscle is made permanent.

2.2 Molecular Communication System

2.2.1 Nanotechnology

The cell communication system exposed in the chapter above is one of the solutions for nano-scale communications scenarios. These systems based on the molecular signaling may be one of the keys for the development of the nanotechnologies. In this new situation appears the figure of the nanomachine, which is, at nano-scale, the most basic functional unit. Nanomachines represent tiny devices consisting in a group of molecules which are able to perform simple tasks such as computation, sensing or actuation. The interconnection between these nanomachines makes possible their cooperation and the exchange of information increasing the capabilities of a single nanomachine. Molecular communication provides a mechanism for one nanomachine to encode or decode the information into molecules and to send information to other nanomachines.

The interconnection of these nanomachines becomes in nanonetworks, and they improve their capacities in the following ways:

- Provides a larger workspace to the nanomachines, which is extremely limited for a single one. Nanonetworks will allow dens deployments of interconnected nanomachines. Thus, larger applications scenarios will be enabled.
- Allows the connection over large areas where the control of a specific nanomachine is difficult because of its small size. By means of broadcasting and multihopping nanonetworks can interact with remote nanomachines
- Nanomachines such as nano-valves, nano switches or nano memories, cannot execute complex task by themselves. The network performed by the connection between these nanomachines will allow them to work in a cooperative manner achieving more complex tasks.

Nanomachines cannot be built yet, but they exist in the nature in the form of biological cells and the chemical processes within those cells. The bionanotechnology is advancing quickly, until the actual point where engineering of biological systems is possible. It has been demonstrated [5] that the modification of the DNA can give a new functionality to a cell. As the bionanotechnology becomes more mature, the study of the molecular communications can be applied in the design of more complex nanomachine systems.

2.2.2 Overview of nanomachines

A nanomachine is defines as a device consisting of nanometer-scale components that performs a useful function at nano-level, such as communicating, data storing, sensing and actuation or computing. The tasks that a single nanomachine can achieve are very simple because of its low complexity and small size.

As it has said before, the fabrication of these nanomachines is still a very promising field in research, but with the exception of the found in the nature, it is not possible to built artificial nanomachines yet. There are three different approaches for their development; the top-down approach in which the nanomachines are developed by means of downscaling the already existing microelectronic technologies. The bottom-up approach consists in the design of nanomachines from molecular components, which are assembled using chemical principles of molecular recognition. Recently has appeared a third approach called bio-hybrid that is based on the use of existing biological nanomachines as models or components for the development of new nanomachines.

2.2.2.1 Nanomachine architecture

The architecture of a nanomachine depends strongly on its complexity. It can be from simple molecular switches up to complete nanorobots. In general a regular nanomachine should include the following architecture components [6]:

- Control unit. The control unit executes the instructions to perform the intended tasks, and all the components of the nanomachines can be controlled by this unit in order to achieve this purpose.
- Communications unit. The communications unit is a transceiver capable of transmitting and receiving messages at nano-scale.
- Power unit. The goal of the power unit is supply all the components of the nanomachine, by obtaining energy from external sources such as light or temperature and store it for a later distribution and consumption.
- Sensor and actuators. In the same way as the communications unit the sensors and actuators acts as interfaces between the environment and the nanomachine.
- Reproduction unit. In many applications the capability of replicate the nanomachine using external elements may be very useful. This is the aim of the reproduction unit. It fabricates each component of the architecture using external elements, and then assembles them to replicate it.

Currently such complex nanomachine cannot be built. However, systems found in the nature like living cells have similar architectures. According to the bio-hybrid approach, the biological cells have served as a template from which we are learning to build nanomachines. Similar to the architecture of a nanomachine, a cell contains the following components:

- Control unit. The chromosome within the nucleus contains all the instructions to

realize the intended cell functions.

- Communications unit. The gap junctions and the receptor proteins located on the plasma membrane act as molecular transceivers for cell-cell communications.
- Power unit. For the power generation cells can include different nanomachines such as the mitochondria, that generate most of the chemical substances used as energy in the cellular processes, and the chloroplast, that converts sunlight into chemical fuel.
- Sensors and actuators. Several sensors and actuators are included in a cell such as the olfactory sensor (smell) or the flagellum which provides a method of locomotion to the cells.
- Reproduction unit. In the biological cells, the code of the nanomachine is stored in molecular sequences, which are duplicated in the cell division. The resulting cells contain a copy of the original DNA sequence.

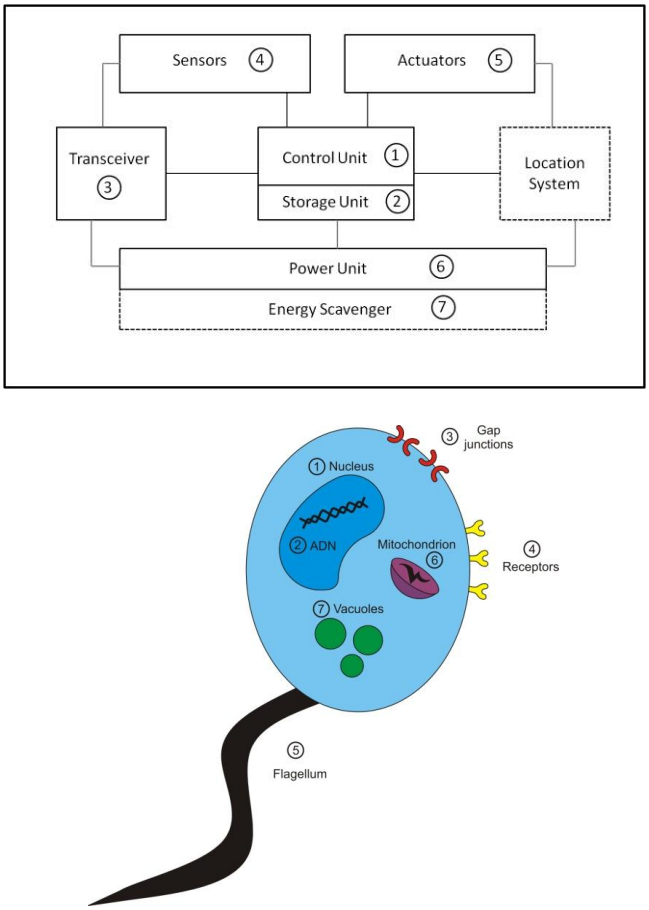

Fig. 2.9 On the top functional architecture of a nanomachine, on the bottom biological architecture of a cell.

The bio-hybrid approach, in addition to be used to develop nanomachines, is very useful as a means to understand their interactions. These interactions, controlled by molecular communication techniques, are essential because their understanding is the key to explore their capabilities to achieve more complex tasks in a cooperative manner.

2.2.2.2 Desirable features of nanomachines

As we have seen desirable features of nanomachines are presents in living cells. For example, nanomachines will have a set of instructions or code to realize specific tasks embedded in their molecular structure, or they will be able to read them from another molecular structure in which the instruction set is stored. The ability of a nanomachine could make a copy of itself would be interesting. In order to achieve this goal, a nanomachine would need the features of self-assembly and self-replication. Self-assembly is defined as the process in which several disordered elements form an organized structure without external intervention. A nano-level this happens naturally due to the molecular affinities between two different elements. Self-replication is defined as the process in which a device makes a copy of itself using external elements. Self-maintenance is another feature very interesting to be considered as well as the locomotion, which would provide the ability to move from one place to another at a nanomachine. Communication among nanomachines is one of the most desired features. It is required to realize more complex tasks in a cooperative manner, and also a nano-to-macro interface with which to access and control the nanomachine.

From the point of view of communication, cells act as multi-interface devices. Cells have hundreds of receivers and are able to communicate using multiple unique channel access techniques such as ligand-recptors or gap junctions. Besides, the cells can be using these mechanisms simultaneously. All cells have a very sensitive transducing signal mechanism. The signal is detected by the receptor, which amplify the signal, integrate the signal with the input received by other receptors, and transmit the resulting signal to the cell. Therefore, a nanomachine should have these features that characterize signal transduction [7]:

- Specificity. Specificity is the ability to detect and react to a specific signal. The signal and the receptor are complementary. The specificity quantifies the precision with which a molecule fits in a complementary receptor, where other signals do not fit.
- Amplification. Amplification is the ability to increase the magnitude of a signal. Amplification by enzyme cascades can amplify a signal in several orders of magnitude within milliseconds.
- Desensitization. Desensitization is the ability to remove the molecules of the signal once this is received.
- Integration. Integration is defined as the ability of a system to receive multiple signals and integrate them into only one, producing the suitable response of the nanomachine.

2.2.3 Overview of nanonetworks

Nanonetworks are communication networks which exist mostly at nano-level scale. The nanonetworks achieve the functionally and performance as the macro-scale networks using nodes of nanometers and channels physically separated by up to

hundreds or thousands of nanometers. Besides, nodes are supposed to be rapidly deployable and mobile, and also are assumed to be self-powered.

Nanonetworks, such as all the other networks have all the features analogous communication networks. The information must be collected, coded, transmitted, received, decoded and delivered to the appropriate target. Thereby, all the concepts presented in the information theory apply in nanonetworks including bandwidth, compression, error detection and correction.

2.2.4 Communications among nanomachines

Since nanonetworks provides to the nanomachines a support on which establish a communication system, two different bidirectional scenarios appear:

- Communications between two or more nanomachines.
- Communications between a nanomachine and a larger system such as electronic micro-device.

Different communication technologies have been proposed to approach each scenario [8] electromagnetic, acoustic or molecular.

The electromagnetic waves have been used for communications since long time, and actually are the most common technique to interconnect microelectronic devices. The losses for these waves are minimal along wires or through air. However, in the nano-scale scenario, wiring large quantity of nano-machines is unfeasible. In this case, wireless technology could be an alternative. In order to establish bidirectional communication, a radiofrequency transceiver would have to be integrated in the nanomachine. Nano-scale antennas can be built for very high frequency communications, but due to the size and the complexity of the transceivers, they cannot be easily integrated in nanomachines yet. In addition, even if this integration could be realized, the nanomachine could not have enough output power to establish a bidirectional communication. Because of that, electromagnetic communication could be used to transmit information from a micro-device to a nanomachine, but not in the opposite direction.

Acoustic communications are based in the transmission if ultrasonic waves, air pressure waves. In the same way to the electromagnetic communications, the acoustic communication would need the integration of ultrasonic transducers in the nanomachines. These transducers are obviously needed to sense the variations of pressure produced by the ultrasonic waves and also to emit acoustic signals. The issue in this case is exactly the same that in the previous case, the size of these transducers makes impossible their integration in the nanomachines.

Molecular communication is established when the information is encoded using molecules. Molecular communication is a new and interdisciplinary field which includes knowledge in nano, bio and communication technologies. Unlike previous

communication techniques, in this case the integration of transceivers in the nanomachine is not an issue because of the intrinsic size of the molecular transceivers. These transceivers are nanomachines which are able to react to specific molecules, and to release others as a response to an internal command. Molecular communications can be used to interconnect different nanomachines, resulting in nanonetworks which increase the capabilities of a single nanomachine.

2.2.4.1 Features of molecular communication

The nanonetworks, as it has said previously, expand the capabilities of a single nanomachine, but in addition, represent a potential solution for some applications where the current communication networks are not suitable. Compared to actual communication network technologies, nanonetworks have the following advantages [7]:

- Biocompatibility: This is defined as the capacity of a device to operate in biological environments without affecting them negatively. Inserting nanomachines into the human body for medical applications requires nanomachines that are biologically friendly. Functions as receiving, interpreting, and releasing molecules would provide to biological nanomachines a mechanism to interface directly with natural processes. Thus, it would not be necessary to include harmful inorganic chemicals. In addition, nanomachines and molecular messages may also be programmed to be broken down after use to avoid procedures for removal or cleanup of devices
- Scale: The reduced size of the nanomachines and the resulting nanonetwork components are a very interesting goal in systems where the dimensions of the system are critic.
- Information representation: Molecules can represent the information using different ways, such as their chemical structure, relative positioning or concentration. Thus, molecular information provides different methods for manipulating and interacting with the information since operation performed are non-binary.
- Energy efficiency: In terms of energy consumption, chemical reactions are highly efficient. These reactions could power nanonetwork nodes and processes. In addition, chemical reaction can represent computation and decision processes, which usually take multiple operations.

2.2.4.2 Traditional communication networks and nanonetworks

The emergence of nanonetworks has implied the development of a new paradigm which is much more complex than a simple extension of the traditional communication networks. Especially due to the size, most of the communication processes are inspired by biological systems found in nature and because of that there are some differences between nanonetworks and traditional communication networks [6]:

- In nanonetworks the message is encoded using molecules instead of

electromagnetic, acoustic or optical signals which are used by the traditional communication networks. There are two different and complementary techniques to encode the information in nanonetworks. The first, called molecular encoding, uses internal parameters of the molecule -such as chemical structure, polarization or relative positioning- to encode the information. In this case the receiver has to be able to detect these parameters in order to decode the information. This technique is similar to the use of encrypted messages, in which only the specific receivers are able to decode the information. The second technique uses temporal sequences to encode the information, such as the temporal concentration of a specific molecule in the medium. Depending on the concentration, the receiver decodes the information in one way or another. This technique is similar to those used in traditional communication where the information is encoded in time-varying sequences.

- Most of the processes in nanonetworks are chemical reactions with low power consumption. In traditional networks, the communication processes consume electrical power which comes from batteries or from external sources such as electromagnetic induction.
- In traditional communication networks, the noise is known as an unwanted perturbation overlapped with the wanted signals. In nanonetworks, according to the molecular encoding techniques the noise can be described in two different ways. The first, as occurs in traditional communication systems, is an overlapping of the molecule signal with some other molecules of the same type. This means, another source emits the same molecules used to encode the message, affecting the concentration sensed by the receiver. The second source of noise in nanonetworks can be understood as undesirable reaction between the information molecules and other molecules present in the medium. Those reactions can modify the structure of the information molecules and then the receiver would not be able to detect the message.
- The propagation speed of signals used in traditional communication networks is much faster than the propagation of molecular messages. In nanonetworks, the information molecules have to be physically transported from the transmitter to the receiver. In addition, molecules can be subjected to random diffusion processes and environmental conditions, such as temperature, that affects the propagation of the molecular message.

Type of communication	*Traditional*	*Molecular*
Signal type	*Electronic or optical*	*Chemical*
Communication carrier	*Electromagnetic waves*	*Molecules*
Noise	*Electromagnetic fields and signals*	*Molecules in medium*
Encoded information	*Voice, video, text, images...*	*Chemical states, phenomena, processes..*
Propagation speed	*Light (3e8 m/s)*	*Very low*
Medium conditions	*Wired: Almost immune Wireless: Affect communication*	*Affect communication*
Energy	*High energy consumption*	*Low energy consumption*

Table 2.1 Main differences between traditional communication networks and nanonetworks enabled by molecular communication [9].

2.2.5 Nanonetwork components

The models used to describe nanonetworks come from those used in Information and Communication Technologies (ICT) for communication networks. In nanonetworks there are seven different components: information source and sink, the transmitter node, the receiver node, the message, the carrier and the medium. These components affects in the communication process, which includes the following steps [10]:

(1) The information source generates information such as reactions, data storing or activation commands.
(2) The transmitter encodes a sensed reaction onto information molecules.
(3) The transmitter sends the information molecule into the environment, by releasing the molecules to the medium or attaching them to molecular carriers.
(4) The message propagates from the transmitter to the receiver.
(5) The receiver detects the transported information molecule.
(6) The receiver decodes the information molecules to cause a desired reaction at an information sink.

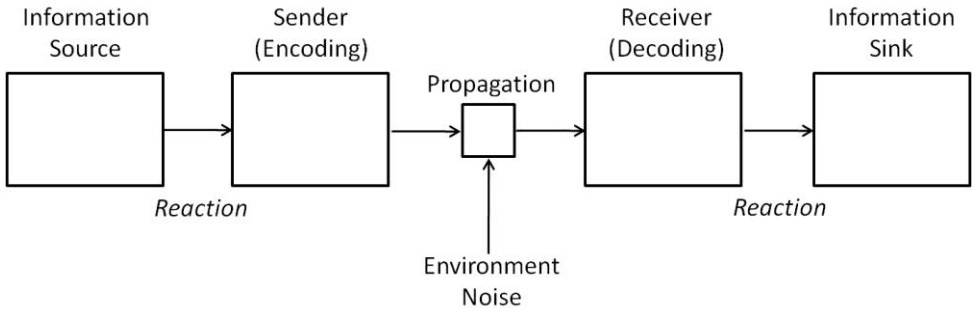

Fig. 2.10 Generic communication architecture.

2.2.5.1 Information source and sink

The information source has the information to send through a sender. This information can be presented as some events, chemical reactions, data storing, etc. The information sink is the destination where the desired reaction is caused.

2.2.5.2 Transmitter and receiver

In nanonetworks, these nodes encode the information by modifying molecules by means of chemical reactions. The transmitter node must be able to send the information into the environment. The receiver should be able to detect and extract the message from the medium and once it is decoded causing a desired reaction at an information sink.

The message contains the information which will be used by the receiver forwarding it, storing it or reacting to it. Since nanomachines are very simple and the messages are basically molecules, handling all of these processes is a hard task. The transmitter and receiver nodes exchange molecules as information, and those molecules are limited in the medium. This has two consequences. First, the transmitter has to be able to collect molecules from external sources, and store them in order to use them later as a message. Second, the receiver has to be able to buffer the molecules that it gets, and it also needs the capability of release those molecules to empty the buffer.

2.2.5.3 Message

In tradition communication networks, the information is usually represented as a binary system, and the transmitted message is a set of bits. In molecular communication, information can be described as a biological reaction at a receiver. Since a biological reaction is an interaction between molecules, a biological reaction can be caused by sending molecules. In molecular communication, the message is the molecule which stores such reaction information.

There are three important features that molecular message should have. Firstly, the molecule should not react with other molecules in the medium. Secondly, the molecules should have an external structure that would allow an easy detection by the receivers. And finally, the molecules should easily be eliminated once they are decoded, and thus, avoid possible interferences between messages.

2.2.5.4 Carrier molecule

In traditional communication networks, the carrier is a signal in which is carried the information to increase the signal features, especially the features related to the propagation. The creation of multiple communication channels is achieved modulating the information on different carriers. In nanonetworks, the carriers are used exactly with the same purpose. In this case a carrier is particular molecule which is able to transport chemical signals or molecule structures which contain the information. The propagation features of these carriers are better than the features presented by single

information molecules by themselves, protecting the information from noise sources and allowing the system to create multiple independent channels using the same medium.

The use of molecules as information carriers has been observed in biological systems; identifying two different carriers in which modulate the information. Molecular motors [10], and calcium ions [11]. Molecular motors are proteins that can generate movement using chemical energy. These proteins transport the information molecule from the transmitter to the receiver [12]. The second types of carriers are calcium ions. In this case the transmitter can modulate the information in the concentration of these ions -modulation of amplitude- or it can do it encoding the information in the frequency at which the transmitter sends these ions -frequency modulation-.

2.2.5.5 Medium

The medium is the space in which the message goes from the transmitter to the receiver. In molecular communication the medium can be wet or dry, and the propagation depends strongly on the medium conditions. In addition, the presence of physical obstacles can hinder the propagation of the message.

2.2.6 Communication systems using calcium signaling

Cell-cell communication based on calcium signaling is one of the most important molecular techniques [13, 14]. It is responsible for many coordinated cellular task, such as, contraction, secretion or fertilization**.** This signaling process is used in two different scenarios, when two cells are in physical contact, or when there is not this physical dependence.

The propagation of the signal is driven by a chemo-signal pathway, in which one messenger transports the information until certain point in the pathway where the information is transferred to another messenger. This transmission from one messenger to another continues until the information reaches its destination. This process is explained in more detail in the previous chapter “Intracellular signal pathways”. As it is presented there, this system has some important advantages, especially the possibility to amplify the information at different levels of the chemo-signal pathway. The ligand-receptor binding principle is the most important process in this information transfer between messengers. As it is explained before this process consists in the bounding between to molecules (the information molecule, or ligand, and the protein receptor) resulting in a local reaction, which in turn can trigger other process.

When cells are physically separated the information molecule binds to the receptors placed on the cell membrane. This binding generates an internal signal which can be decoded by cell components.

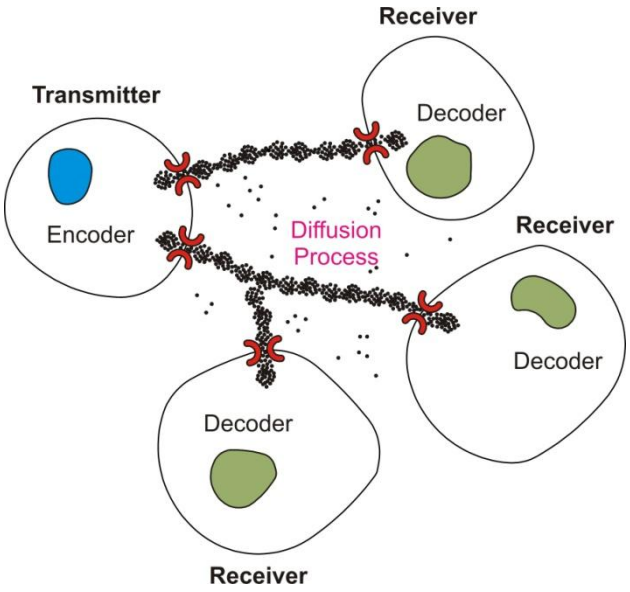

Fig. 2.11 Signal propagation in calcium signaling communication systems by diffusion.

In this case the information molecule is considered as the first messenger, while the internal signal is considered as the second messenger. The first messenger in the signal that transports the information outside the cell while the second messenger is the signal which transports the information inside the cell. Membrane receptors transforms first messenger into second messengers by chemical reactions.

If cells are located next to each other, existing physical contact between them, they can be connected through gap junctions. These biological gates allow molecules and ions to pass from one cell to another.

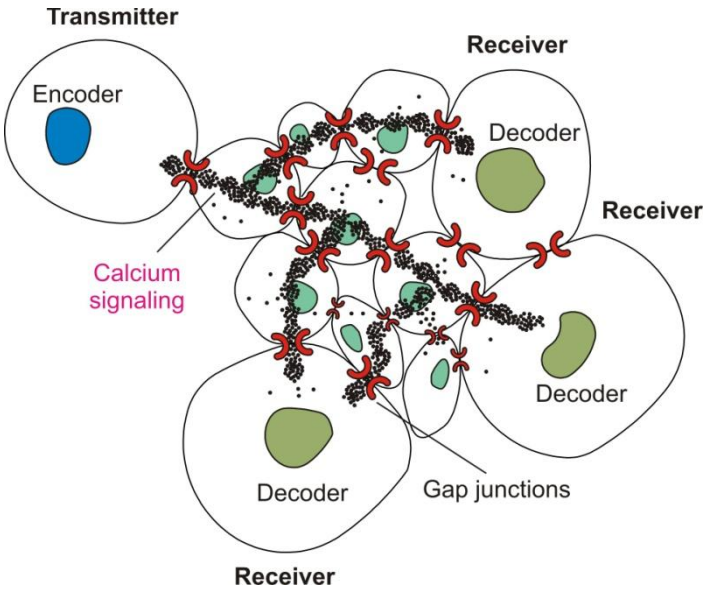

Fig. 2.12 Signal propagation in calcium signaling communication systems by gap junctions signal forwarding.

In this case the information travels along cells using only second messengers such IP3 (inistor 1,4,5-triphosphate) without intervention of first messengers. IP3 is a messenger that propitiates the secretion of calcium ions (Ca^{2+}) by cell organelles. Therefore, diffusion of IP3 through gap junctions propagates waves of Ca^{2+} along the interconnected cells.

The propagation of Ca^{2+} is very complex task in which several cell components participate in order to make this signal propagation possible. Ca^{2+} buffers or reservoirs are needed inside the cell when it needs to release molecules to the medium, or when it is passing those molecules through the gap junctions to the next cell. These buffers can be certain proteins of the cytoplasm and organelles such as the endoplasmatinc reticulum. Also ion channels located on the cell membrane are involved in this process, maintaining this finite resource.

Calcium signaling provides a method to maintain neighboring cells interconnected. Using calcium signaling surrounding nanomachines can receive a message sent it only from one nanomachine, in a similar way that is done in traditional communication networks in processes such as multicasting or broadcasting.

2.2.6.1 Communication features

Calcium signaling would be used in communications over short-range (nm up to μm) among nanomachines [11]. Similar to natural models, this method would be used by nanomachines when these placed near each other. Following natural models, the propagation of the information can be performed in two different ways depending on the deployment of the nanomachines:

- **Direct access.** In this case, nanomachines should have to be physically connected. Thereby, Ca^{2+} signals would travel from one nanomachine to another through the gates in a similar way that is shown in the figure Fig. 2.12. These gates would act as gap junctions allowing the flux of calcium waves from one nano-machine to the interior of the next.
- **Indirect access.** For indirect access, nanomachines should have to be separated, and the transmitter should be able to release molecules to the medium as a first messenger in the chemical pathway. These information molecules would move to the destination following a diffusion process. There, they would be detected by the receptors and the second messengers would be produced inside the nanomachine. The transmitters should be able to encode the information varying the concentration of the first messenger. Biological systems can encode the information on frequency and amplitude of concentration changes, usually referred to as Ca^{2+} oscillation and Ca^{2+} spikes.

These two propagation methods enable the formation of networks supporting multicast or broadcasting transmission mechanisms.

2.2.6.2 Communication process using calcium signaling

The communication process is set of steps for which the message travels from the transmitter to the receiver. Usually this process consists of the following steps: encoding, transmission, signal propagation, reception and decoding. These steps may present differences for direct access or indirect access.

2.2.6.2.1 Direct access communication process

In this scenario there is one transmitter and many other cells or nanomachines that are able to propagate the message. As it is said above these components are located one next to each other, existing physical contact between them, and they are interconnected through gap junctions or functional gates. In this case, the target cell or nanomachine can be any of those components of the network.

- **Encoding.** This step generates the information molecules. When the nanomachines are used to propagate the signal, the transmitter encodes the information using Ca^{2+}. These calcium waves are encoded varying the concentration of the ions in amplitude or frequency. These encoding methods are known as amplitude modulation (AM) or frequency modulation (FM), and they can be understood in a similar way to the conventional radio-electric modulations.
- **Transmission.** This task refers to the signaling initiation. The transmitter stimulates neighboring nanomachines and then the signaling process starts. The signaling generates the initiation of propagation of Ca2+ waves. IP3 generated by the transmitter, starts flowing into neighboring nanomachines through the gates, and therefore, neighboring nanomachines release more Ca^{2+} driven by the presence of IP3 substance.
- **Signal propagation.** IP3 transmitted to neighboring nanomachines induces the release of Ca^{2+} from the Ca^{2+} stores which are sensitive to this substance. The diffusion of IP3 continues to the next nanomachine inducing again the release of Ca^{2+} on this nanomachine. Because of this chain reaction, the concentration of Ca^{2+} increases, and as a result, the Ca^{2+} wave propagates along the networked nodes affected by IP3. This propagation can be controlled changing the permeability of the function gates.
- **Reception.** Receiver nanomachine is connected to their neighbors through the gap junctions and perceives the Ca^{2+}concentration waves from inside them. Once the message is received, receiver nanomachine closes its gates, and thus, it stops the propagation of IP3.
- **Decoding.** The receiver nanomachine reacts to the internal concentration of Ca^{2+}. The signal can be encoded in amplitude or frequency enabling the activation of different processes. The difference between the receiver and all of the participating components in the propagation is the capacity to decode the message. The other nanomachines just receive the signal and forward it to the next component.

2.2.6.2.2 Indirect access communication process

The indirect scenario is formed by nanomachines deployed separately and where the signals propagate along the medium where the nanomachines are deployed.

- **Encoding.** The transmitter encodes the information in the molecule to be used as a first messenger. The first messenger can also be encoded using AM of FM techniques.
- **Transmission.** Transmitter initiates signaling by releasing calcium to the environment.
- **Signal propagation.** In indirect access, the signal diffuse along the medium to reach with the receiver. This scenario is much more sensitive to the medium conditions than the direct access. Transmitter nanomachines should consider the medium conditions to ensure that the signal will arrive to the receiver.
- **Reception.** The receptors placed on the receiver have to translate the information molecule into internal Ca^{2+} signals. A nanomachine needs several different receptors in order to be able to detect many different information molecules. This could be used to establish many parallel communications channels using the same medium.
- **Decoding.** The receiver nanomachine reacts to the internal concentration of Ca^{2+}. This depends on the bindings between information molecules and nanomachine receptors. Again the information can be encoded in AM or FM and the only nanomachine which is able to decode the information is the receiver, while other nanomachines only forward the signal. Since calcium signaling can be considered as a broadcast scheme, multiple receivers can decode the same message.

2.2.7 Communication systems using other methods

There are so many communication systems which are used in the nature depending on the distance between transmitter and receiver. Because the main work in this thesis is based on calcium signaling using indirect access, this system has been explained in more detail. Now the intention is present some other communication systems more briefly which are use by biological cells in different scenarios.

2.2.7.1 Molecular motors

Similar to the calcium signaling, the communication systems based on molecular motors are used in tiny scenarios. They cover the necessities in short-ranges from nm to a few μm. Molecular motors are used in most of the intra-cellular communications and they are proteins that converts chemical energy into mechanical work at nano-scale [15].

The information molecule is carried on the motor, in this move directionally along cytoskeletal tracks. Inside the cells, molecular motors are aimed to transport molecules

among organelles. They travel along molecular rails performs a complete railway network inside the cell for intra-cell substance transportation.

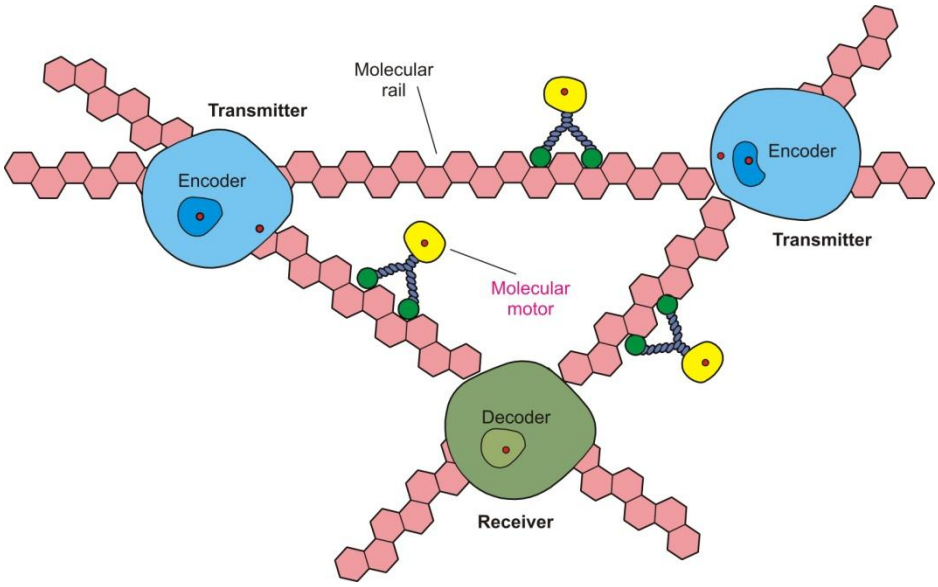

Fig. 2.13 System components in molecular motors communication systems.

This communication system includes one transmitter and only one receiver. The ability to move molecules makes molecular motors a feasible way to transport information packets. But this system applied in nanonetworks should be able to adapt to more complex scenarios. In this case techniques as multihoping would be needed and because of that the nanomachines should be able to amplify, decode and redirect the information.

2.2.7.2 Pheromones

Pheromones are a system very useful when the distance between transmitter and receiver nanomachines ranges from mm up to km. Nanonetworks in long-range scenario are also inspired in biological systems found in nature. Many animals such as butterflies, bees, many mammals or ants use pheromones in their communications. Butterflies use pheromones and molecular messages can reach the range of a few kilometers [7].

Communication using pheromones is similar to the techniques based on the release molecules that can be detected by a receiver. Once the molecules are released to the medium, they can be affected by factors, temperature, medium flow, antagonist agents, and the can be considered as noise sources.

Probably, the most important feature in this kind of log-range communication system is the coding system. In the nature only the animals of the same species can detect the pheromones in the air. While in traditional communication networks, the information is usually encoded in a binary system, in pheromone systems the information is encoded in the molecule itself. The messages can be encoded using different molecules which imply more combinations to encode the information.

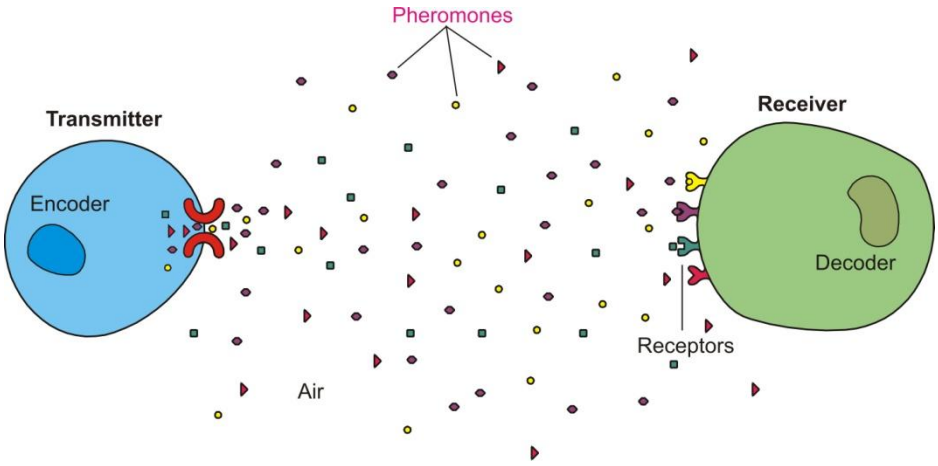

Fig. 2.14 System components in pheromone communication systems.

The reception of the transmitted molecules is realized by molecular receptors located on the receiver. In a similar way to the calcium signaling scenarios, the process is based on the ligand-receptor binding. In molecular communication using pheromones, the receptor proteins can be considered as the receiver nanomachine antenna, which transforms energy contained in the message into a reaction at the receiver.

2.2.8 Conclusion and research challenges

The study of cellular communications is basic in the development of reliable communication techniques at nano-scale. Sciences such as biology, chemistry, electronics or communication sciences converge in nanotechnology, creating a new multidisciplinary science. Biology and chemistry describe the processes in the nature which yield in the development of functions at nano-scale. Engineers should be able to model such processes with the purpose of create devices with the same characteristics.

Paracrine communications used by cells, and especially those driven by mean of calcium ions signaling, are an interesting point of study to understand the communications at nanometric scales. This work pretends study the process of modulation in amplitude and frequency realized by cell with the objective of determine under what conditions the information must be encoded using one method of the other. This study could be highly useful in the developing of communication systems in nanomachines or at the same time their medical applications are very promising.

2.3 Microfluidics Fundamentals

Microfluidics is the study of flows that are simple or complex which are circulating in artificial microsystems [16].

In the recent years, important progress has been made in the field of miniaturization. Nowadays is completely feasible to miniaturize many kind of systems – e.g. mechanical, electromechanical, fluidic or thermal- to micrometric scales. In the 1980s, due to these achievements, a new field known as MEMS (microelectronic-

mechanical systems) showed up. Later in 1990s these systems began to be used in many different fields, being manufactured MEMS for chemical, biological and biomedical applications. These systems utilized fluid flows operating in unusual and unexplored conditions, which inevitable led to the creation of a new discipline known as microfluidics.

In microfluidics the systems manipulate small amounts of liquids, from 10-18 to 10-9 liters, using channels with dimensions of tens to hundreds of micrometers [17]. It takes advantage of its most obvious characteristic, small size, but also it exploits a less obvious characteristic of fluid in microchannels, the laminar flow.

Microfluidics offers a number of interesting capabilities such as the ability to use very small quantities of samples, low cost or short time of analysis which are very useful in analysis applications. It offers fundamentally new capabilities in the control of concentration of molecules in space and time.

2.3.1 Low Reynolds number

In fluid mechanics, the Reynolds number is the ratio between the inertial forces and the viscous forces, and quantifies the relative importance between these two types of forces.

$$Inertial = \frac{\rho \bar{v}^2}{d} \qquad (2.1)$$

$$Viscous = \frac{\mu \bar{v}}{d^2} \qquad (2.2)$$

Where ρ is the density of the fluid (kg/m^3), $\bar{v}$ is the mean velocity of the fluid (m/s), d is the characteristic length of the flow (m) and μ is the dynamic viscosity of the fluid (kg/m·s).

This dimensionless number can be used to characterize different flow regimes, such as laminar flow or turbulent flow. For low values of the Reynolds number (less than 2300 [18])the fluid flows in a laminar way, on the other hand for large values of this number (more than 10000 [18]) the behavior of the fluid is turbulent. Laminar flow is characterized by smooth, constant fluid motion. The motion of the particles of fluid is very orderly with all particles moving in straight lines parallel to the pipe walls [19], while turbulent flow tend to create vortices, chaotic eddies and other flow instabilities.

$$\mathrm{Re} = \frac{\rho \bar{v} d}{\mu} = \frac{\bar{v} d}{\upsilon} \qquad (2.3)$$

Where υ is the kinematic viscosity (m2/s). The characteristic length of closed channel flow is the hydraulic diameter of the channel:

$$d_h = \frac{4A}{P} \qquad (2.4)$$

Where A is the cross-sectional area and P is the wetted perimeter, the perimeter of the channel which is wetted by the fluid.

In microfluidic systems, typical fluid velocities do not exceed a centimeter per second and widths of canal are on the order of tens to hundreds of micrometers; therefore, in general, Reynolds number in microfluidic systems do not exceed 10e-1. In fact, we can say that a microfluidic system whose channels have one of the three dimensions (height, width or depth) lower than 100μm, always will work in laminar regime.

2.3.2 Velocity profile in microchannels

In the situation of two parallel planes close together filled with fluid the gap space between them. In fluid dynamics there are two ways of provoke movement in the fluid between the planes: by applying shear stress through the channel or by a playing a pressure gradient along the channel [20].

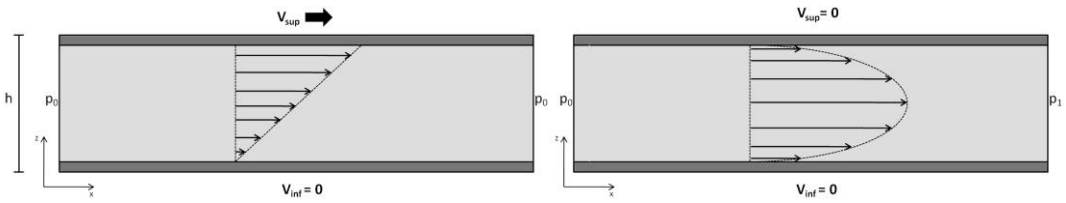

Fig. 2.15 On the left velocity profile applying shear stress of the superior plane. On the right, velocity profile applying a pressure gradient along the channel.

The second one, which is called *Poiseuille* flow, is the most common situation in microfluidic systems because in these systems the walls are usually resting in the same position.

The flow forced by a hydrodynamic pressure gradient is called Pressure-Driven Flow (PDF) and it is conditioned by the velocity of the channel walls. As it has been said before, in pressure-driven flow the walls are at rest forcing the velocity of the fluid at the channels walls is zero. On the other hand, the pressure applied to the fluid volume generates a uniform force over the whole cross-sectional area of the channel. The combination of the no-slip condition at the walls and the uniform force applied to the entrance provokes a parabolic velocity profile of the flow, that is, zero velocity at the walls and maximum a velocity at the center of the channel.

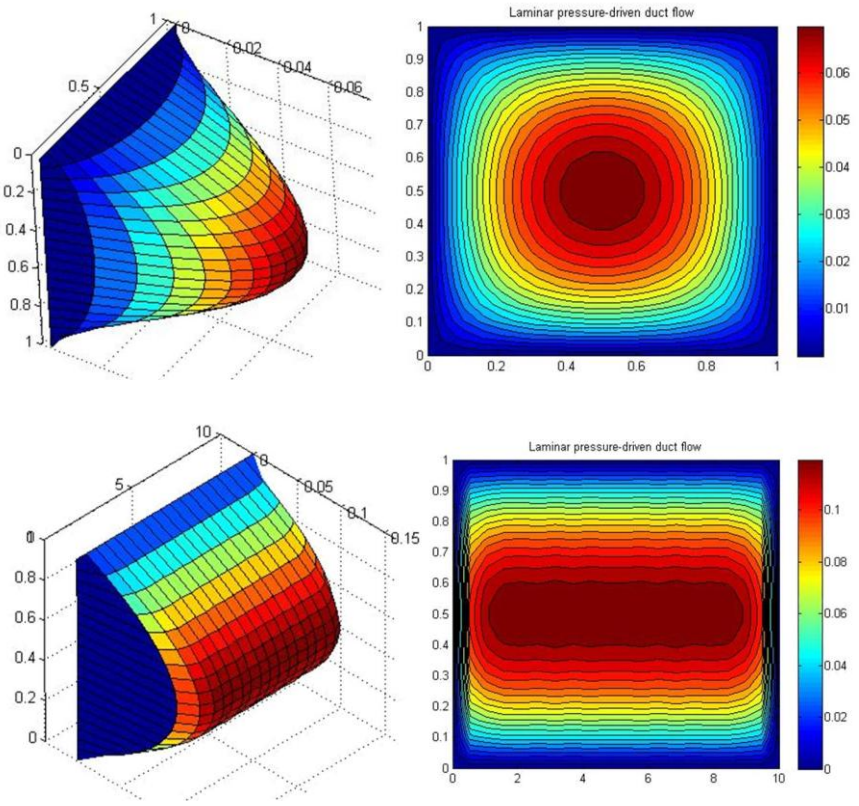

Fig. 2.16 Fluid velocity profiles within two rectangular ducts of different height:width ratios. On the top aspect ratio AR=1, on the bottom AR=10.

In laminar flow the particles of the fluid follow straight paths, so they do not cross each other. Thus, the flow may be considered as a series of concentric cylinders flowing over each other.

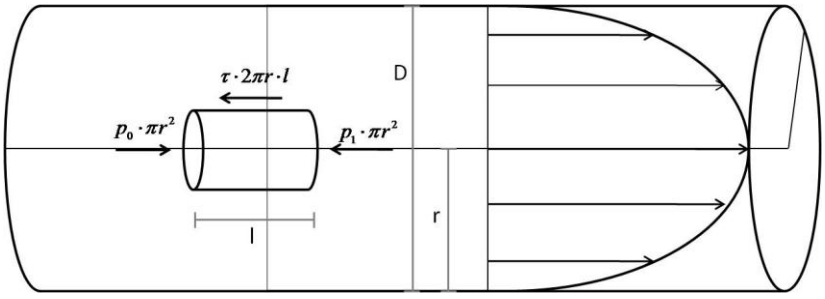

Fig. 2.17 Steady flow in a circular pipe.

The forces applied to a steady state laminar flow are in equilibrium conditions. In a horizontal pipe, the pressure force in the flow is balances by the shear stress force on the wall.

The shear stress is defined as an inertial force which is applied parallel to the liquid.

$$\tau = \frac{F}{A} \qquad (2.5)$$

Where τ is the shear stress (N/m2), F is the force applied (N) and A is the cross-sectional area (m2).

By the Newton's law of viscosity, the shear stress for laminar flow is linearly related to the fluid viscosity:

$$\tau = \mu \frac{\partial v}{\partial r} \qquad (2.6)$$

Hence, in equilibrium conditions:

$$F_0 - F_1\big|_{\text{Pressure}} = F_{Shear} \qquad (2.7)$$

$$-\Delta P \cdot \pi r^2 = \tau \cdot 2\pi r \cdot l \rightarrow \tau = -\frac{r}{2} \cdot \frac{\Delta P}{l} \qquad (2.8)$$

Combining the equations (2.6) and (2.8):

$$\mu \frac{\partial v}{\partial r} = -\frac{r}{2} \cdot \frac{\Delta P}{l} \qquad (2.9)$$

And solving this simple differential equation, the velocity is:

$$v(r) = -\frac{1}{4\mu} \frac{\Delta P}{l} r^2 + C \qquad (2.10)$$

And the integration constant C can be found using the no-slip at the walls condition v(r)=0 when r=R.

$$\begin{aligned} v(R) = 0 &= -\frac{1}{4\mu} \frac{\Delta P}{l} R^2 + C \rightarrow C = \frac{1}{4\mu} \frac{\Delta P}{l} R^2 \\ v(r) &= \frac{1}{4\mu} \frac{\Delta P}{l} \left(R^2 - r^2 \right) \end{aligned} \qquad (2.11)$$

We can observe that the velocity has a parabolic relationship with the distance. Re-arranging the equation above:

$$v(r) = \frac{1}{4\mu} \frac{\Delta P}{l} \cdot R^2 \left(1 - \left(\frac{r}{R} \right)^2 \right) \qquad (2.12)$$

The equation (2.12) shows that the velocity at the walls, $v(r = R)$, is 0, while the velocity at the center of the pipe, $v(r = 0)$ is maximum:

$$v_{\max} = \frac{1}{4\mu} \frac{\Delta P}{l} \cdot R^2 \qquad (2.13)$$

Similar to the *Poiseuille* flow, the velocity profile in a pipe is also parabolic. Actually, the three dimensional flow has a velocity profile which a form of a paraboloid, having its maximum at the axis of the pipe, and its zeros at the walls. For non-circular three dimensional channels, the solution is not analytical so microfluidic devices have to be studied through simulation tools.

2.3.3 Fick's laws of diffusion

In microfluidics is very common to find situations where the particles in the liquid move inside it following diffusion processes.

Molecular diffusion is the thermal motion of all molecules at temperatures above absolute zero. This principle establishes that when in a certain point exists a non-uniform distribution of particles, then they tend to diffuse away in order to reach uniform concentration through all the space [21]. Molecular diffusion can be also considered a specific case of random walk or Brownian motion, which is used to model the movement of particles suspended in a fluid.

Molecular diffusion is typically described using the Fick's laws of diffusion.

Fick's first law:

The Fick's first law permits relate the net flux of particles to the concentration of particles, establishing that the flux goes from regions of high concentration to regions of low concentration, with a value proportional to the concentration gradient.

$$J\left(\bar{x},t\right) = -D\nabla C\left(\bar{x},t\right) \qquad (2.14)$$

J represents the net flux of particles in a specific position x and at a specific time t (mol/m2·s). C is the concentration of particles (mol/m3) and D is the diffusion coefficient or diffusivity (m2/s). The diffusion coefficient is a parameter which specifies how "easy" is for a particle to move in a fluid. It provides the idea of the speed at which the particles move from positions with high concentration to positions with low concentrations. This coefficient depends strongly on the size of the particles. Small particles have high values of diffusivity while big particles provide low values of this parameter.

Fick's second law:

The Fick's second law predicts how diffusion causes the change of the concentration with the time. This law depends on the combination of the Fick's first law and the law of conservation of mass. The law of conservation of mass states that the particles cannot be created or destroyed, and thus, all the particles entering or leaving the global system must be the same.

In a first approximation, the variation of the particles concentration in time must be opposite to the gradient of the particle flux in the same location.

Hence:

$$\frac{\partial C\left(\bar{x},t\right)}{\partial t} = -\nabla J\left(\bar{x},t\right) \qquad (2.15)$$

And then, substituting the expression of the first Fick's law (2.14) into the law of conservation of mass (2.15) the Fick's second law is obtained:

$$\frac{\partial C\left(\bar{x},t\right)}{\partial t} = D \cdot \nabla^2 C\left(\bar{x},t\right) \qquad (2.16)$$

A more detailed expression for the Fick's second law takes into account two more terms that can affect in the ratio of appearance of disappearance of particles in the system.

The four terms are [22]:

- Rate of increase of particles per unit volume:

$$\frac{\partial C\left(\bar{x},t\right)}{\partial t} \qquad (2.17)$$

- Net rate of addition of particles per unit volume by convection:

$$\bar{v} \cdot \nabla C\left(\bar{x},t\right) \qquad (2.18)$$

- Rate of addition of particles per unit volume by diffusion:

$$-\nabla J\left(\bar{x},t\right) = D \cdot \nabla^2 C\left(\bar{x},t\right) \qquad (2.19)$$

- Rate of production or elimination of particles per unit volume by reactions:

$$R\left(\bar{x},t\right) \qquad (2.20)$$

Then, the variation of particles concentration is the result of the addition of molecules by convection, by diffusion or by reaction:

$$\frac{\partial C\left(\bar{x},t\right)}{\partial t} = -\left(\bar{v} \cdot \nabla C\left(\bar{x},t\right)\right) - \left(\nabla J\left(\bar{x},t\right)\right) + R\left(\bar{x},t\right) \qquad (2.21)$$

Arranging the previous equation and assuming the simplification that the diffusion coefficient is constant [22]:

$$\frac{\partial C\left(\bar{x},t\right)}{\partial t}+\bar{v}\cdot\nabla C\left(\bar{x},t\right)=D\cdot\nabla^2 C\left(\bar{x},t\right)+R\left(\bar{x},t\right) \qquad (2.22)$$

Where $\bar{v}$ is the velocity and R is the production or elimination (source or sink) of particles. There are two important: when the velocity is zero, then, the system works in a pure diffusion mode, while if the velocity is not zero, then, is the system is produces the dispersion phenomena.

The equation (2.22) is also known as the **Diffusion Equation**. It provides the value of the future concentration of particles in one point if the concentration in that point and in its vicinities is known.

2.3.4 Micorfabrication

The most common technique of microfabrication of microfluidic systems is the one known as Soft-Lithography. It is based in two steps, the fabrication of a master using lithography techniques, and the replica of this master by casting of some plastics or polymers.

The use of microelectronic techniques such as photolithography over silicon wafer to fabricate the master is especially due to two reasons. The first one is that the microelectronic fabrication techniques are a very well known source of knowledge in the fabrication of all kind of devices at micrometric scale. The second one is because of the low roughness of the silicon wafers (around 2nm [23]), which is essential in the replication of structures. The use of glass substrates is being used more frequently due to its characteristics of softness and its lower cost.

2.3.4.1 Photolithography

One process that plays a central role in microfabrication is photolithography. It consists in the exposition of a photosensitive resist through a mask, which has been deposited on a substrate.

The photolithography **masks** are generally plates of quartz on which deposits of chrome form the pattern that is desired to replicate. Obviously is not possible to fabricate objects with geometric precision superior to that of the mask. These masks are often made using electron beams with a precision on the order of a fraction a micrometer. When this high precision is not required methods like high quality printout on a transparency can be used.

The mold will appear when the light through the mask cure the photosensitive resist. This resist is **deposited** in a thin layer on a solid substrate of silicon or glass. The deposit is made using a spin coater.

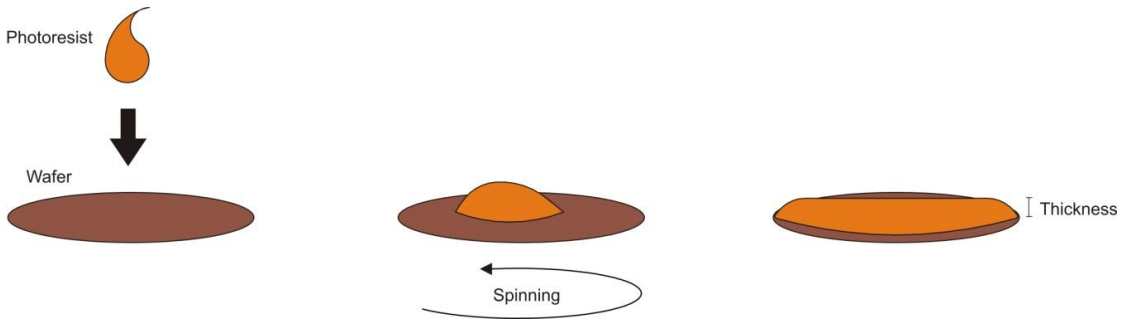

Fig. 2.18 Spinning process. Firstly a droplet of photoresist is poured over the wafer, after that the wafer starts turn obtaining finally the photeresist uniformly spreaded on the wafer.

This piece of equipment consists in a disk that turns at high velocities and allows the spreading of a drop of liquid initially deposited in the center of the disk. The thickness of the layer spread can be controlled changing the rotation speed of the disk. Over the last few years, highly photosensitive polymers such as SU-8 or AZ-series resists have been selected to create structures on glass or silicon substrates.

Once the resist is deposited, the film is **exposed** to a luminous flux produced by a source crossing the mask. In this way dark and light zones appear on the polymer, forming the same pattern that had been designed on the mask. Basically, the light initiates chemical reactions in the polymer, which modify the solubility in certain solvents. There are two types of resists, positive and negative.

- **Positive resist**. The light zone become soluble in a particular solvent, the other zones remain insoluble. That means, the zones affected by the luminous flux are susceptible to be dissolved in presence of a specific solvent, while the zones that have been protected of the luminous flux remain without changes in presence of the same solvent.
- **Negative resist**. The light zones become insoluble in a particular solvent, while the other zones can be dissolved in that same solvent.

Thus, for positive resists, radiation across a mask defines the zones that will form holes in the resist film after the immersion in the solvent (this process is known as development), leaving the other parts of the film permanently polymerized. On the other hand, for negative resists, radiation across the mask defines zones that will remain after the immersion in the solvent, erasing the rest of the polymer that has not exposed.

2.3.4.2 PDMS-Base Molding

Molding is one of the three methods of replication, molding, casting and microinjection. In this study only the molding method is described. A mix containing a catalyst and a polymer is poured on a mold and heated. After curing, the structure is peeled off the mold and it contains the pattern of the mold.

PDMS (polydimethylsiloxane) is a polymer thermo curable that plays a very important role in the fabrication of microfluidic structures. This polymer, when is heated beyond its polymerization temperature and in presence of a curing agent, forms a transparent elastomeric. There are three basic steps in the fabrication of a replica using PDMS-based molding: fabrication of the mold, pouring and curing and separation.

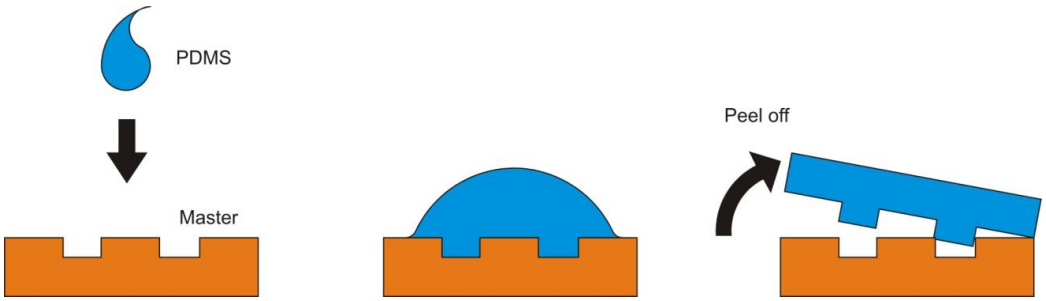

Fig. 2.19 Molding process. Firstly a droplet of polymer is poured over the master, after that the polymer is cured and finally the replica is separated from the master.

The mold is usually made using soft-lithography techniques, such as it is explained previously. A mix of PDMS and curing agent is poured onto the mold. The system is taken to a moderately elevated temperature (on the order of 65°C). During this phase the PDMS polymerizes, cures, and the mix becomes solid. After peeling off the PDMS and object representing the negative of the mold structure is obtained.

Some of the specific properties of PDMS are:

- Its transparency, which allows the visualization of flows.
- The elasticity of the material, which allows the fabrication of micro-valves or micro-pumps using flexible membranes.
- Hydrophobicity in untreated PDMS. It becomes hydrophilic after oxidation of the surface by oxygen plasma. Oxidized PDMS adheres by itself to glass, silicon or polyethylene, as long as those surfaces were themselves exposed to oxygen plasma.
- Permeability to gases such as oxygen or carbon dioxide.
- Non-toxic.

All of these characteristics have made PDMS the most used polymer in lab-on-chip systems.

3 THEORETICAL ANALYSIS OF MOLECULAR COMMUNICATION SYSTEMS

Previously the concept of molecular modulation has been presented. Cells are able to encode the information using amplitude modulation or frequency modulation depending on the requirements of the communication. Understand which are the criteria that cells use to decide whether the communication should be modulated in amplitude or frequency is a key point to design future communication systems for nanonetworks.

In this section a mathematical model for a paracrine communication system is calculated. Whit it, the behavior of these system is predicted and it allows us to find a criterion for which the information shod be encoded using amplitude or frequency modulation.

3.1 Introduction

In the previous chapters, molecular communications systems based on the diffusion of particles in the medium have been presented, such as paracrine signaling or contact-dependent signaling. In these systems the particles move through the medium following diffusion processes and the concentration of these particles can be predicted using the diffusion equation (2.22).

Usually in partial differential equations, such as the diffusion equation, it is not possible to find an analytical closed solution, but sometimes when the geometry of the region where the equation applies is simple and the initials and boundary conditions permit it, it is possible to find a closed solution.

3.2 Closed Solution for the Diffusion Equation

We suppose a biological scenario where a cell cultivated in a cuvette is secreting molecules to the medium and these molecules diffuse until reach to their targets. If we restrict this system to a one dimensional situation where the molecules only can diffuse in one direction, and we assume that the fluid in which the cells are immersed is at rest and the molecules do not react with others, then, the equation (2.22) can be simplified to:

$$\begin{aligned} &\frac{\partial C(x,t)}{\partial t} = D\frac{\partial^2 C(x,t)}{\partial x^2} \\ &0 \le x \le H \\ &0 \le t \le T_{final} \end{aligned} \qquad (3.23)$$

In some cases cells send information by secretion of spikes of molecules periodically. For this case, we assume a simplification of that. A cell secretes a constant concentration of molecules for a period of time and then forces zero concentration of molecules around it. Thus, the concentration of molecules around the cell follows a square function between maximum and zero concentration.

The intention is to solve the equation (3.23) under the situation that the concentration at x=0 is changing from maximum to minimum periodically, following a square function.

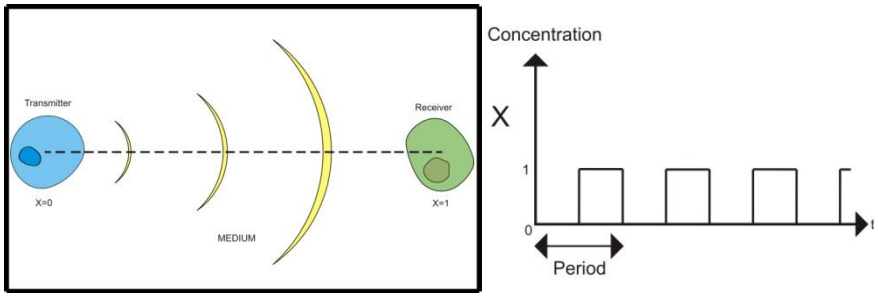

Fig. 3.20 Cell communications situation with a source transmitting a square concentration wave with frequency 1/period.

Under this situation, concentration at the source changing in time, approaching the complete system difficult the obtaining of the real solution, but if we take two different systems, one when the concentration at x=0 is maximum and one when the concentration at x=0 is 0, then we can find a closed solution for the diffusion equation.

In order to normalize the equation (3.23) we take these variables:

$$\Phi(x,t) = \frac{C(x,t)}{C_{\max}(x,t)} \qquad (3.24)$$

$$X = \frac{x}{H} \qquad (3.25)$$

$$T = \frac{t}{T_{final}} \qquad (3.26)$$

Applying these equations on (3.23) we obtain:

$$\frac{\partial\Phi(X,T)}{\partial T} = \frac{D}{H^2 \cdot t_{final}} \cdot \frac{\partial^2\Phi(X,T)}{\partial X^2} \qquad (3.27)$$

Finally if we take $T_{final} = \frac{H^2}{D}$ the diffusion equation becomes:

$$\frac{\partial\Phi(X,T)}{\partial T} = \frac{\partial^2\Phi(X,T)}{\partial X^2}$$
$$0 \le X \le 1$$
$$0 \le T \le 1 \qquad (3.28)$$

The equation (3.28) is known as "Parabolic Second-Order Partial Differential Equation" and initial and boundary conditions are needed to solve this equation. There are two different situations in order to define the initial and the boundary conditions. One when the concentration at X=0 changes from 1 to 0, and the other one when the

concentration at the beginning changes from 0 to 1. We call "Discharge" the first situation and "Charge" the second one.

3.2.1 Discharge conditions

When the concentration at the source changes from maximum to minimum producing a descendent step, in the medium starts a discharge process due to the minimum concentration forced by the transmitter.

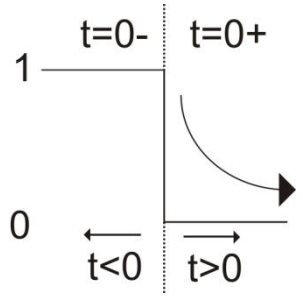

Fig. 3.21 Graphic of the conditions in the instant of change from concentration 1 to 0

The whole medium is filled with particles having maximum concentration at every point, and suddenly ($t = 0^+$), the concentration at the source changes to zero.

Hence, the initial condition in this case is:

$$\Phi(X, 0^-) = 1 \qquad (3.29)$$

And the boundary conditions are:

$$\Phi(0, T > 0^+) = 0 \qquad (3.30)$$

$$\frac{\partial \Phi(1,T)}{\partial X} = \Phi_X(1,T) = 0 \qquad (3.31)$$

Since the cell is placed into a cuvette, when the molecules diffuse to the end, the wall is not permeable to these molecules and as a result, the flux of particles from the source is always zero. This is the meaning of the condition (3.31), which is usually called no-flux boundary condition.

The method of separation of variables can convert a partial differential equation into a different group of ordinary differential equations. We must express the concentration as the product of two single variable functions:

$$\Phi(X,T) = F(T) \cdot G(X) \qquad (3.32)$$

The combination of (3.32) and (3.28) generates:

$$\frac{\partial F}{\partial T}\cdot\frac{1}{F}=\frac{\partial^2 G}{\partial X^2}\cdot\frac{1}{G} \qquad (3.33)$$

Because $F(T)$ and $G(X)$ depend on different variables, the equation (3.33) must be equal to an arbitrary constant:

$$\frac{\partial F}{\partial T}\cdot\frac{1}{F}=\frac{\partial^2 G}{\partial X^2}\cdot\frac{1}{G}=k \qquad (3.34)$$

The partial differential equation (3.28) has become in two different ordinary differential equation:

$$\frac{\partial F}{\partial T}=F\cdot k \qquad (3.35)$$

$$\frac{\partial^2 G}{\partial X^2}=G\cdot k \qquad (3.36)$$

The solution of the equation (3.35) is:

$$F(T)=e^{kT} \qquad (3.37)$$

For positive values of k, the equation (3.37) becomes monotically increasing and would be infinite at infinite values of T which is impossible. So the constant k must be negative:

$$k=-\lambda^2,\quad \lambda\geq 0 \qquad (3.38)$$

The solution for the equation (3.36) is:

$$G(X)=A\cdot\cos(\lambda X)+B\cdot\sin(\lambda X) \qquad (3.39)$$

Therefore the combination of (3.37) and (3.39) provides the complete solution:

$$\Phi(X,T)=\left(A\cdot\cos(\lambda X)+B\cdot\sin(\lambda X)\right)\cdot e^{-\lambda^2 T}+C \qquad (3.40)$$

Where C is a constant that disappears when the concentration equation is derivative.

Now the boundary and the initial conditions will be used in order to find the constants A, B, C and λ.

The substitution of the first boundary condition in (3.40) gives the equation (3.41):

$$\Phi(0,T)=\left(A\cdot 1+B\cdot 0\right)\cdot e^{-\lambda^2 T}+C=0 \qquad (3.41)$$

Because 0 does not have any time dependence:

$$A = 0 \tag{3.42}$$

And then:

$$C = 0 \tag{3.43}$$

Using the second boundary condition in (3.40):

$$\Phi_X(1,T) = B \cdot \lambda \cdot \cos(\lambda \cdot 1) \cdot e^{-\lambda^2 T} = 0 \tag{3.44}$$

The equation (3.44) has infinite solutions:

$$\lambda_n = (2n-1)\frac{\pi}{2} \qquad n \geq 0 \tag{3.45}$$

Adding all the possible solutions we obtain the general solution of the diffusion equation (superposition principle):

$$\Phi(X,T) = \sum_{n=1}^{\infty} B_n \cdot \sin(\lambda_n X) \cdot e^{-\lambda_n{}^2 T} \tag{3.46}$$

$$\Phi(X,T) = \sum_{n=1}^{\infty} B_n \cdot \sin((2n-1)\frac{\pi}{2} \cdot X) \cdot e^{-\left((2n-1)\frac{\pi}{2}\right)^2 \cdot T} \tag{3.47}$$

Finally to find the last constant B, we use the last information that we know, the initial condition. So using (3.29) in (3.47):

$$\Phi(X,0) = \sum_{n=1}^{\infty} B_n \cdot \sin(\lambda_n X) \cdot e^{-\lambda_n{}^2 0} = \sum_{n=1}^{\infty} B_n \cdot \sin(\lambda_n X) = 1 \tag{3.48}$$

Using the concept of orthogonal functions, taking f(x) as:

$$f(X) = \sum_{n=1}^{\infty} B_n \cdot \sin(\lambda_n X)$$

We can say:

$$\int_0^1 f(X') \cdot \sin(\lambda_m X') \cdot dX' = \int_0^1 \sum_{n=1}^{\infty} B_n \cdot \sin(\lambda_n X') \cdot \sin(\lambda_m X') \cdot dX' \tag{3.49}$$

Because the operator integral is linear:

$$\sum_{n=1}^{\infty} B_n \int_0^1 \sin(\lambda_n X') \cdot \sin(\lambda_m X') \cdot dX' \tag{3.50}$$

Arranging the product of sinus we obtain:

$$\sum_{n=1}^{\infty} B_n \int_0^1 \frac{\cos\left((n-m)\pi \cdot X'\right) - \cos\left((n+m-1)\pi \cdot X'\right)}{2} \cdot dX' \qquad (3.51)$$

When $n \neq m$:

$$\sum_{n=1}^{\infty} B_n \cdot \left\{ \frac{\sin\left((n-m)\pi \cdot X\right)}{2}\bigg|_0^1 - \frac{\sin\left((n+m-1)\pi \cdot X\right)}{2}\bigg|_0^1 \right\} = 0 \qquad (3.52)$$

When $n = m$:

$$\sum_{n=1}^{\infty} B_n \cdot \int_0^1 \sin^2\left(\lambda_n X'\right) \cdot dX' = \sum_{n=1}^{\infty} B_n \cdot \int_0^1 \frac{1-\cos\left(2\lambda_n X'\right)}{2} \cdot dX' \qquad (3.53)$$

Solving this equation we obtain that:

$$\int_0^1 f(X') \cdot \sin(\lambda_m X') \cdot dX' = \frac{B_n}{2} \qquad (3.54)$$

So at this point we can say:

$$B_n = 2 \cdot \int_0^1 f(X') \cdot \sin(\lambda_n X') \cdot dX' \qquad (3.55)$$

And as the initial conditions forces and we have found in (3.48):

$$f(X) = \sum_{n=1}^{\infty} B_n \cdot \sin\left(\lambda_n X\right) = 1 \qquad (3.56)$$

So finally using (3.56) in (3.55):

$$B_n = 2 \cdot \int_0^1 1 \cdot \sin(\lambda_n X') \cdot dX'$$
$$B_n = \frac{2}{\lambda_n} = \frac{4}{(2n-1)\pi} \qquad (3.57)$$

Once the four constants have been found the solution for the diffusion equation is ready:

A	*0*
B	$B_n = \frac{4}{(2n-1)\pi}$
C	*0*
λ	$\lambda_n = (2n-1)\frac{\pi}{2}$

Table 3.2 Resume of the constants values for the Discharge situation

Using these values the solution for the diffusion equation in the Discharge case is:

$$\Phi(X,T) = \sum_{n=1}^{\infty} \frac{4}{(2n-1)\pi} \cdot \sin((2n-1)\frac{\pi}{2} \cdot X) \cdot e^{-\left((2n-1)\frac{\pi}{2}\right)^2 \cdot T}$$

$$X = \frac{x}{H}$$

$$T = \frac{t}{D/H^2} \qquad (3.58)$$

$$\Phi = \frac{C(X,T)}{C_{\max}(X,T)}$$

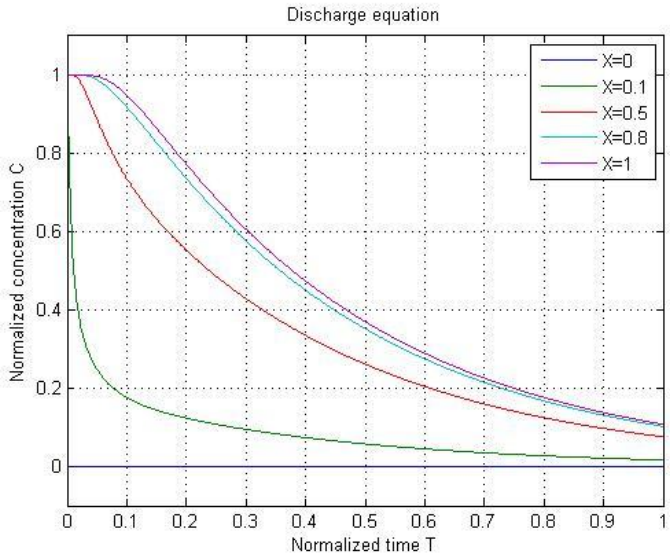

Fig. 3.22 Plot of the discharge equation.

The figure Fig. 3.22 shows the normalized concentration of molecules in different points of the container during the time. We can appreciate how the medium is being emptied of molecules, or in other words how the medium is being "discharged". Further positions take more time to get emitted.

3.2.2 Charge conditions

When the concentration at the source changes from minimum to maximum producing an ascendant step, the medium charges of molecules due to the maximum concentration at the source. The transmitter releases molecules in the container, and because of they cannot leave it, the container gets filled of particles.

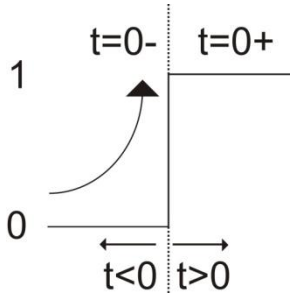

Fig. 3.23 Graphic of the conditions in the instant of change from concentration 0 to 1.

Just in the instant before to the change, the medium is completely empty of molecules, and suddenly the concentration at X=0 changes to its maximum value filling the system of particles and increasing the concentration in each point of X.

The initial condition in this case is:

$$\Phi(X,0)=0 \qquad (3.59)$$

And the boundary conditions are:

$$\Phi(0,T)=1 \qquad (3.60)$$

$$\frac{\partial\Phi(1,T)}{\partial X}=\Phi_X(1,T)=0 \qquad (3.61)$$

The solution is exactly the same until the equation (3.40).

Now using the first boundary condition in (3.40):

$$\Phi(0,T)=\left(A\cdot 1+B\cdot 0\right)\cdot e^{-\lambda^2 T}+C=1 \qquad (3.62)$$

Because 0 does not have any time dependence:

$$A=0 \qquad (3.63)$$

And then:

$$C=1 \qquad (3.64)$$

Using the second boundary condition in (3.40):

$$\Phi_X(1,T) = B \cdot \lambda \cdot \cos(\lambda \cdot 1) \cdot e^{-\lambda^2 T} = 0 \qquad (3.65)$$

The equation (3.44) has infinite solutions:

$$\lambda_n = (2n-1)\frac{\pi}{2} \qquad (3.66)$$
$$n \geq 0$$

Adding all the possible solutions we obtain the general solution of the diffusion equation (superposition principle):

$$\Phi(X,T) = 1 + \sum_{n=1}^{\infty} B_n \cdot \sin(\lambda_n X) \cdot e^{-\lambda_n{}^2 T} \qquad (3.67)$$

Again the last constant is determinate by the initial condition:

$$\Phi(X,0) = 1 + \sum_{n=1}^{\infty} B_n \cdot \sin(\lambda_n X) = 0 \qquad (3.68)$$

Arranging the previous equation:

$$f(X) = \sum_{n=1}^{\infty} B_n \cdot \sin(\lambda_n X) = -1 \qquad (3.69)$$

And now using the orthogonal principle again the constant is:

$$B_n = -\frac{2}{\lambda_n} = -\frac{4}{(2n-1)\pi} \qquad (3.70)$$

Now we have all the constants found:

A	*0*
B	$B_n = -\frac{4}{(2n-1)\pi}$
C	*1*
λ	$\lambda_n = (2n-1)\frac{\pi}{2}$

Table 3.3 Resume of the constants values for the Charge situation

So finally the solution of the diffusion equation for the Charge case is:

$$\Phi(X,T) = 1 - \sum_{n=1}^{\infty} \frac{4}{(2n-1)\pi} \cdot \sin((2n-1)\frac{\pi}{2} \cdot X) \cdot e^{-\left((2n-1)\frac{\pi}{2}\right)^2 \cdot T}$$

$$X = \frac{x}{H}$$

$$T = \frac{t}{D/H^2} \qquad (3.71)$$

$$\Phi = \frac{C(X,T)}{C_{\max}(X,T)}$$

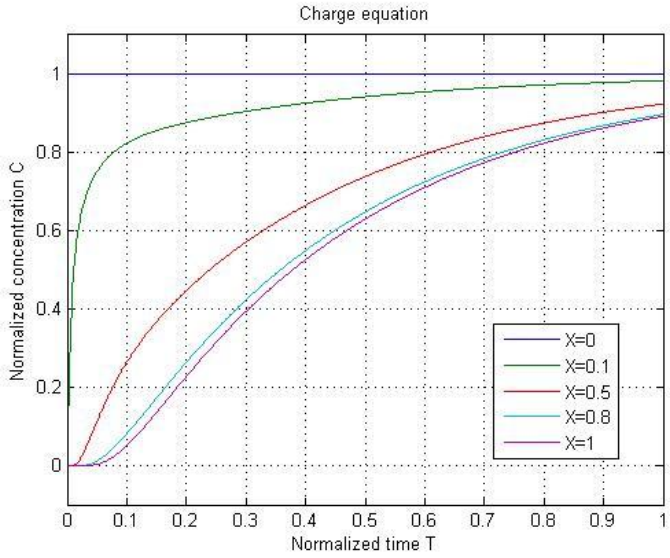

Fig. 3.24 Plot of the charge equation.

The figure Fig. 3.24 shows the concentration in different points along the container during the time. We can appreciate how the system increases the concentration in each point X from 0 to 1. The system is being filled of particles or in other words the medium is "charging".

3.2.3 Complete solution

In order to achieve a solution for a source secreting a square wave of molecules we combine the two previous solutions (3.58) and (3.71) alternating each solution during one semi-period. The only think to be care is the fact that we have been assuming that the initial condition for the charge was initial concentration 0 and for discharge initial concentration 1. If there is no complete charge or discharge the initial conditions do not are 0 o 1 respectively. The initial condition for the charge is the last value in the previous discharge, and the initial condition for the discharge is the last value in the previous charge. This affect to the calculus of the constant B.

Combining the two equations the constant B is:

- **Discharge case:**

$$B_n = \frac{2}{\lambda_n} \cdot IC \qquad (3.72)$$

- **Charge case:**

$$B_n = -\frac{2}{\lambda_n} \cdot (1 - IC) \qquad (3.73)$$

In the **Appendix F** there is a MATLAB code which combines the two equations in order to solve the diffusion equation with a square wave as a source.

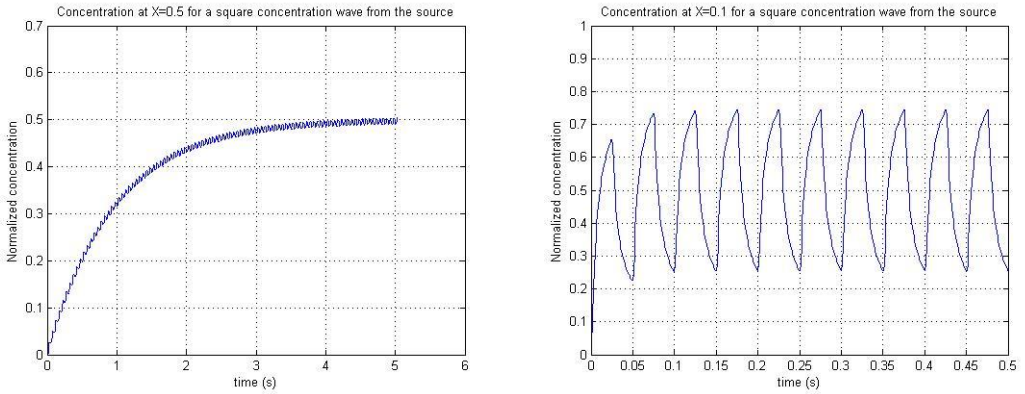

Fig. 3.25 Solution for the diffusion equation complete. On the right the position where we are calculating the concentration is X=0.5, on the left is X=0.1.

3.3 Frequential Analysis

In frequency modulations, the information is carried in periodic signals that are called carriers. In biological communications the information is carried in periodic waves of calcium, and the real information is encoded in the frequency of those waves. Therefore, a wave of calcium with frequency F1 may indicates the duplication of the target cell, but the same wave with a frequency F2 may indicates the transformation of the target cell.

Because of the information in frequency modulations depend on the carrier's frequency; a frequential study for the solution of the diffusion equation is required. Because the solution has two forms, one per each semi-period in a periodic square signal, the frequential analysis will be done for each solution.

3.3.1 Discharge conditions

Denormalizing the equation (3.58) we obtain the real solution for the diffusion equation:

$$\Phi(x,t)=\sum_{n=1}^{\infty}\frac{4}{(2n-1)\pi}\cdot\sin((2n-1)\frac{\pi}{2}\cdot\frac{x}{H})\cdot e^{-\left((2n-1)\frac{\pi}{2}\right)^2\cdot\frac{D}{H^2}t} \qquad (3.74)$$

Appling the Laplace transform the equation (3.74) becomes:

$$\mathrm{O}(x,s)=\sum_{n=1}^{\infty}\frac{4}{(2n-1)\pi}\cdot\sin((2n-1)\frac{\pi}{2}\cdot\frac{x}{H})\cdot\frac{1}{s+\left((2n-1)\frac{\pi}{2}\right)^2\cdot\frac{D}{H^2}} \qquad (3.75)$$

The frequency response results of taking $s=j\omega$. Doing this we observe that the system is the summation of infinite first order systems, each with a pole situated at:

$$p_n=-\left((2n-1)\frac{\pi}{2}\right)^2\cdot\frac{D}{H^2} \qquad (3.76)$$

Each of those systems by itself is a low pass band filter whose frequency corner is situated according with its pole. The amplitude decreases with n with the relation:

$$\frac{4}{(2n-1)\pi}$$

Using an approximation of the system for its first component $n=1$ we would obtain a simple low pass band filter whose corner frequency would be at:

$$\omega_1=\left(\frac{\pi}{2}\right)^2\cdot\frac{D}{H^2} \qquad (3.77)$$

This frequency depends on the coefficient diffusion and the distance between the source and the sink. But before to be able to use this approximation we must demonstrate that it is sufficiently faithful.

Following is shown the bode plots for a system using the approximation only for the first component, and another using 47 terms.

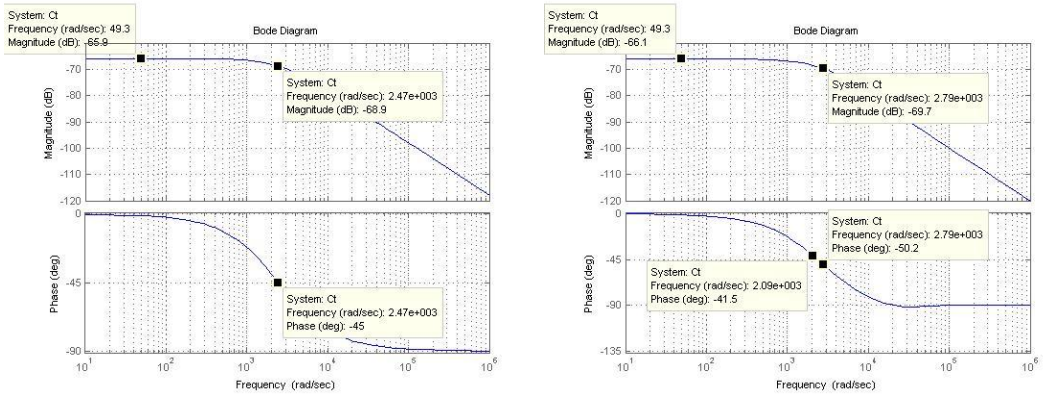

Fig. 3.26 Bode plots for the cases n=1 (left) and n=47 (right). H=1 μm, x=0.9 μm, D=1000 μm2/s

This Bode plots show that the systems act as a low pass band filter and also shows big similitude between them.

	n=1	***n=47***
Initial Amplitude	*-65.9 dB*	*-66.1 dB*
Corner Frequency	*2.47e3 rad/s*	*2.44e3 rad/s*

Table 3.4 Comparison of the frequential response for n=1 or n=41

The value of the corner frequency in n=47 comes from the mean value of amplitude at the frequencies of 2.79e3 and 2.09e3 rad/s which have been taken from the phase plot, around the 45°.

With these results it is reasonable to think that the relevant frequency information is presented only in the first component of the infinite series.

$$\mathrm{O}(x,s) \approx \frac{4}{\pi} \cdot \sin\left(\frac{\pi}{2}\frac{x}{H}\right) \cdot \frac{1}{s + \left(\frac{\pi}{2}\right)^2 \frac{D}{H^2}} \qquad (3.78)$$

And the approximate corner frequency of the system is:

$$\omega_c = \left(\frac{\pi}{2}\right)^2 \frac{D}{H^2} \qquad (3.79)$$

3.3.2 Charge conditions

In this case denormalizing the equation (3.74) we obtain the real solution for the diffusion equation:

$$\Phi(x,t) = 1 - \sum_{n=1}^{\infty} \frac{4}{(2n-1)\pi} \cdot \sin((2n-1)\frac{\pi}{2} \cdot \frac{x}{H}) \cdot e^{-\left((2n-1)\frac{\pi}{2}\right)^2 \cdot \frac{D}{H^2} t} \qquad (3.80)$$

Appling the Laplace transform the equation (3.80) becomes:

$$O(x,s) = \frac{1}{s} - \sum_{n=1}^{\infty} \frac{4}{(2n-1)\pi} \cdot \sin((2n-1)\frac{\pi}{2} \cdot \frac{x}{H}) \cdot \frac{1}{s + \left((2n-1)\frac{\pi}{2}\right)^2 \cdot \frac{D}{H^2}} \qquad (3.81)$$

In this case a pole at the beginning appears. That makes us think that for this system the response is not a first order low pass band filter.

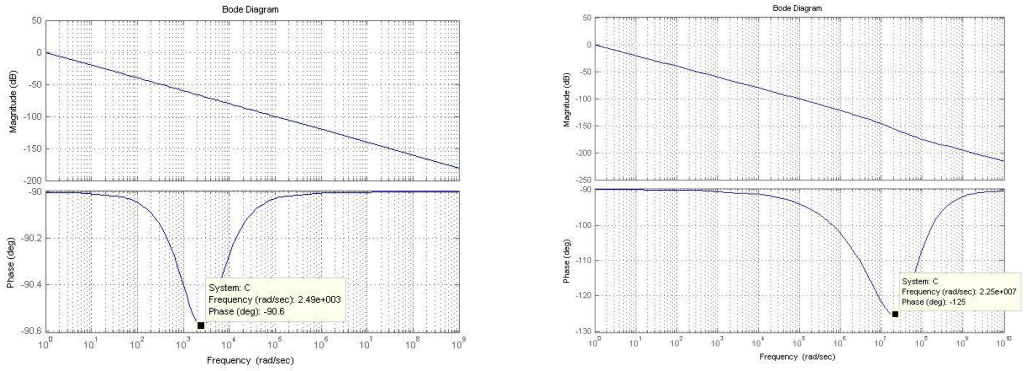

Fig. 3.27 Bode plots for the cases n=1 (left) and n=47 (right). H=1 μm, x=0.01μm, D=1000 μm2/s

Although this bode plots show that the high frequencies are attenuated, they are not a first order low band pass filter.

	n=1	***n=47***
Initial Amplitude	*0 dB*	*0 dB*
A(1e5)	*-100 dB*	*≈-100 dB*
A(1e9)	*-180 dB*	*≈-180 dB*
Minimum Phase	*-90.6°*	*-125°*
Freq. Minimum Phase	*2.49e3 rad/s*	*2.25e7 rad/s*

Table 3.5 Comparison of the frequency response for n=1 or n=41

These results show us that there are many similarities in the amplitude plot, they are almost equals, but the phase is completely different. The addition of terms causes a shift in the phase and at the same time increases the phase delay.

3.4 Stability

In systems that work with transfer functions a study of their stability is always needed. The value of the poles and zeros in these systems are defined by physical parameters such as the diffusivity, the size of the container H or the position in the cuvette where the concentration is being calculated. The values of the parameters that yield instable poles or zeros must be determined in order to predict when the solution will present instabilities.

3.4.1 Non-minimum phase systems

The transfer functions that do not have poles or zeros in the right half-plane s are minimum phase transfer functions, while those that at least have one pole or one zero in the right half-plane s are non-minimum phase transfer functions. The systems that include non-minimum phase transfer functions are called non-minimum phase systems [24].

Considering the transfer function $G(s)$:

$$G(s)=\frac{K\cdot(1-T_a s)}{s\cdot(Ts+1)}\rightarrow T_a>0 \qquad (3.82)$$

This function has non-minimum phase, due to there is a zero place in the right half-plane s.

The systems with all their roots (poles and zeros) in the left half-plane, are always stable. When a system has only one pole in the right half-plane (it is positive) this system is always instable. The systems with only stable poles, but with at least one zero in the right half-plane can be stable or unstable.

Closing the loop for the system $G(s)$:

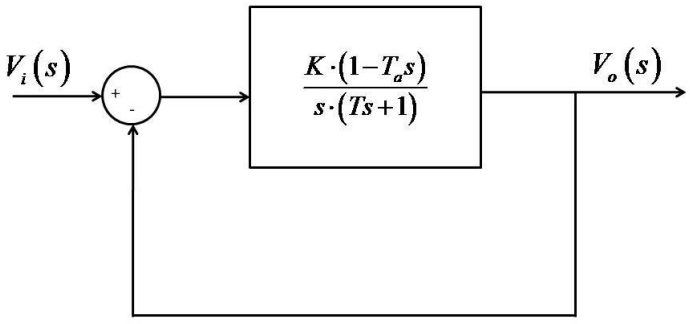

Fig. 3.28 Non-minimum phase system.

We can obtain the root locus. This graphic shows what values of the gain K may yields instabilities.

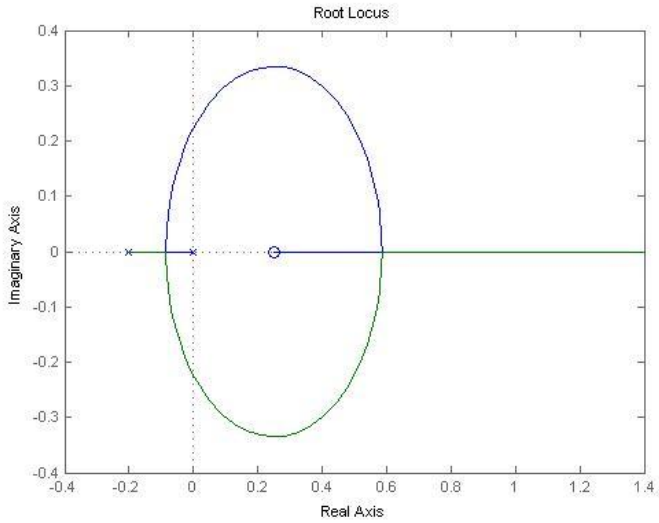

Fig. 3.29 Root locus for a system with a non-minimum phase zero.

The figure Fig. 3.29 shows how depending on the gain value the system may be stable or unstable only because there is one positive zero.

Being $R(s)$ the transfer function that describes the charge conditions and $S(s)$ the transfer function that describes the discharge conditions, the mathematical model of the molecular communication systems is:

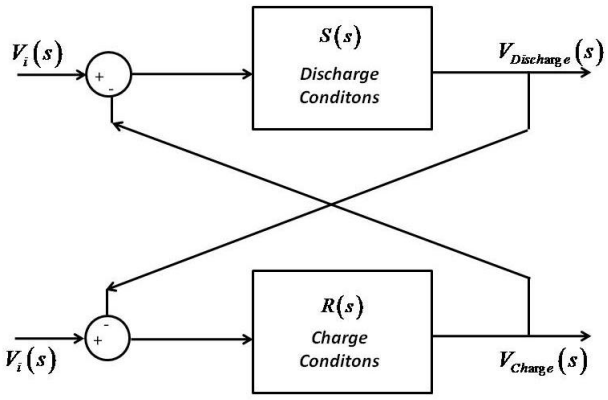

Fig. 3.30 Mathematical model of a Molecular Communication System.

This system is formed by two transfer functions with negative feedback. The unstable poles and zeros of the open loop may affect to the stability of the closed loop.

Then, the stability depends on finding when the poles and the zeros are positive or negative depending on the parameters of the equation.

3.4.2 Discharge conditions

A study of the stability is necessary always when we work with pole-zero systems.

The approximation n=1 is always stable. It has only a pole in the negative half plane so there is no possibility for instabilities. In the approximation n=2 the Laplace transform is:

$$O_2(x,s)=\frac{2}{\lambda_1}\sin\left(\lambda_1\frac{x}{H}\right)\frac{1}{s+\lambda_1^2\frac{D}{H^2}}+\frac{2}{\lambda_2}\sin\left(\lambda_2\frac{x}{H}\right)\frac{1}{s+\lambda_2^2\frac{D}{H^2}} \qquad (3.83)$$

Taking:

$$A_1=\frac{2}{\lambda_1}\sin\left(\lambda_1\frac{x}{H}\right)$$

$$A_2=\frac{2}{\lambda_2}\sin\left(\lambda_2\frac{x}{H}\right)$$

$$a_1=\lambda_1^2\frac{D}{H^2}$$

$$a_2=\lambda_2^2\frac{D}{H^2}$$

The equation (3.83) becomes:

$$O_2(x,s)=\frac{A_1}{s+a_1}+\frac{A_2}{s+a_2}=\frac{A_1\cdot(s+a_2)+A_2\cdot(s+a_1)}{(s+a_1)\cdot(s+a_2)} \qquad (3.84)$$

There are two stable poles because $a_1\geq 0$ and $a_2\geq 0$ always. There is one zero, and we must find if this zero is stable or not.

$$z=-\frac{A_1\cdot a_2+A_2\cdot a_1}{A_1+A_2} \qquad (3.85)$$

So the stability condition is:

$$\frac{A_1\cdot a_2+A_2\cdot a_1}{A_1+A_2}\geq 0 \qquad (3.86)$$

Arranging the equation above:

$$\frac{\sin\left(\lambda_1\frac{x}{H}\right)\cdot\frac{\lambda_2^2}{\lambda_1}+\sin\left(\lambda_2\frac{x}{H}\right)\cdot\frac{\lambda_1^2}{\lambda_2}}{\frac{\sin\left(\lambda_1\frac{x}{H}\right)}{\lambda_1}+\frac{\sin\left(\lambda_2\frac{x}{H}\right)}{\lambda_2}}\geq 0 \qquad (3.87)$$

We have to demonstrate that the numerator and the denominator have the same sign:

$$\lambda_1 = \frac{\pi}{2}$$
$$\lambda_2 = 3\frac{\pi}{2} \qquad (3.88)$$

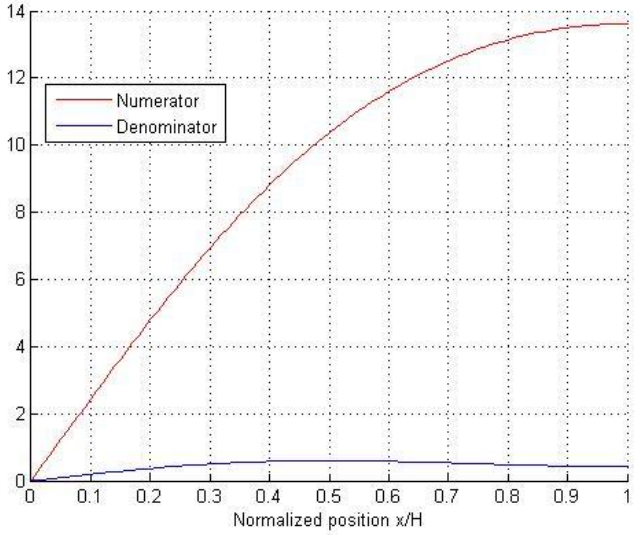

Fig. 3.31 Value of the numerator and the denominator.

As we can see in Fig. 3.31, either the numerator or the denominator is positive in the whole domain. Thus, we can affirm that the condition (3.88) applies and then, the zero is placed in the negative half plane. After that it is reasonable to think that this system is stable for any value of $n \geq 0$.

3.4.3 Charge conditions

For the charge conditions, the existence of a pole at $s = 0$, causes that the first term in the series has a zero instead of the discharge case that only had poles in the first term.

For n=1:

$$O_1(x,s) = \frac{1}{s} - \frac{4}{\pi} \cdot \sin\left(\frac{\pi}{2} \cdot \frac{x}{H}\right) \cdot \frac{1}{s + \left(\frac{\pi}{2}\right)^2 \cdot \frac{D}{H^2}} \qquad (3.89)$$

And taking:

$$A_1 = \frac{4}{\pi} \cdot \sin\left(\frac{\pi}{2} \cdot \frac{x}{H}\right)$$
$$a_1 = \left(\frac{\pi}{2}\right)^2 \cdot \frac{D}{H^2}$$

The equation (3.89) becomes:

$$O_1(x,s)=\frac{(1-A_1)s+a_1}{s\cdot(s+a_1)} \qquad (3.90)$$

In this case there are 2 poles, one at 0 and the other is negative so both are stable, and one zero. We must know when this zero is unstable:

$$z_1=-\frac{a_1}{1-A_1}=-\frac{\left(\frac{\pi}{2}\right)^2\frac{D}{H^2}}{1-\frac{4}{\pi}\sin\left(\frac{\pi}{2}\frac{x}{H}\right)} \qquad (3.91)$$

The condition is this zero must be negative. The numerator is always positive so the only condition remains in the denominator. Then the stability condition is:

$$\frac{x}{H}<\frac{2}{\pi}\arcsin\left(\frac{\pi}{4}\right)\approx 0.575 \qquad (3.92)$$

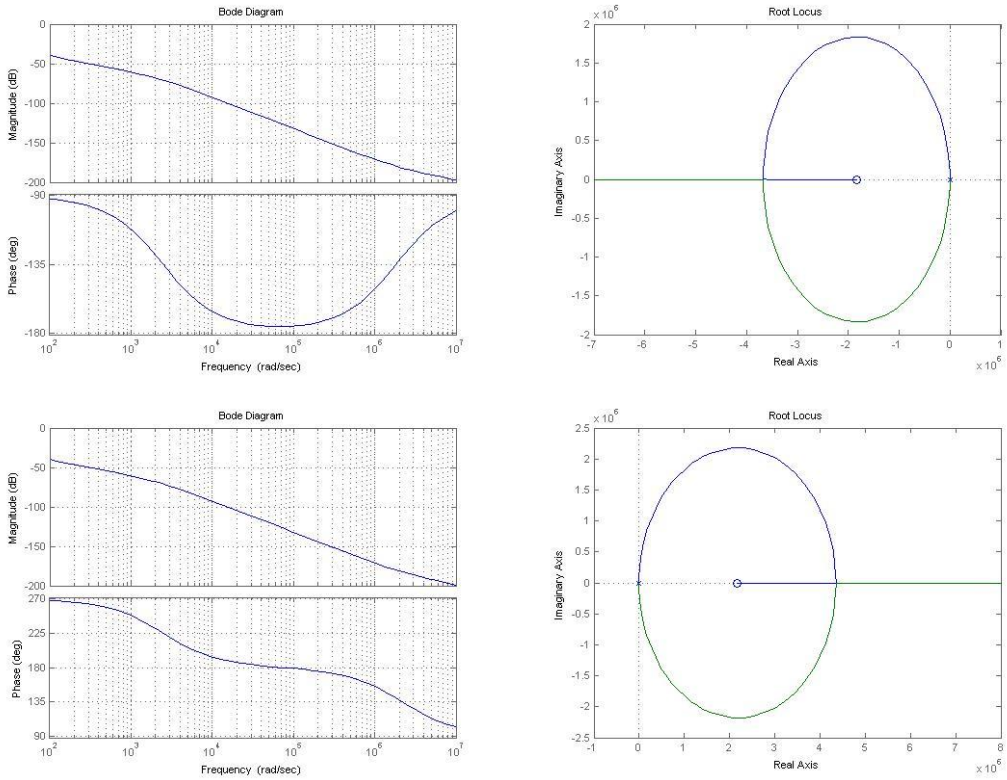

Fig. 3.32 Bode plots (on the left) and root locus (on the right) for the case n=1. The two plots on the top have been done with a ratio x/H=0.574. The two plots on the bottom have been done with a ratio x/H=0.576.

We can see in this graphics how the stability condition complies. In the image on the top at the right, the root locus show us how the zero is in the half negative plane, instead of the image on the bottom at the right which shows the zero in the unstable plane. In the bode plot this is reflected because we can see that it is a non-minimum phase system.

The temporal evolution for these cases is presented below:

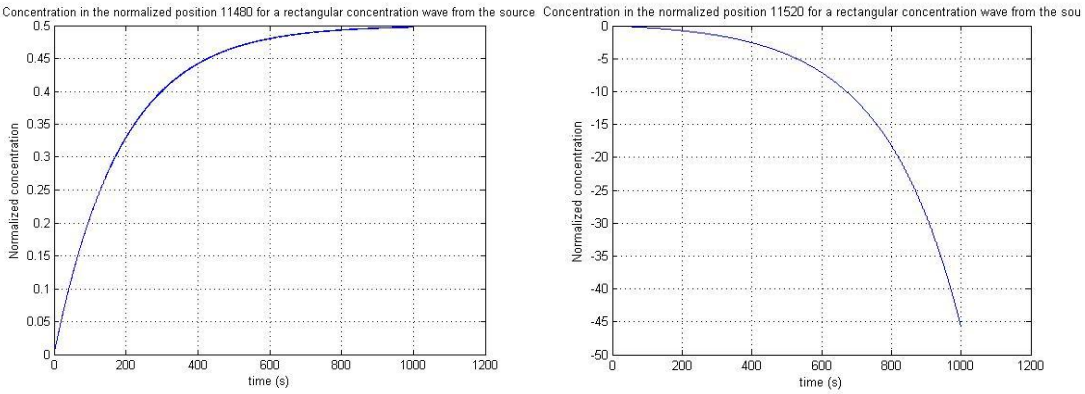

Fig. 3.33 Concentration at the sink positions for the stable case x/H=0.574 (rigth) and the unstable case x/H=0.576 (left) for a system with a longitude of H=2cm and diffusion coefficient D=1000μ2/s.

We can appreciate in the previous figure how the stability condition restricts the point in which we can calculate the complete solution. In the image on the left, the concentration increases during the time as we expect, reaching the mean value of the maximum and the minimum concentration, 0.5 if it is normalized. On the other hand, the image on the right shows how for further positions, the solution becomes unstable.

For n=2:

$$O_2(x,s)=\frac{1}{s}-\frac{2}{\lambda_1}\sin\left(\lambda_1\frac{x}{H}\right)\frac{1}{s+\lambda_1^2\dfrac{D}{H^2}}+\frac{2}{\lambda_2}\sin\left(\lambda_2\frac{x}{H}\right)\frac{1}{s+\lambda_2^2\dfrac{D}{H^2}} \qquad (3.93)$$

And taking:

$$A_1=\frac{2}{\lambda_1}\sin\left(\lambda_1\frac{x}{H}\right)$$

$$A_2=\frac{2}{\lambda_2}\sin\left(\lambda_2\frac{x}{H}\right)$$

$$a_1=\lambda_1^2\frac{D}{H^2}$$

$$a_2=\lambda_2^2\frac{D}{H^2}$$

The equation (3.93) becomes:

$$O_2(x,s)=\frac{1}{s}-\frac{A_1}{s+a_1}-\frac{A_2}{s+a_2}=\frac{(1-A_1-A_2)s^2+(a_1+a_2-A_1a_2-A_2a_1)s+a_1a_2}{s\cdot(s+a_1)\cdot(s+a_2)} \qquad (3.94)$$

This equation has three stable poles and two zeros. The stability depends on the position of those zeros. In order to know if there are positive roots in the numerator the Routh-Hurwitz method is used.

$$\begin{array}{c|cc} s^2 & 1-A_1-A_2 & a_1a_2 \\ s & a_1+a_2-A_1a_2-A_2a_1 & 0 \\ 1 & \dfrac{\left(a_1+a_2-A_1a_2-A_2a_1\right)\cdot a_1a_2-\left(1-A_1-A_2\right)\cdot 0}{\left(a_1+a_2-A_1a_2-A_2a_1\right)} & 0 \end{array}$$

Arranging the result above we obtain:

$$\begin{array}{c|cc} s^2 & 1-A_1-A_2 & a_1a_2 \\ s & a_1+a_2-A_1a_2-A_2a_1 & 0 \\ 1 & a_1a_2 & 0 \end{array}$$

The number of unstable roots is the number of sign changes in the elements in the first column. Because $a_1>0$ and $a_2>0$ then the all column must be positive.

The first stability condition is:

$$1-A_1-A_2=A_1=1-\frac{2}{\lambda_1}\sin\left(\lambda_1\frac{x}{H}\right)-\frac{2}{\lambda_2}\sin\left(\lambda_2\frac{x}{H}\right)>0 \qquad (3.95)$$

$$\frac{1}{2}>\frac{\sin\left(\lambda_1\frac{x}{H}\right)}{\lambda_1}+\frac{s\sin\left(\lambda_2\frac{x}{H}\right)}{\lambda_2} \qquad (3.96)$$

The second stability condition is:

$$a_1+a_2-A_1a_2-A_2a_1=\lambda_1^2\frac{D}{H^2}+\lambda_2^2\frac{D}{H^2}-\frac{2}{\lambda_1}\sin\left(\lambda_1\frac{x}{H}\right)\cdot\lambda_2^2\frac{D}{H^2}-\frac{2}{\lambda_2}\sin\left(\lambda_2\frac{x}{H}\right)\cdot\lambda_1^2\frac{D}{H^2} \qquad (3.97)$$

$$\frac{1}{2}>\frac{\sin\left(\lambda_1\frac{x}{H}\right)\cdot\lambda_2^3+\sin\left(\lambda_2\frac{x}{H}\right)\cdot\lambda_1^3}{\lambda_1\lambda_2\cdot\left(\lambda_1^2+\lambda_2^2\right)} \qquad (3.98)$$

Plotting these two conditions we can find what is the range of x/H that satisfies the two conditions.

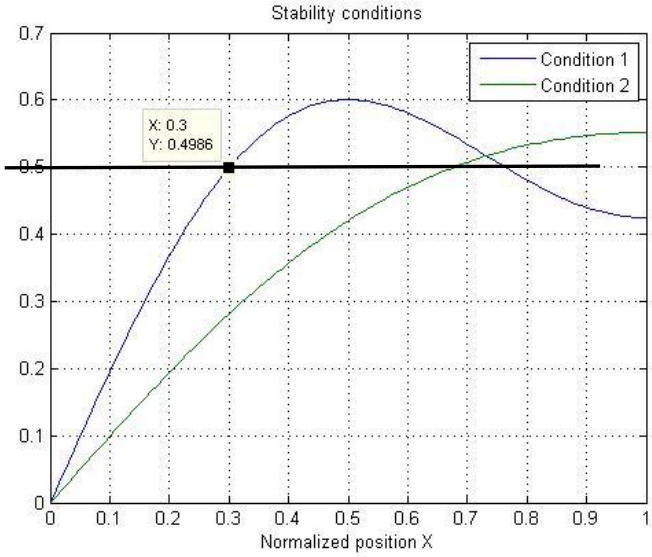

Fig. 3.34 Stabilities conditions for n=2.

As we can see in the figure above the range of stability is $0 \le \frac{x}{H} \le 0.3$

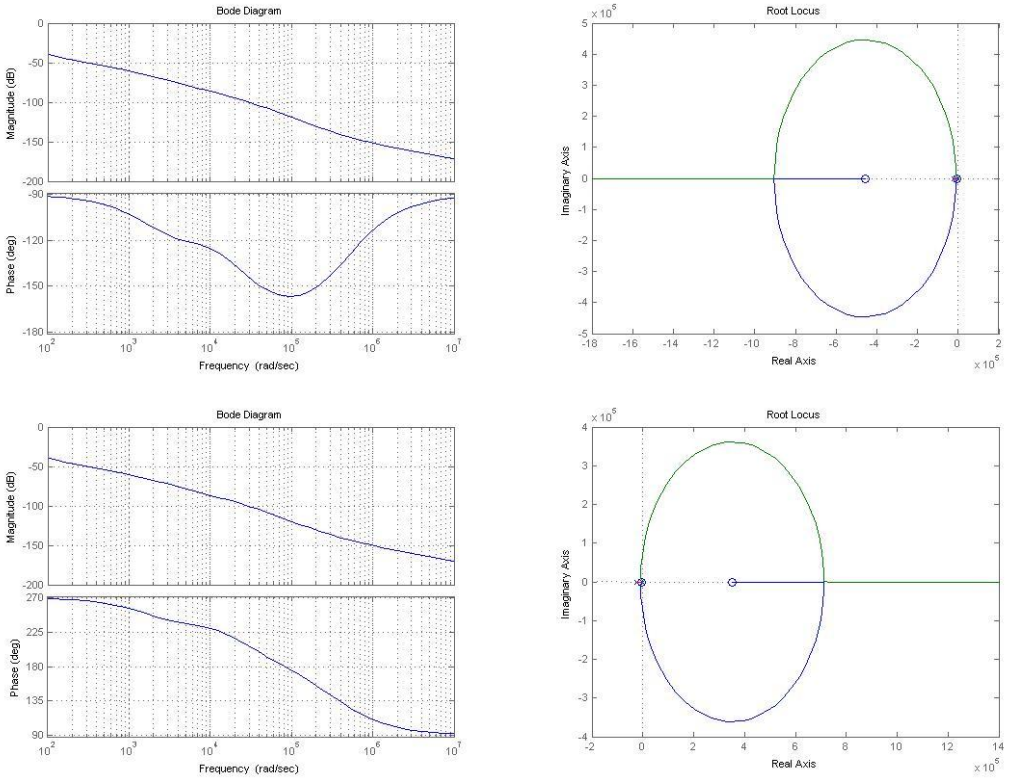

Fig. 3.35 Bode plots (on the left) and root locus (on the right) for the case n=2. The two plots on the top have been done with a ratio x/H=0.29. The two plots on the bottom have been done with a ratio x/H=0.31.

We can see the position of the zeros depending on the stability condition. Below is shown the temporal effects for these conditions:

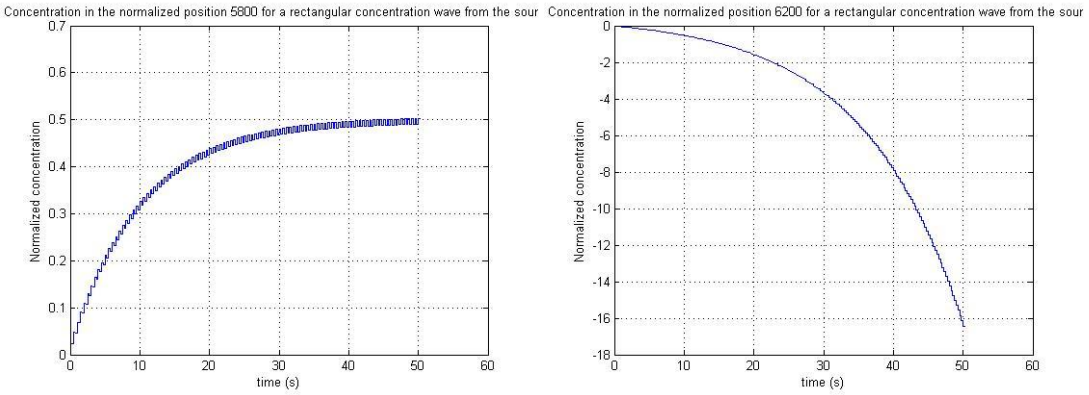

Fig. 3.36 Concentration at the sink positions for the stable case x/H=29 (right) and the unstable case x/H=0.31 (left).

The figure Fig. 3.36 shows how the stability depends on the position where the concentration is being calculated. These stability conditions say us that we cannot measure the concentration in all range of x.

3.5 Results and Discussions

The solution for the diffusion equation in a scenario with a cell placed in a cuvette secreting molecules to the medium has been found when the wave of molecules follows a square signal. This solution provides a mathematical model for this system that describes the biological scenario as a low pass band filter whose frequency corner depends on the diffusivity, D, and the size of the container where the cell is placed, H.

The frequency corner takes a key role to understand when a cell is able to encode the information using amplitude or frequency modulation. The frequency modulation has several advantages over the amplitude modulation, such as the less amount of molecules that are needed or a better noise immunity.

Assuming that the cells encode the information in frequency when they can do it instead of use amplitude modulation, a cell will modulate in frequency when the carrier frequency belongs to the pass band of the filter.

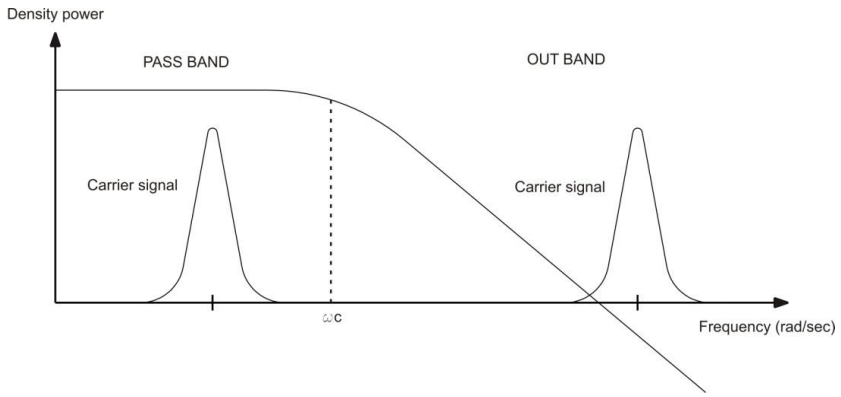

Fig. 3.37 Low pass band filter

In a low pass filter, the band pass goes from 0 Hz to the frequency corner so if the carrier frequency is lower than the frequency corner a cell is able to use frequency modulation. The frequency corner can be determined approximately according to the expression (3.79)

$$\omega_c = \left(\frac{\pi}{2}\right)^2 \frac{D}{H^2}$$

The equation says that for large values of the diffusion equation the band pass increases, and in consequence, the range of possible carrier frequencies is bigger. This means that large values of diffusivity make easier the frequency modulation. Physically this represents that systems with high diffusivity allows the rapid diffusion of particles, and thus all changes at the source may be propagated quickly through the system.

The figure Fig. 3.38 represents a system with a longitude of 10μm in which a cell placed at the position x=0μm is secreting a square wave of molecules with a frequency of 2Hz.

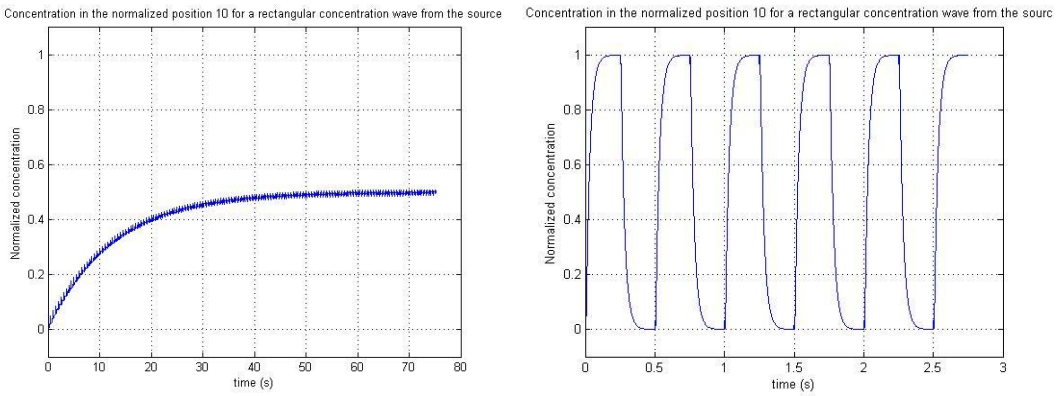

Fig. 3.38 Normalized concentration in a system with H=10μm, at the position in the cuvette x=10μm for an input square signal with a frequency F=2Hz. On the left diffusivity D=30μ2/s on the right D=1500μ2/s.

In the image on the left, the system is working with low diffusivity conditions. Under this situation, because of the low diffusion coefficient, the molecules released to the medium move slowly along the cuvette, and all the changes from maximum to minimum concentration forced by the source cannot be detected at further positions. The molecules have not diffuse enough when the concentration imposed by the source changes. For this reason the concentration detected in further positions is the mean value of the maximum and the minimum concentration transmitted.

Mathematically, the image shows the signal transmitted is being filtered. The system has an approximated frequency corner of:

$$\omega_c = \left(\frac{\pi}{2}\right)^2 \frac{D}{H^2} = \left(\frac{\pi}{2}\right)^2 \frac{30}{10^2} = 0.740\, rad/s$$

And the input signal frequency is:

$$\omega_i = 2\pi F = 2\pi \cdot 2 = 12.56 \, rad/s$$

AS we can observe $\omega_c << \omega_i$ so the system is filtering the input signal.

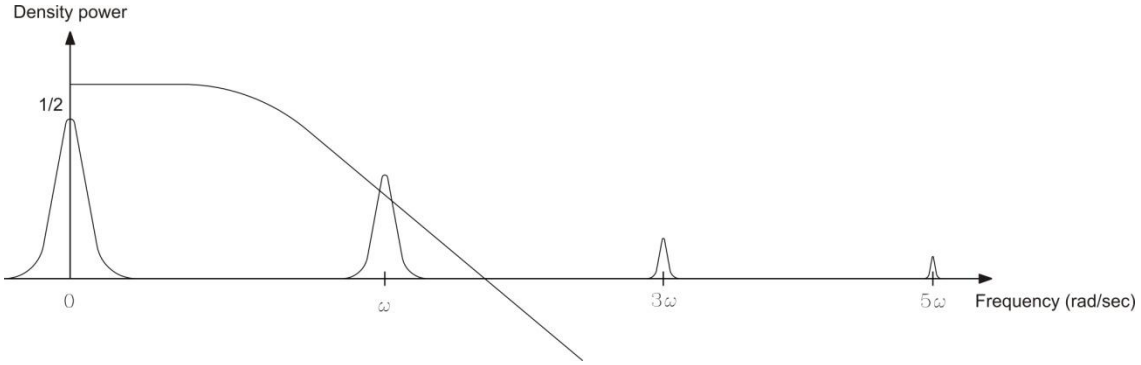

Fig. 3.39 Square signal filtered by a low pass filter.

The square waves present infinite frequential components at the odd harmonics $(\omega_i, 3\omega_i, 5\omega_i, 7\omega_i, ...)$ and a dc component which is the mean average of the signal. In this case the bandwidth of the filter only includes the dc component, and all harmonics are filtered. Because of that the signal tends to be a dc component placed around 0.5.

On the other hand, the image on the right shows a system working with high diffusivity conditions. In this case the molecules released move quickly along the medium, and they arrive to further positions before the change occurs at the source. the concentration detected at the end of the container follows the changes forced by the source, remaining the frequency information unchanged.

Mathematically the meaning is that the signal transmitted has its frequency inside the pass band. In this case the system has a pass band of:

$$\omega_c = \left(\frac{\pi}{2}\right)^2 \frac{D}{H^2} = \left(\frac{\pi}{2}\right)^2 \frac{1500}{10^2} = 37.011 \, rad/s$$

And the input signal is the same. In this case the signal is not filtered because of $\omega_c > \omega_i$.

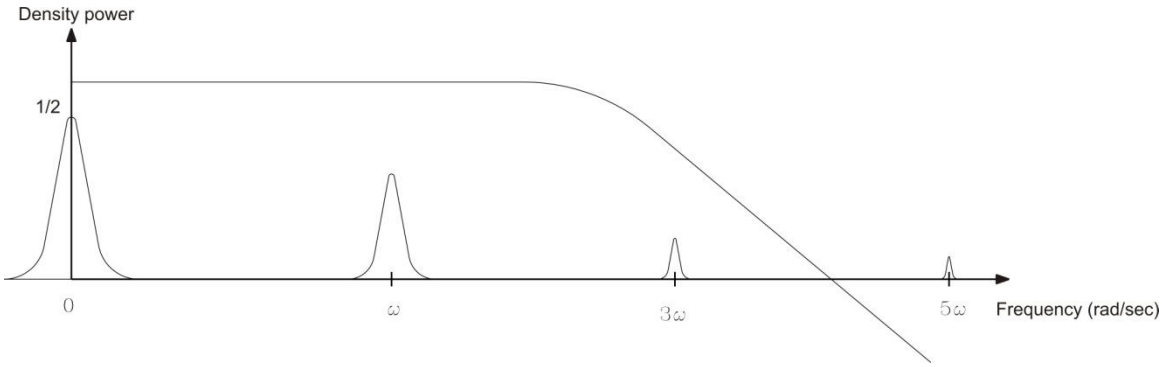

Fig. 3.40 Square signal with two harmonics in the band pass.

The bandwidth includes the dc component, the first and the second harmonics (which are the harmonics with higher amplitude). Because of that the signal detected has a shape that is almost a square wave. The information of high frequency filtered, provokes that the signal detected is not a perfect square.

The pass band depends also on the size of the container that is being filled of molecules. Small containers (low value of H) produce systems with high bandwidth. Physically that means that small containers can be filled or emptied quicker, and thus, variations of the concentration at the source are detected more easily at the end of the cuvette. For big containers the molecules have to travel long distance until to diffuse along the whole system. They need a lot of time to reach the end, and during this time the concentration at the source is continuously changing. In this case the concentration detected at the end of the container will be again the mean average of the maximum and the minimum concentration of the square signal transmitted by the source.

The figure Fig. 3.41 describes the behavior of a system with a constant diffusivity of 2000μm2/s in which at the position x=0μm it is being secreted molecules following a square wave of concentration with a frequency of F=2Hz.

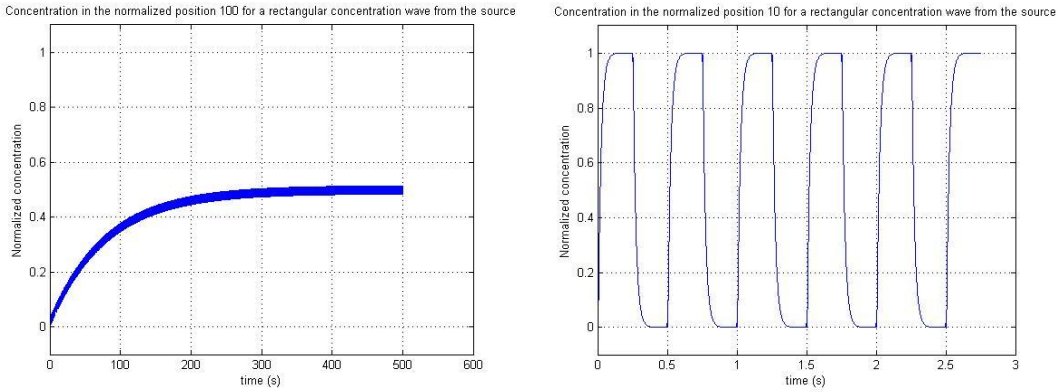

Fig. 3.41 Normalized concentration in a system with D=2000μm²/s for an input square signal with a frequency F=2Hz. On the left the size of the container is H=100μm on the right the size is H=10μm. In both cases the detection is made it at the end of the cuvette.

The image on the left shows how for big containers the input signal is filtered. The concentration measured at the end of the cuvette is the average of the input signal concentration. In this case the frequency corner is:

$$\omega_c = \left(\frac{\pi}{2}\right)^2 \frac{D}{H^2} = \left(\frac{\pi}{2}\right)^2 \frac{2000}{100^2} = 0.493 \, rad/s$$

Much lower than the signal frequency $\omega_i = 12.57 \, rad/s$. The signal is out of band in this case, and for this reason only the average is detected.

The image on the right represents a system which is formed for a small container. That makes easier the process of filling and emptying, and the changes at the sources are transported by the medium faster. The frequency corner in this situation is:

$$\omega_c = \left(\frac{\pi}{2}\right)^2 \frac{D}{H^2} = \left(\frac{\pi}{2}\right)^2 \frac{2000}{10^2} = 49.35 \, rad/s$$

In this bandwidth covers the dc component and the two first harmonics. How the output signal follows the input signal frequency is clear.

In frequency modulation the information is encoded in the carrier frequency. When the frequency of the carrier is bigger than the filter's bandwidth, the carrier cannot cross the system, and it gets attenuated, losing the information that is carrying. For this reason the systems which are able to accept information modulated in frequency are those that have high diffusivities or that are small enough. In either of these two situations, a cell would encode the information using frequency modulation. In other case it would encode it in amplitude modulation.

The solution purposed to model paracrine communications is very useful to understand the needed conditions for the biological modulation of signals. With this model we have found a criterion which decides when the information can be encoded in amplitude or in frequency. But important stability issues have been detected using this method.

Since the complete solution is formed from the two partial solutions (charge and discharge) if one of them is unstable, the complete system also is. The discharge solution is always stable, but the charge solution presents some instabilities.

Not always it is possible to find a solution for the whole system. It has been demonstrate that under specific conditions, the stability depends on the relative position x/H. In the worst approximation of the real solution (the approximation of n=1) the stability threshold is x/H=0.576 which means that we can calculate the concentration only until the half of the range.

For this reason a tool able to simulate the paracrine communication system will be programmed. The intention is, once the mathematical model has been described, to design a simulator based on numerical methods which provides an approximate solution of the diffusion equation. With this simulator the concentration at every point in the system will be known solving all the stability issues that the real solution presents.

4 FABRICATION AND CHARACTERIZATION OF A MICROFLUIDIC DEVICE

The aim of this chapter is to fabricate a microfluidic device known as T-SENSOR whose operating principle is basically the same of the one that governs the molecular communication systems. With this device we can study the diffusion process in a more experimental way, and also doing experiments with this device we will get experimental data that will be used to validate the simulator of diffusion.

4.1 T-SENSOR

The T-Sensor [25] is a microfluidic analytical device which uses the low Reynolds numbers to ensure laminar flow inside it. It has two inlets for which are introduced different fluids that flow together side-by-side, and one outlet which drop the mixed fluid. The mixing between them is only due by diffusion process because of the flow is strictly laminar. Diffusion of molecules between streams flowing side-by-side may be observed directly and monitored optically through the downstream direction.

The T-Sensor is a microfluidic analytical device which uses the low Reynold numbers to ensure laminar flow inside it. It has two inlets channels that join in a one main channel. Two different fluids are introduced for the inlets and when they converge in the main channel flow together side-by-side mixing only by diffusion process. Diffusion of molecules between streams flowing side-by-side may be observed directly and monitored optically through the downstream direction.

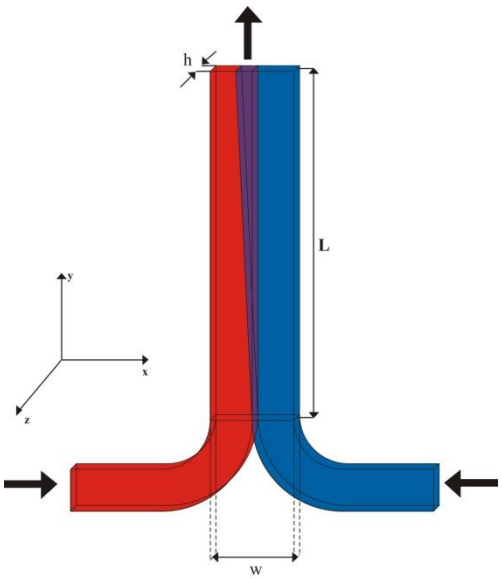

Fig. 4.42 Schematic representation of the T-Sensors shape. Two fluid enter for the channels at the bottom and one mixed fluid drop for the outlet at the top.

The T-SENSOR is the most common passive mixer. The two fluid mix along the main channel, and if this channel was long enough a fluid with uniform concentration would be achieved.

The zone where the two fluids are mixes is called "interdiffusion zone" and it is very dependent of the flow velocity. When the velocity is slow, it takes more time to the particles to travel along the whole channel, and during this time these particles can diffuse a through the interdiffusion direction $\vec{x}$. Otherwise, when the fluid is fast the particles leave the main channel before they can diffuse.

The T-Sensor is a microfluidic device which is fabricated using the known as "Soft Lithography" process. The soft-lithography process can be separated in two parts:

fabrication of an elastomeric element and use of this element to pattern the geometric features defined by a relief structure. The structure from which the stamp is derived is called 'master'. It can be fabricated by any method which is capable to reproduce a well defined structure of relief on a surface. Commonly the regular lithography technique is used to define a master. The elastomeric element is generated by casting a polymer against the master. The most common elastomeric used is the Polydimethylsiloxane or PDMS which is a heat curable polymer.

In this work a much easier way to fabricate the master was used [26]. The main idea is the fabrication of a master made by Scotch Tape. It is easier, quicker and more inexpensive than a master made it by lithography.

4.2 Design

In order to study the diffusion process of particles in a fluid the microfluidic device T-SENSOR will be fabricated and characterized.

The basic features for this device are:

$$w = 2mm$$
$$h = 60\mu m$$
$$L = 3cm$$

This dimensions have been chosen because the device will be fabricated using a hand-made technique, and the features must be easy to handle using regular tools such as scalpels or rulers.

Even being big features in microfluidics, because of the height is lower than 100μm we can ensure that the flux will be laminar. The equations (2.3) and (2.4) allows us to calculate the Reynolds number.

w	*2000 μm*
h	*60 μm*
Re	$\frac{\bar{v}d}{\upsilon}$
d	$\frac{4A}{P} = 4\frac{h \cdot w}{2(h+w)}$
υ_{water}	$1.13 \cdot 10^{-6}\ m^2/s$

Table 4.6 Parameters to calculate the Reynolds number

It has been assumed that the channels have a rectangular cross-sectional shape and that the fluids used in this scenario are dissolutions in water.

Following the specifications in the Table 4.6 the Reynolds number will be:

$$\mathrm{Re} = 2\frac{h\cdot w}{h+w}\cdot\frac{\bar{v}}{\upsilon}\approx 2w\cdot\frac{\bar{v}}{\upsilon} \qquad (4.99)$$

As it was said in the **Chapter 2** values below 2300 of the Reynolds number ensure laminar flow. The velocity needed to comply this limit is:

$$\mathrm{Re} = 2\frac{h\cdot w}{h+w}\cdot\frac{\bar{v}}{\upsilon}\approx 2w\cdot\frac{\bar{v}}{\upsilon}$$
$$\mathrm{Re} < 2300 \Leftrightarrow \bar{v} < \frac{2300\cdot\upsilon}{2w} = 21.7\,{}^{m}\!/_{s} = 78.12\,{}^{km}\!/_{h} \qquad (4.100)$$

This is a huge velocity in terms of microfluidics, so we can state that the system's dimensions ensure laminar flow inside the device.

Some drawing software can be used to design the device's layout. Corel DrawX4 was used in order to achieve these layouts.

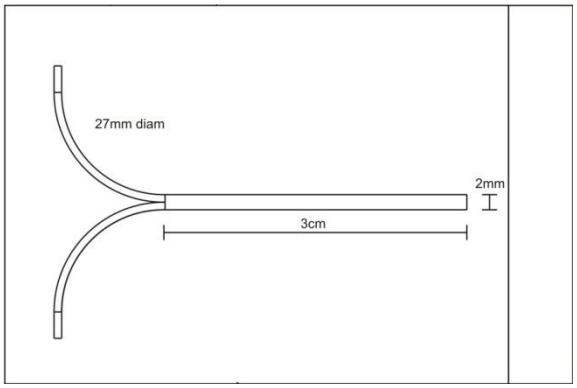

Fig. 4.43 Layout T-Sensor

4.3 Fabrication

Usually the fabrication of microfluidic devices is limited to people who have access to a clean room that allows the fabrication with features of micrometers. For the features needed in the device presented in Fig. 4.43, a much easier technique can be used without the need of accessing to the clean room. The soft lithography techniques are base on the replication of masters in some curable polymers. How this master is fabricated is up to the designer. The adhesive tape can be used as a powerful tool in the fabrication of masters for microfluidic applications due to its features.

Scotch tape presents a uniform height of ~ 60 μm, so cutting this tape following the shape of the device required will yield a relief structure completely useful to be replicated. As it has been demonstrated in the condition (4.100) the height that Scotch tape has ensures laminar flow inside the channels.

Next are detailed the all the steps in the fabrication of devices using the Scotch tape patterned method.

4.3.1 Required materials

One of the most important advantages of the master fabricated using Scotch tape is its low cost. This is due especially to two factors, firstly only bench-top tools are required for the fabrication of these masters, and secondly accessing to the clean room is not required.

The needed materials for the fabrication of microfluidic devices are presented below:

- Glass slides, pre-cleaned from Manufacturer (Fisher Scientific, 75mm x 50mm x 1mm, Cat. No. 12-550-C).
- Scotch tape (3M Scotch® Transparent Tape 600).
- Stainless steel Scalpel or surgical blade with (Feather Safety Razor Co., LTD, Cat. No. 2976#11).
- Polystyrene Petri dish (Fisher Scientific, 100mm x 15mm, Cat. No. 08-757-12).
- Oven or hot plate (to work at 65°C).
- Tweezers.
- Gloves (do not use latex gloves).
- PDMS silicone elastomer base and curing agent (Sylgard 184, Dow Corning). Heptane H-350-1 (Fisher Scientific, Cat. No. 102258).
- Plasma oxidazer (Harrick Plasma PDC-001).
- Isoproppyl Alcohol (Isopropanol), (Fisher Scientific, Cat. No. 67-63-6, Lot #: 102109).
- 1.22 mm diameter biopsy puncher (Harris Uni-Core, Prod #15074).

4.3.2 Fabrication process

Once the device's layout is designed, a piece of Scotch tape has to be attached on the top of a glass slide. Usually this thickness is around 60μm which is perfectly useful for microchannels designing. The height can be increased by the adhesion of more layers of tape, achieving larger dimensions always multiples of 60μm.

Fig. 4.44 Attaching the film of Scotch tape on the glass slide

Once done it, the glass slide has to be placed on the printed layout (with the attached piece of tape facing up) and fix it to the printout in order to avoid any movement. Then using a scalpel the tape on the glass can be cut following the shape indicated by the printed layout.

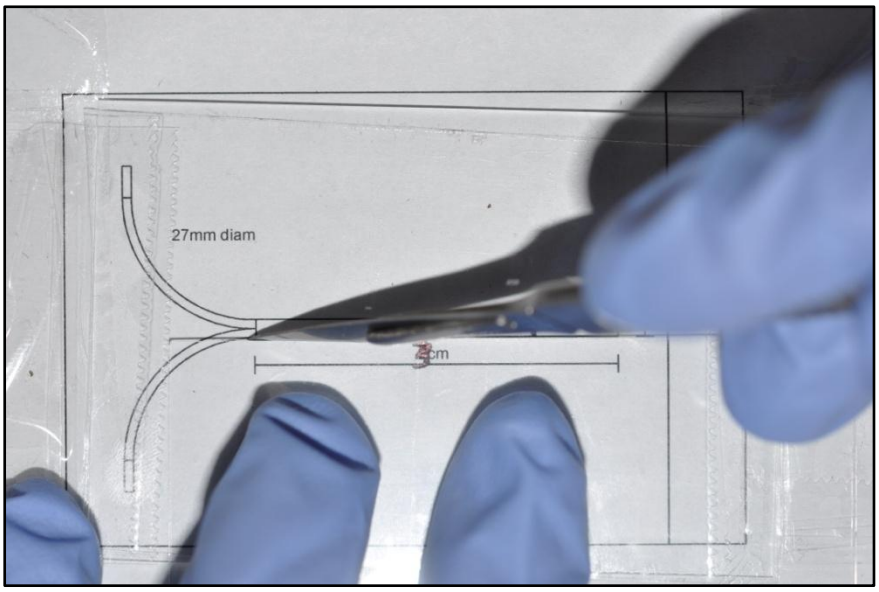

Fig. 4.45 Cutting the Scotch tape according with the layout

The next step is to take out the useless Scotch tape from the glass slide (all the tape except that in the layout of the microchannel) and clean the edges of the remained tape using isopropanol in order to remove the extra glue.

After that the glass slide with patterned Scotch tape has to be heated in oven at 65°C for 2 or 3 minutes that will provide a better adhesion of the Scotch tape to de glass

substrate. At this point the Scotch tape pattern fixed on the glass slide is ready to be used as a master for soft lithography uses.

Then mix the base and the curing PDMS components such as the manufacturer recommends (in this case 10 parts of base by 1 part of curing agent). Once the master is put in a petri dish the PDMS mixture is poured in the dish until it is totally covered.

PDMS has to be degassed in a vacuum chamber for at least 1 hour in order to remove all the air bubbles that can deform the device, and after that the petri dish can be placed in the oven at 65°C. After 1 hour the PDMS is totally cured and ready to be separated from the master.

Once the PDMS is cured, it should cut the slab containing the pattern using a scalpel. At this point the replica is ready to be peeled it off.

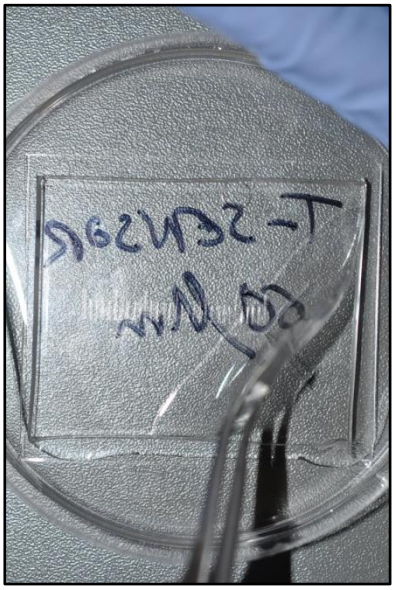

Fig. 4.46 Peeling of the PDMS from the master.

The next step is to punch holes in the replica for the inlets and the outlets of the device. Finally replica is sealed to a substrate (another clean glass slide) using an oxygen plasma oxidizer.

This sealing process is based in two steps, first the oxidation of the substrate by introducing the glass slide into the plasma oxidizer (with the surface that will be sealed to the replica facing up) at maximum power for 3 minutes. Then the PDMS replica has to be placed into the plasma oxidizer (with the surface that will be sealed to the glass substrate facing up) with the glass slide for 3 minutes more. At the end, the glass slide is exposed to the plasma for 6 minutes while the PDMS replica is exposed only for 3 minutes. After that putting the two faces in contact produce a chemical reaction that

makes a covalent union between the glass and the PDMS yielding an irreversible bounding between them.

The last step is heating the device in the oven at 65°C for ten minutes to finalize the adhesion.

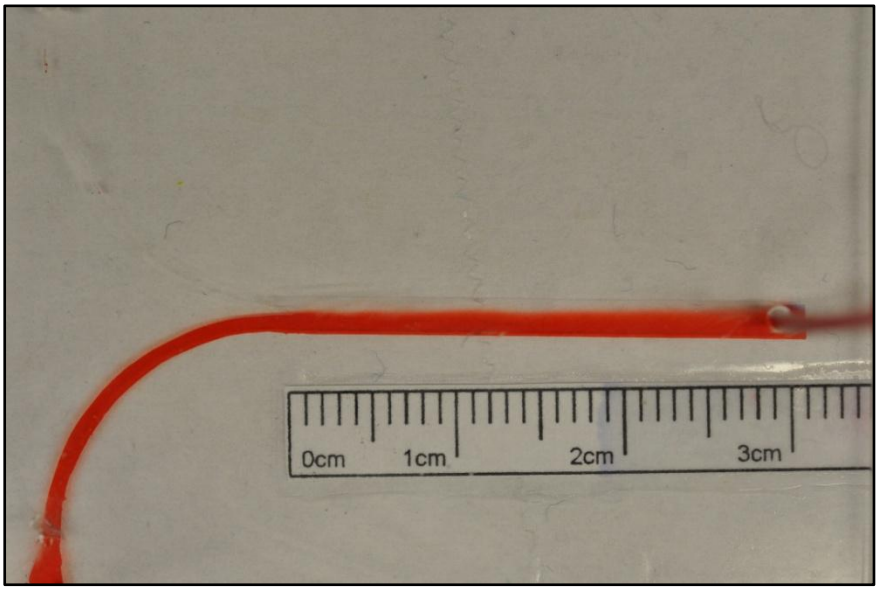

Fig. 4.47 T-Sensor filled with DI water and diluted red ink.

The figure Fig. 4.47 shows the behavior of a T-Sensor fabricated using the Scotch tape patterned method. It is possible to appreciate the laminar flow in the main channel and how the interdiffusion zone increases along the channel.

4.4 Characterization

The design and the fabrication of a T-SENSOR has been presented already, at this point is time to characterize the behavior of this microfluidic device. As it was said before the diffusion of molecules between streams may be observed through the downstream direction.

Two different devices will be fabricated with the same features except the thickness of the channels, and the same fluid will be infused with the same flow rate in each one. In one case the thickness will be 60 μm in the other case the thickness will be 120 μm. According to the theory more diffusion is expected for the system with lower fluid velocity, which is the device with higher thickness if the flow rate is the same for the two cases. This is because the mean velocity in the microchannel is:

$$\overline{V} = \frac{Q}{A} \qquad (4.101)$$

So, as soon as the cross section area increases the mean velocity decreases, and it means that the diffusion zone grows because the molecules have more time to diffuse.

Then if the fluids are colored, the interdiffusion zone is visible, and it can be determined.

The most important characteristics for the systems are presented in the next table:

	Device 1	***Device2***
w *(width)*	*2 mm*	*2 mm*
h *(height)*	*60 µm*	*120 µm*
L *(Longitude)*	*3 cm*	*3 cm*
Q *(Flow Rate)*	*20 nL/s*	*20 nL/s*
V *(Velocity)*	*166.66 µm/s*	*83.33 µm/s*

Table 4.7 T-Sensor features

Using a syringe pump, 2 fluids can be infused at the same time. In this experiment were used as fluids, a dissolution of red and blue ink in DI water, that produced and interdiffusion zone of black color clearly differentiated.

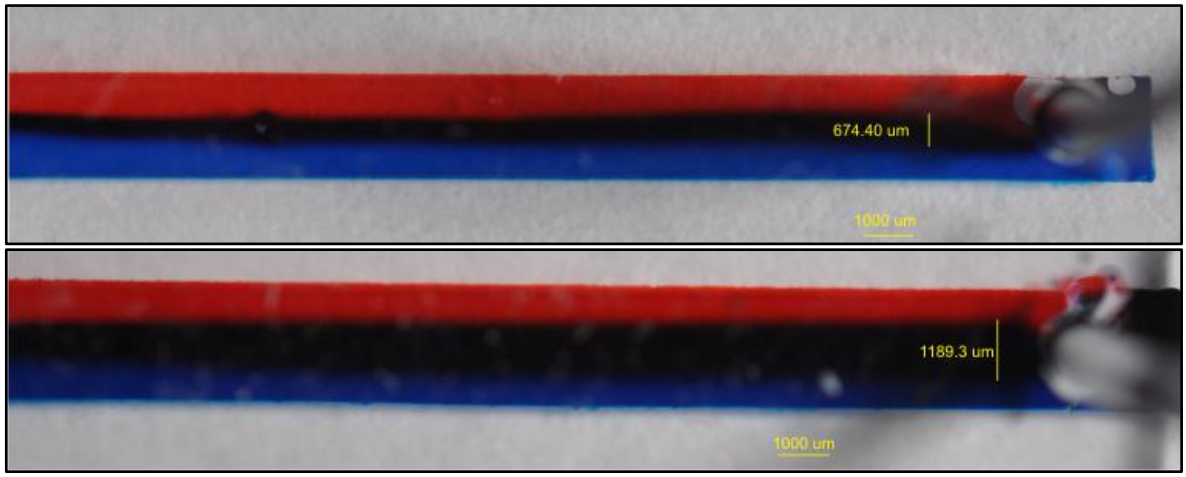

Fig. 4.48 On the top a T-Sensor with height of 60µm filled with red and blue ink. Its interdiffusion zone is 674.40µm. On the bottom a T-Sensor with height of 120µm filled with red and blue ink. Its interdiffusion zone is 1189.30µm.

The results in the figure Fig. 4.48 agree with the hypothetical results expected, the interdiffusion distance is almost double for the device with higher thickness. For low velocities the molecules can diffuse for more time, but the goal now is to know how the concentration of molecules is distributed along the main channel.

In a first approximation we suppose at the beginning (when the two fluids meet) there is maximum concentration of particles in one channel and minimum concentration in the other, yielding a gradient of concentration. Then, as soon as the particles flow downstream the two fluid mixes until a uniform concentration in the interdiffusion direction is achieved. It is possible to find out the concentration profile across the interdiffusion zone by optical monitorization along the main channel.

In order to characterize these concentration profiles, a simple inspection does not enough. The use of a microscope is needed to achieve more detailed images. The experiment consists in the observation of the interdiffusion zone in a T-Sensor introducing DI water in one inlet and a dissolution of fluorescein disodium 1Mm with DI water in the other. Fluorescein is a molecule commonly used in microscopy that reacts to ultraviolet light making it visible. The molecules of fluorescein can be detected under the microscopy, and pictures at different points downstream can be taken at microscopic scale. Applying some image processes to these pictures it is possible to extract the concentration information of each one.

The proportion elected for this dissolution was made after the study of the fluorescence in eight different samples using different proportions. The final proportion elected was 16:1 (in 16 parts of dissolution 1 is fluorescein) according with the best results observed in the microscope.

The lent with minimum augment in the microscope was 4x. For this reason the width of the cannel cannot be bigger than 1mm if we can see the whole channel only in one picture. In order to solve this issue a device with 1mm width was fabricated.

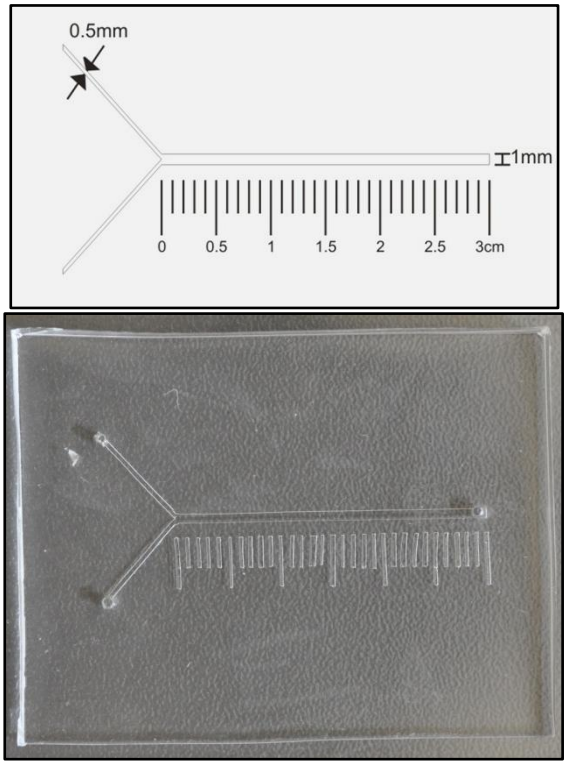

Fig. 4.49 On the top the layout for the T-Sensor. On the bottom the T-Sensor fabricated using the Scotch tape patterned method. The reason for which the inlets do not have a curved shape is for the complication in cutting this pattern of Scotch tape when the width is less than 1mm.

$$w = 1mm$$
$$h = 120\mu m$$
$$L = 3cm$$

The composition for the experiment was a syringe-pump with two 10mL syringe connected by 1.22 mm diameter polyethylene tubes to the T-Sensor. For observe the interdiffusion zone the microscope Nikon Eclipse Ti was used. The lent used is Nikon Plan Flour 4x/0.13 and to be able to see the fluorescein flowing through the channel a fluorescent lamp was needed. The lamp was the Nikon Intensilight C-HGFIE. The images were acquired by the computer using de video camera CoolSnap HQ2.

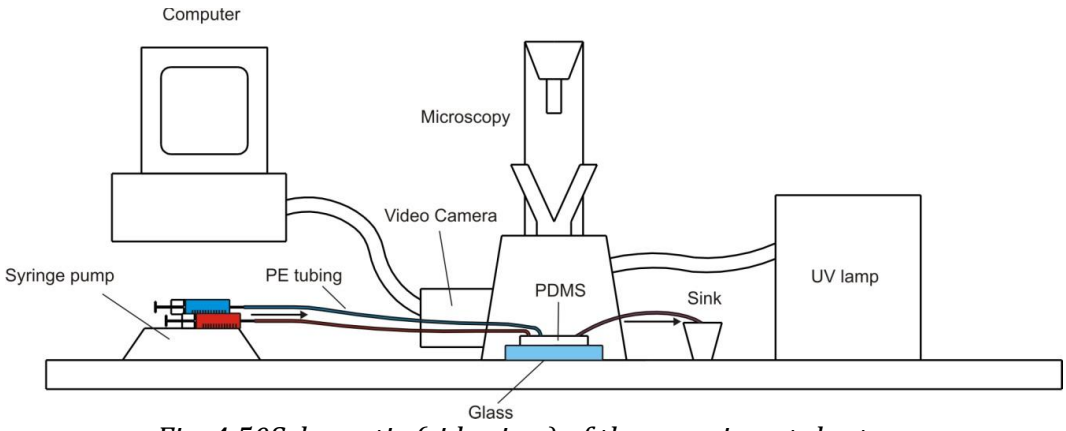

Fig. 4.50Schematic (side view) of the experimental setup.

Under this conditions the fluid were infused into the T-Sensor for different flow rates in order to find which one gave a better images of the interdiffusion zone.

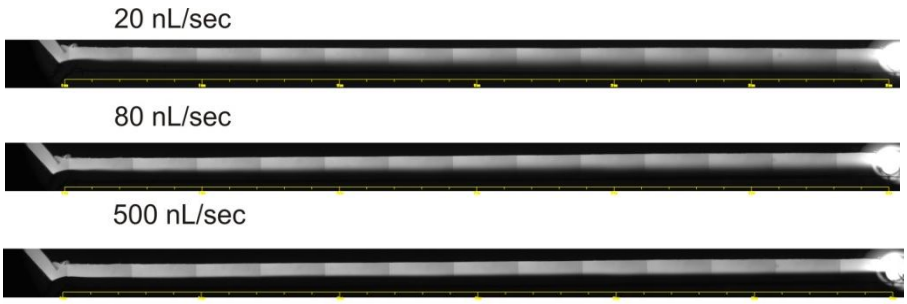

Fig. 4.51 T-Sensor infused with DI water and Fluorescein Disodium diluted in DI water with the proportion 16:1 for different flow rates. The images were taken using the microscope Nikon Eclipse Ti with the lent 4x, a fluorescent lamp with filter TRI. The images were taken with an exposure time of 60ms. The temperature in the room when the images were taken was 17°C

In the figure Fig. 4.51 are presented the pictures taken for three different flow rates. The white color shows the molecules of fluorescein, and it is easy to see how they diffuse along the interdiffusion direction. The image on the top (at 20 nL/s) provides the most

clear interdiffusion zone, and it was selected to be processed for obtaining the concentration profiles at different points of the main channel.

4.4.1 Data acquisition and image processing

The image at 20nL/s was divided in 6 different JPEG images of 1mm width each at the positions 0, 5, 10, 15, 20, 25 and 30mm using Adobe Photoshop.

With MATLAB R2009b 10 randomly-distributed vertical lines [20] were chosen per each image and the pixel intensity light was extracted for each vertical line of pixels. The sum average of these lines provides the light intensity profile for each image which is proportional to the concentration profile.

In order to normalize the curve, we subtracted the minimum value of intensity and then we divided the intensity of each pixel by the maximum intensity value.

In the **Appendix C** the code written for do this is shown.

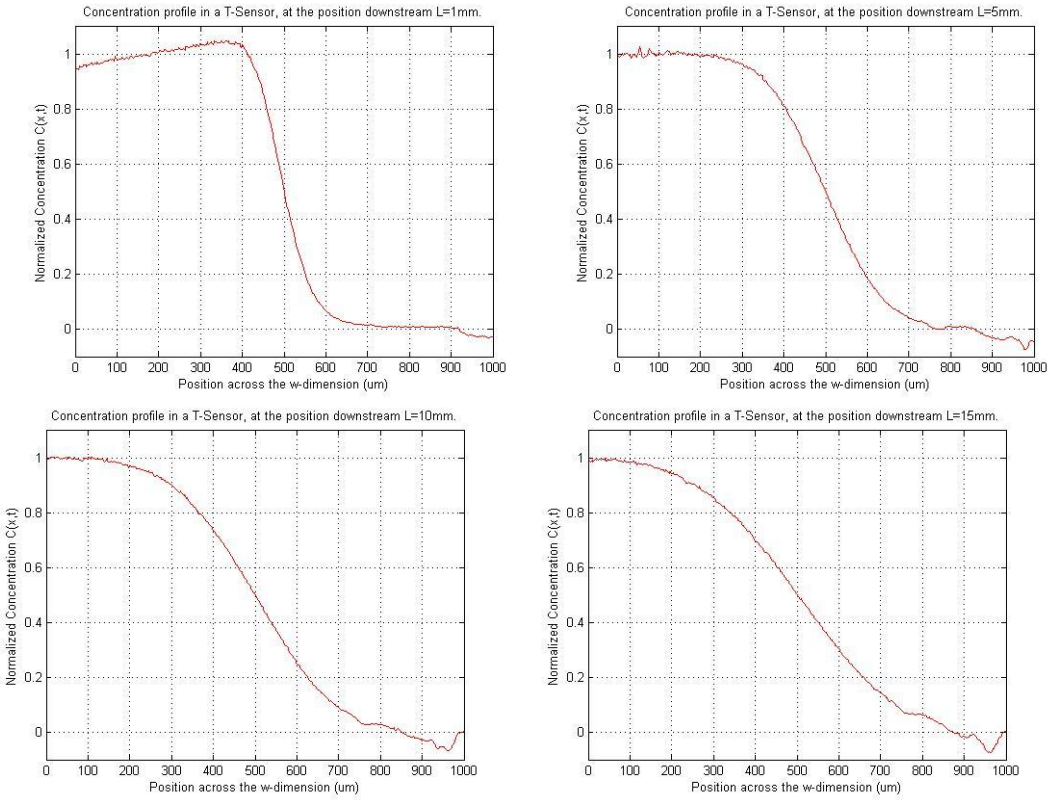

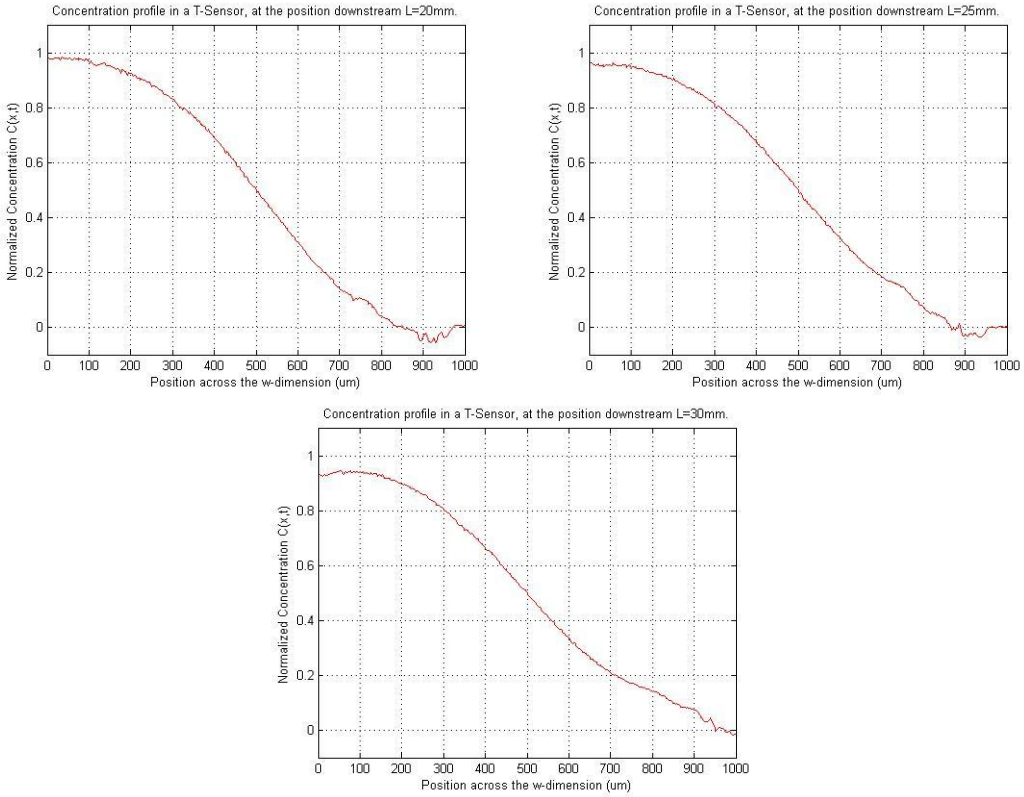

Fig. 4.52 Normalized concentration profiles in a T-Sensor of fluorescein disodium at different points downstream. Flow rate of 20 nL/s.

The image Fig. 4.52 shows a set of images that provide the concentration profile across the interdiffusion direction. We can see how as soon as the concentration is obtained in further positions downstream the tendency is to achieve a uniform concentration along the channel.

The persistent error at the end of the curve, when the position is around 900μm belongs from the shadows in the picture taken with the microscope.

4.5 Results and Discussions

The fabrication of microfluidic devices using a very simple and inexpensive technique has been presented. As we have demonstrated this technique is completely useful for the fabrication of micro-devices with width up to 300μm. For devices below 1mm it is possible to use magnificent glasses in the fabrication process, but when the features are smaller than 300μm this technique is not suitable.

By the realization of two different experiments using three different devices we have demonstrate that this method is completely useful, and it is much easier, faster and inexpensive that all those methods that need the use of a clean room for the fabrication of the master.

One of the most important applications of the T-SENSOR is the calculus of the diffusivity of molecules. In these cases what it is done is the extraction of the

concentration profiles of these molecules such as it has been done before. After that a simulator can be used to find out which is the diffusion coefficient that fits better with the experimental results.

In the following chapters a simulator of the diffusion will be programmed, and the results that we have got before will be use to verify the reliability of that simulator.

The T-SENSOR is a microfluidic device that allows the study of the diffusion of particles. It may provide us a better understanding of this phenomenon, and utilize this knowledge in the study of molecular communication based on diffusion processes.

5 SIMULATION OF A T-SENSOR

As it was commented in previous section, the analytical solution of molecular communication systems presents instability issues. For this reasons a simulator of this process has to be programmed.

In this chapter firstly we discuss about numerical methods and specifically we present the method of "Finite Differences". Using this method we find a simulator able to predict the theoretical behavior of a T-Sensor. This simulator is done in 1 and 2 dimensions and is validated using the experimental data got in Chapter 4.

Using this simulator as model, in future sections the molecular communication simulator is programmed.

5.1 Introduction

Previously the T-Sensor has been presented as the perfect device to study the diffusion of particles in fluids.

A simulator that characterizes the theoretic behavior of this device may help in a better understanding of the diffusion process. As it has seen in previous chapters a closed analytical solution for the diffusion equation is hard to find and in the most cases is not possible to obtain. For this reason it is simpler to use a simulator based on numerical methods which provides an approximation as reliable as it is required of the real solution.

Two streams traveling in the main channel of a T-Sensor flow in a strictly laminar regime, yielding a gradient of concentration between fluids and starting the diffusion process of particles. The diffusion between two fluids which flow side by side with laminar flow is given by the equation of continuity for incompressible fluid (2.22):

$$\frac{\partial C\left(\bar{x},t\right)}{\partial t}+\bar{v}\cdot\nabla C\left(\bar{x},t\right)=D\cdot\nabla^2 C\left(\bar{x},t\right)+R\left(\bar{x},t\right)$$

Specifying this equation in a three dimensional space, the equation becomes:

$$\frac{\partial C}{\partial t}+\left(\bar{v}_x\frac{\partial C}{\partial x}+\bar{v}_y\frac{\partial C}{\partial y}+\bar{v}_z\frac{\partial C}{\partial z}\right)=D\left(\frac{\partial^2 C}{\partial x^2}+\frac{\partial^2 C}{\partial y^2}+\frac{\partial^2 C}{\partial z^2}\right)+R\left(\bar{x},t\right) \quad (5.102)$$

Where the coordinate axis are as in Fig. 4.42. The region where this equation is defined is:

$$0\le x\le w$$
$$0\le y\le L$$
$$0\le z\le h$$

In a T-Sensor we can assume laminar flow because of the low Reynolds numbers complies, therefore there is only diffusion in the directions $\vec{x}$ and $\vec{z}$. All entry effects are ignored so it assumes that the fluids velocities in the directions $\vec{x}$ and $\vec{z}$ directions have to be zero, the fluid is only flowing downstream. Finally this simulation does not include any chemical reaction.

Application of these assumptions leads to [25, 27]:

$$\frac{\partial C}{\partial t}=V_y\frac{\partial C}{\partial y}=D\left(\frac{\partial^2 C}{\partial x^2}+\frac{\partial^2 C}{\partial z^2}\right) \quad (5.103)$$

This equation is a three dimensional parabolic differential equation and it can be solved a numerical method known as "finite differences".

5.2 Simulation Using Numerical Methods

The science and the technology describe real phenomena by mathematical models. The study of these models allows large in-depth knowledge of the phenomenon as well as its future evolution. Unfortunately, applying classic analytical methods to obtain these mathematical models is not always possible. This can be due to different reasons:

They do not fit to the particular model. The analytical solution is so complicated, and makes impossible further interpretations. Their application is excessively complicated. It does not exist any analytical method able to provide solutions to the problem.

In these cases numerical methods are useful. They provide approximate solutions which are always numerical. These methods depend on a very large number of calculi, and their use requires computational devices.

In the field of partial differential equations one of the most well known numerical methods is the "Finite Difference Method".

5.2.1 Finite difference method

In mathematics, finite difference methods are numerical methods approximating the solutions to differential equations using finite differences equations to approximate derivatives.

The first derivative of a function is defined by:

$$f'(x) = \lim_{\varepsilon \to 0} \frac{f(a+\varepsilon) - f(a)}{\varepsilon} \qquad (5.104)$$

Then a reasonable approximation for that derivative when ε has a small value would be:

$$f'(x) \approx \frac{f(a+\varepsilon) - f(a)}{\varepsilon} \qquad (5.105)$$

Using this and similar formula to replace derivative expressions in differential equations, it is possible to approximate their solutions without the need for calculus.

The main idea for this method is discretize the continuous domain in a finite number of points, building a two dimensional mesh.

Being $f(x,t)$ a function defined in the domain $0 \le x \le X$ and $0 \le t \le T$, this function can be approximated in a limited number of points discretizating its domain.

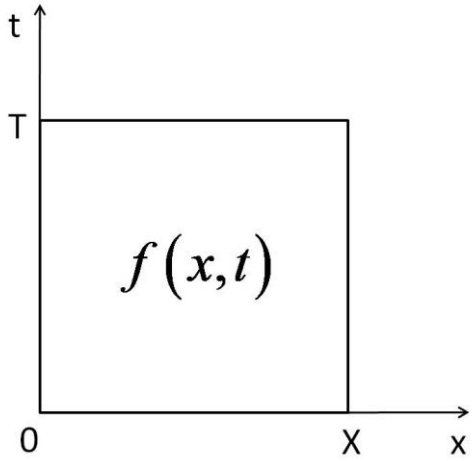

Fig. 5.53 Function f(x,t) defined only in a region.

The region $0 \le x \le X$ becomes a group of L discrete points $x_l \to l = 0,1,2,3,...,L-1$ separated a distance dx each other, with $x_0 = 0$ and $x_{L-1} = X$. The same reasoning applies for the region $0 \le t \le T$, obtaining M discrete points separated dt in the t-dimension.

The built mesh has a size of L x M points which specifies the two dimensional region where the function applies. This method is very useful to calculate an approximation of the real solution of systems defined by differential equations. The quality of this approximation depends on the space between those points.

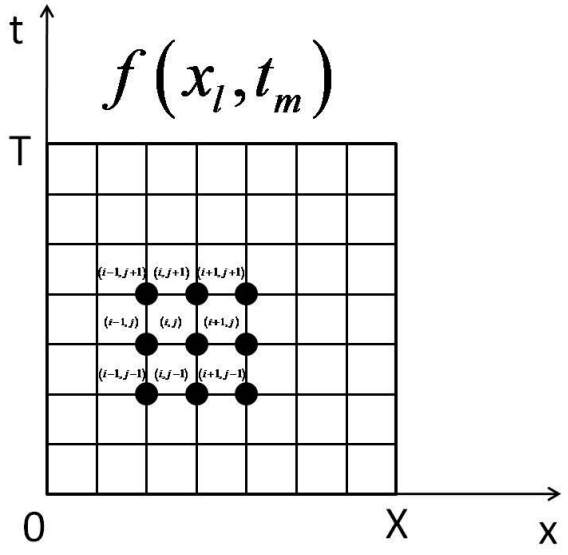

Fig. 5.54 Time-Spatial mesh for finite difference

Using the Taylor's series it is possible to say:

$$f(x_{i+1}) = f(x_i + dx) = f_i + f_i' \cdot dx + f_i'' \cdot \frac{dx^2}{2!} + f_i''' \cdot \frac{dx^3}{3!} + f_i'''' \cdot \frac{dx^4}{4!} + ... \qquad (5.106)$$

$$f(x_{i-1}) = f(x_i - dx) = f_i - f_i' \cdot dx + f_i'' \cdot \frac{dx^2}{2!} - f_i''' \cdot \frac{dx^3}{3!} + f_i'''' \cdot \frac{dx^4}{4!} + \ldots \qquad (5.107)$$

Now rearranging these formulas they become:

$$f_i' = \left.\frac{\partial f}{\partial x}\right|_i = \frac{f_{i+1} - f_i}{dx} - \frac{dx}{2} \cdot f_i'' + \ldots \qquad (5.108)$$

$$f_i' = \left.\frac{\partial f}{\partial x}\right|_i = \frac{f_i - f_{i-1}}{dx} + \frac{dx}{2} \cdot f_i'' + \ldots \qquad (5.109)$$

These equations are called Forward and Backward approximation respectively. The error in both cases has an order of $o(dx)$.

In order to reduce the order of the error we can use more terms from the Taylors series approximation. Subtracting the equations (5.106) and (5.107), and then isolating the first order derivative, the approximation becomes:

$$f_i' = \left.\frac{\partial f}{\partial x}\right|_i = \frac{f_{i+1} - f_{i-1}}{2 \cdot dx} - \frac{dx^2}{3!} \cdot f_i''' + \ldots \qquad (5.110)$$

This equation is called the central approximation and its errors is of order $o(dx^2)$. A better approximation is obtained comparing with the forward and the backward approximations.

The next step is to find the approximation for the second order derivative. Adding the equations (5.106) and (5.107) and arranging the result we can obtain:

$$f_i'' = \left.\frac{\partial^2 f}{\partial x^2}\right|_i = \frac{f_{i+1} - 2 \cdot f_i + f_{i-1}}{dx^2} - \frac{2 \cdot dx^2}{4!} \cdot f_i'''' + \ldots \qquad (5.111)$$

This is the approximation for the second derivative, and its error has an order of $o(dx^2)$.

In resume the approximations for the first and second derivative are the following:

	Approximation	Error
Forward approximation	$\left.\frac{\partial f}{\partial x}\right\|_i \approx \frac{f_{i+1} - f_i}{dx}$	$o(dx)$
Backward approximation	$\left.\frac{\partial f}{\partial x}\right\|_i \approx \frac{f_i - f_{i-1}}{dx}$	$o(dx)$
Central approximation	$\left.\frac{\partial f}{\partial x}\right\|_i \approx \frac{f_{i+1} - f_{i-1}}{2 \cdot dx}$	$o(dx^2)$
Second order Derivative	$\left.\frac{\partial^2 f}{\partial x^2}\right\|_i \approx \frac{f_{i+1} - 2 \cdot f_i + f_{i-1}}{dx^2}$	$o(dx^2)$

Table 5.8 Resume of finite difference approximations in the x-dimension

The same reasoning applies in order to obtain the approximations for the derivatives in the t-dimension.

	Approximation	Error
Forward approximation	$\left.\frac{\partial f}{\partial t}\right\|_j \approx \frac{f_{j+1} - f_j}{dt}$	$o(dt)$
Backward approximation	$\left.\frac{\partial f}{\partial t}\right\|_j \approx \frac{f_j - f_{j-1}}{dt}$	$o(dt)$
Central approximation	$\left.\frac{\partial f}{\partial t}\right\|_j \approx \frac{f_{j+1} - f_{j-1}}{2 \cdot dt}$	$o(dt^2)$

Table 5.9 Resume of finite difference approximations in the t-dimension

Approximations presented in Table 5.8 and Table 5.9 can substitute the derivatives in differential equations. That transforms these deferential equations into simple algebraic equations which are easily computed. Many mathematical models of real phenomenon based on partial differential equations such as the behavior of a steel sheet with a uniform charge q, the conductive heat transport, or the movement of particles by Brownian motion can be computed using finite differences.

5.3 1-Dimensional Simulation

A one dimensional model of the T-Sensor would be:

$$\frac{\partial C}{\partial t} = D \frac{\partial^2 C}{\partial x^2} \qquad (5.112)$$

Hence, the equation (5.112) can be expressed using the finite differences method in a discrete environment. To do this, the derivatives are substituted by its approximations presented in Table 5.8 and Table 5.9 thus obtaining [28]:

$$\frac{C_i^{j+1}-C_i^j}{dt}=D\cdot\left(\frac{C_{i+1}^j-2\cdot C_i^j+C_{i-1}^j}{dx^2}\right) \qquad (5.113)$$

And arranging the equation (5.113) and isolating the term n+1:

$$C_i^{j+1}=\frac{D\cdot dt}{dx^2}\cdot\left(C_{i+1}^j-2\cdot C_i^j+C_{i-1}^j\right)+C_i^j \qquad (5.114)$$

The index i determines the position dependence and the index j determines the temporal point. The equation (5.114) shows that the value of the concentration in the instant $j+1$ is fixed by the value of the concentration in the instant before j and by its neighbor points. So it is possible to solve the diffusion equation by iteration using mathematical software as MATLAB.

The behavior of this device is easily described using the diffusion equation. The only point needed at this time is to define the boundary and the initial conditions in this system.

The no flux boundary condition applies in both walls. The T-Sensor is made using PDMS which is not permeable to liquids and as a result, the flux of fluids will always be zero at the walls. As initial condition the concentration at the beginning in one channel is maximum and in the other channel minimum. The boundary conditions prohibit the flux at the walls:

- **Initial Condition:**

$$\begin{aligned} C(x,t=0)\big|_{x\in(0,\frac{w}{2})}&=1\\ C(x,t=0)\big|_{x\in(\frac{w}{2},w)}&=0 \end{aligned} \qquad (5.115)$$

- **Boundary Conditions:**

$$\left.\frac{\partial C(x=0,t)}{\partial x}\right|_{t\geq 0}=0 \qquad (5.116)$$

$$\left.\frac{\partial C(x=w,t)}{\partial x}\right|_{t\geq 0}=0 \qquad (5.117)$$

Using the finite difference method these two equations become like:

$$\left.\frac{\partial C(x=0,t)}{\partial x}\right|_{t\geq 0} \approx \frac{C_2^j - C_1^j}{dx} = 0 \rightarrow C_2^j = C_1^j \qquad (5.118)$$

$$\left.\frac{\partial C(x=w,t)}{\partial x}\right|_{t\geq 0} \approx \frac{C_w^j - C_{w-1}^j}{dx} = 0 \rightarrow C_w^j = C_{w-1}^j \qquad (5.119)$$

With these equations it is possible to program a simulator which will be able to calculate a non closed solution as good as we want. The only limitation is the stability condition (5.124).

A T-Sensor simulator programmed by MATLAB R2009b is provided in the **Appendix A**.

The results obtained for a device with the following features is presented below.

***w** (width)*	*550 μm*
***L** (Longitude)*	*3 cm*
***D** (Diffusion Constant)*	*800 μm2/s*
***V** (Velocity)*	*333.33 μm/s*

Table 5.10 T-Sensor features

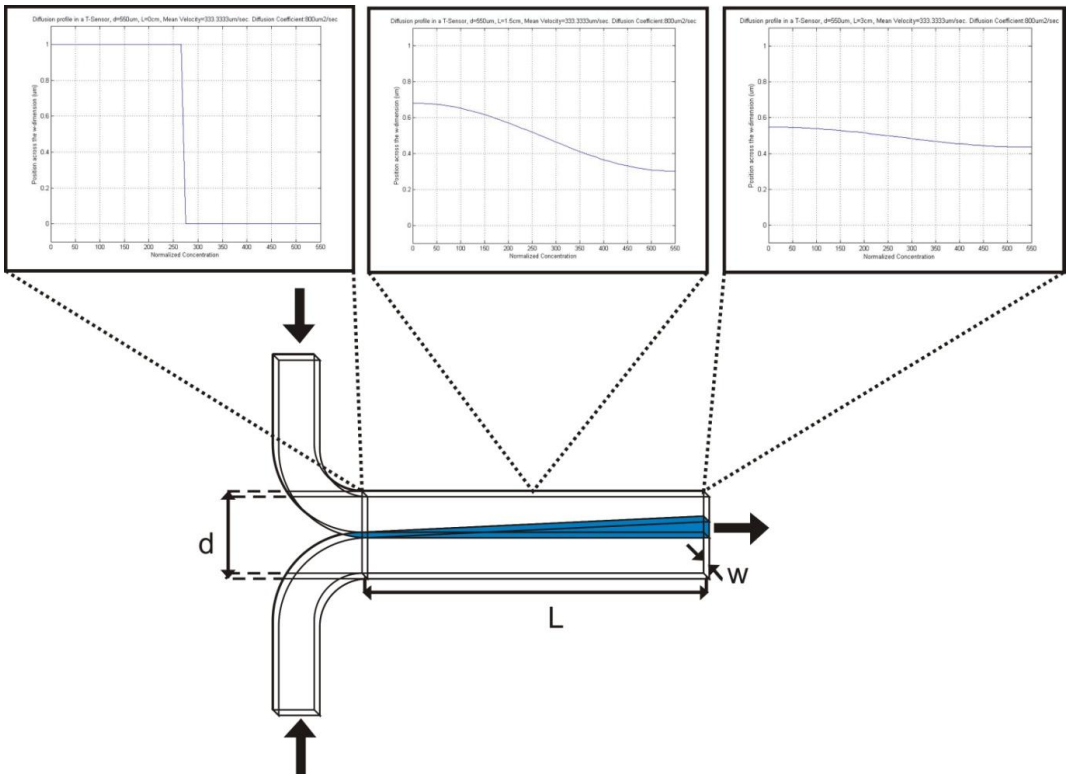

Fig. 5.55 Concentration across the w-dimension in a T-Sensor at distances 0cm, 1.5cm and 3cm downstream.

As it was expected at the beginning the concentration in the inlet 1 is maximum and the concentration in the inlet 2 is minimum. If we move downstream, the molecules start to diffuse across the w-dimension. This is reflected in the image because the concentration in the channel 1 decreases in the same way that it does the channel 2. This is the consequence of the boundary conditions, since the PDMS in not permeable, all the molecules must remain inside the device, so the global concentration of particles have to be constant.

At the end if the device was large enough the concentration would be 0.5 in every point across the w-dimension. This would mean that it would have been perfect mixing between the two fluids.

The diffusion of particles depends also on the velocity of the fluid where the molecules are suspended.

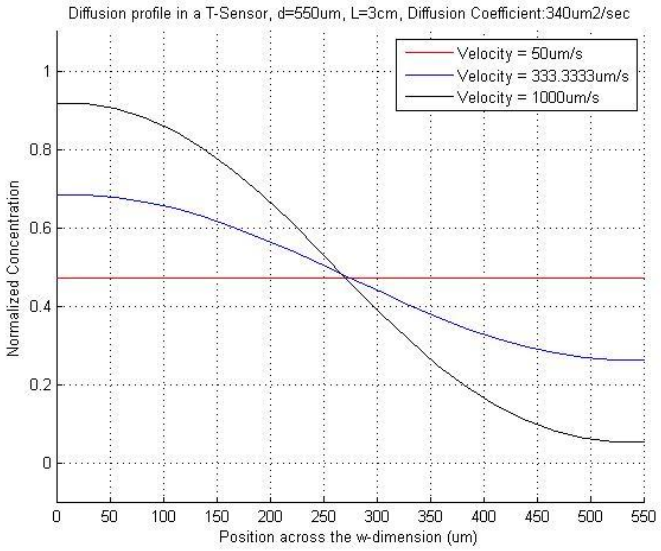

Fig. 5.56 Concentration across the w-dimension in a T-Sensor at 3cm downstream for three different fluid velocities. w=550μm, L=3cm, D=340μm²/s.

For faster velocities the molecules cross the T-Sensor in less time, what means that they cannot diffuse large zones. On the other hand for low velocities those molecules are flowing in the device for more time so they have can diffuse further distances.

In the figure Fig. 5.56 the concentration profile for a T-Sensor for three different velocities have been simulated. We assume that the particles have diffused a distance if the concentration in that point is at least the 40% of the initial bulk concentration, otherwise they have not. Using this threshold it states for a velocity of 1000μm/s the particles diffuse up to ~300μm, for 333.333 μm/s they diffuse up to ~330μm and for 50μm/s the particles have diffused completely.

Velocity(μm/s)	*Diffusion time(s)*	*Distance diffused(μm)*
1000	*30*	*~25*
333.333	*90*	*~55*
50	*600*	*225 (totally diffused)*

Table 5.11 Relationship between the diffusion time and the distance diffused depending on the fluid velocity.

The last parameter that controls the diffusion of molecules is the diffusivity. The diffusion coefficient gives an idea of how easy is for a molecule to move in a medium.

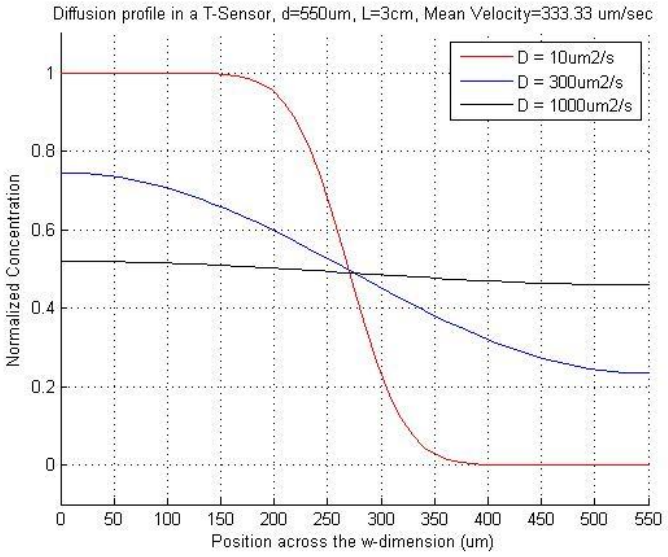

Fig. 5.57 Concentration across the w-dimension in a T-Sensor at 3cm downstream for three different diffusivities. w=550μm, L=3cm, V=333.33μm/s.

Diffusivity is a parameter that depends strongly on the size of the particle. Big molecules yield small values of diffusivity, because they are harder to move or they move slowly, while small particles have large diffusivities. In Fig. 5.57 for a very low value of the diffusion coefficient, the molecules have not diffused almost, while for larger values they diffuse further distances or even they achieve to diffuse completely.

The simulator provides the theoretical behavior of the T-Sensor according to the velocity of the fluid and the diffusivity of the particles.

5.3.1 Stability in finite difference 1-D

The approximation of real solutions using finite differences is a very simple an powerful tool. The only issue is this method may produce unstable solution under different situations.

Following the next theorem [28] for the finite difference method:

$$C_i^{j+1} = A \cdot C_{i+1}^j + B \cdot C_i^j + C \cdot C_{i-1}^j \qquad (5.120)$$

If an equation as (5.120) is obtained using finite difference, then the scheme is stable and the errors die out when A, B, and C are positive and $A+B+C \leq 1$. In the case above:

Taking $\alpha = \frac{D \cdot dt}{dx^2}$ then (5.114) can be written as:

$$C_i^{j+1} = \alpha \cdot C_{i+1}^j + (1-2\alpha) \cdot C_i^j + \alpha \cdot C_{i-1}^j \qquad (5.121)$$

And comparing with (5.120):

$$A = C = \alpha = \frac{D \cdot dt}{dx^2} \qquad (5.122)$$

$$B = 1-2\alpha = 1-2 \cdot \frac{D \cdot dt}{dx^2} \qquad (5.123)$$

Is easy to see that $A+B+C \leq 1$is always true:

$$\alpha + (1-2\alpha) + \alpha = 1$$

A and C are always positive constants, so the only term which affects in the stability is B.

$$B = 1-2\alpha \geq 0 \Leftrightarrow \alpha \leq \frac{1}{2}$$

$$\frac{D \cdot dt}{dx^2} \leq \frac{1}{2} \rightarrow dt \leq \frac{dx^2}{2 \cdot D} \qquad (5.124)$$

(5.124) is the stability condition to solve the diffusion equation using finite difference.

The practical explanation is that, given a spatial resolution and the velocity by which the molecules diffuse away, the temporal resolution has to be enough to "see" without mistake the evolution of all the particles.

5.4 2-Dimensional Simulation

A two dimension model of the T-Sensor is presented in the equation (5.103). This system is defined by a three dimensional grid which comprehend the two spatial dimension $\vec{x}$ and $\vec{z}$, ant the temporal dimension t.

Using the finite differences approximations in this model we are able to find an approximation for the two-dimensional diffusion equation:

$$\frac{C_{i,j}^{n+1}-C_{i,j}^{n}}{dt}=D\cdot\left(\frac{C_{i+1,j}^{n}-2\cdot C_{i,j}^{n}+C_{i-1,j}^{n}}{dx^{2}}+\frac{C_{i,j+1}^{n}-2\cdot C_{i,j}^{n}+C_{i,j-1}^{n}}{dz^{2}}\right) \qquad (5.125)$$

Where the indexes i and j describe the spatial position in the mesh and the index n indicates the temporal position in the grid.

Arranging this equation and isolating the component $n+1$ we obtain:

$$C_{i,j}^{n+1}=\frac{D\cdot dt}{dx^{2}}\cdot\left(C_{i+1,j}^{n}+C_{i-1,j}^{n}\right)+\frac{D\cdot dt}{dz^{2}}\cdot\left(C_{i,j+1}^{n}+C_{i,j-1}^{n}\right)+C_{i,j}^{n}\cdot\left(1-2\cdot\frac{D\cdot dt}{dx^{2}}-2\cdot\frac{D\cdot dt}{dz^{2}}\right) \qquad (5.126)$$

Once again it is possible to calculate the concentration in the next instant $n+1$ using the known values in the instant before n.

Since this model can be considered as an extension of the one dimensional situation, the boundary conditions and the initial condition must be the same. Maximum concentration in one channel and minimum in the other as initial condition; and no flux at the walls.

- **Initial Condition:**

$$\begin{aligned} &C(x,z,t=0)\big|_{\substack{x\in(0,\frac{w}{2})\\ z\in(0,h)}}=1\\ &C(x,z,t=0)\big|_{\substack{x\in(\frac{w}{2},w)\\ z\in(0,h)}}=0 \end{aligned} \qquad (5.127)$$

- **Boundary Conditions:**

$$\left.\frac{\partial C(x=0,\forall z,t)}{\partial x}\right|_{t\geq 0}=0 \qquad (5.128)$$

$$\left.\frac{\partial C(x=w,\forall z,t)}{\partial x}\right|_{t\geq 0}=0 \qquad (5.129)$$

$$\left.\frac{\partial C(\forall x,z=0,t)}{\partial z}\right|_{t\geq 0}=0 \qquad (5.130)$$

$$\left.\frac{\partial C(\forall x, z=h, t)}{\partial z}\right|_{t\geq 0} = 0 \qquad (5.131)$$

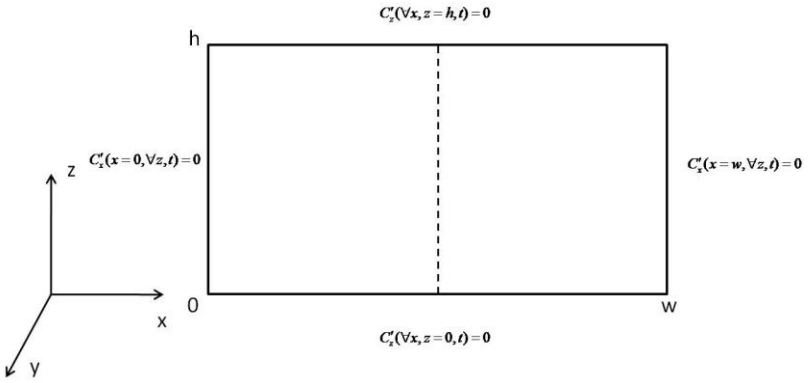

Fig. 5.58 Distribution of the boundary conditions in the device

Using finite difference the boundary conditions become:

$$\left.\frac{\partial C(x=0, \forall z, t)}{\partial x}\right|_{t\geq 0} = 0 \approx \frac{C_{2,j}^n - C_{1,j}^n}{dx} = 0 \rightarrow C_{2,j}^n = C_{1,j}^n \qquad (5.132)$$

$$\left.\frac{\partial C(x=w, \forall z, t)}{\partial x}\right|_{t\geq 0} = 0 \approx \frac{C_{w,j}^n - C_{w-1,j}^n}{dx} = 0 \rightarrow C_{w,j}^n = C_{w-1,j}^n \qquad (5.133)$$

$$\left.\frac{\partial C(\forall x, z=0, t)}{\partial y}\right|_{t\geq 0} = 0 \approx \frac{C_{i,2}^n - C_{i,1}^n}{dz} = 0 \rightarrow C_{i,2}^n = C_{i,1}^n \qquad (5.134)$$

$$\left.\frac{\partial C(\forall x, z=h, t)}{\partial y}\right|_{t\geq 0} = 0 \approx \frac{C_{i,h}^n - C_{i,h-1}^n}{dz} = 0 \rightarrow C_{i,h}^n = C_{i,h-1}^n \qquad (5.135)$$

A T-Sensor simulator programmed by MATLAB R2009b is provided in the **Appendix B**. The results obtained for a device characterized in the following table will be presented below.

***w** (width)*	*550 μm*
***h** (height)*	*60 μm*
***L** (Longitude)*	*3 mm*
***D** (Diffusion Constant)*	*320 μm2/s*
***Q** (Flow Rate)*	*11 nL/s*
***V** (Velocity)*	*333.33 μm/s*

Table 5.12 T-Sensor features

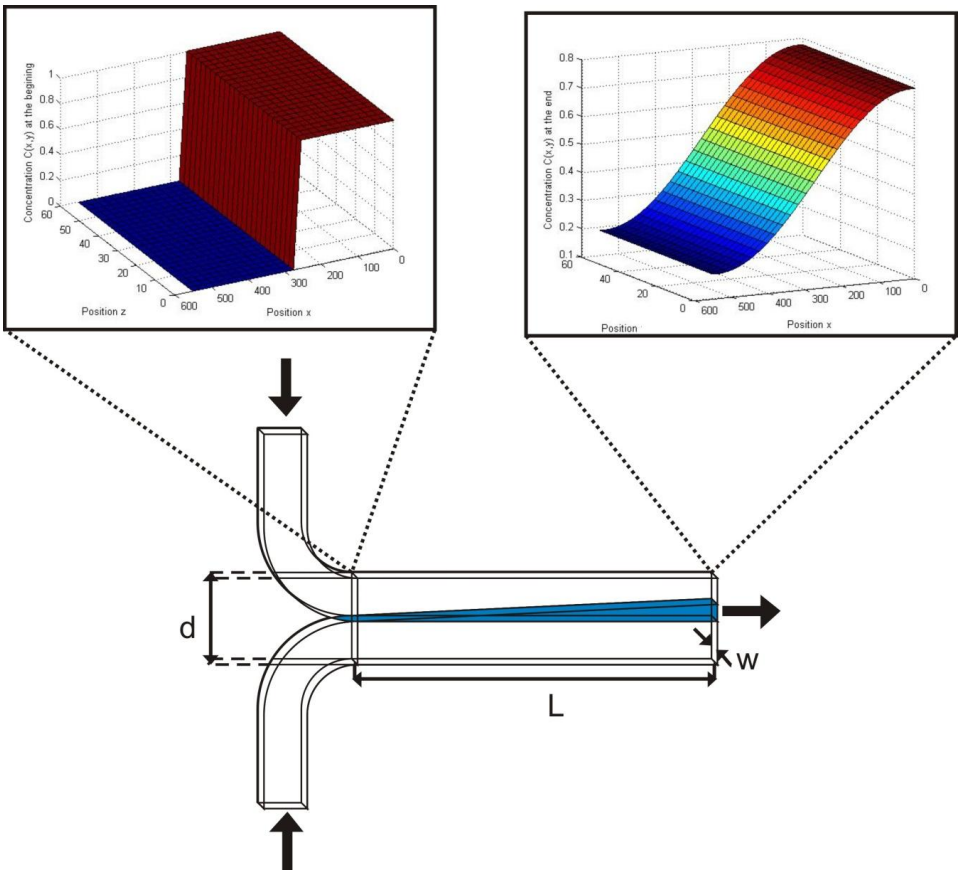

Fig. 5.59 Concentration profile across the w-dimension in a T-Sensor at distances 0cm and 3cm downstream.

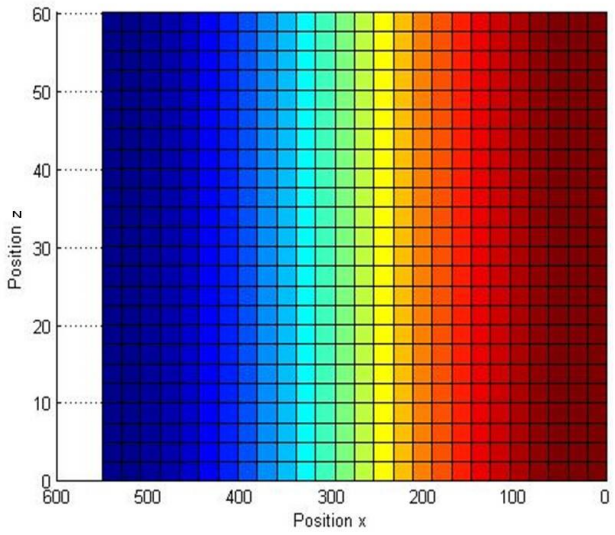

Fig. 5.60 X-Z view of the concentration in a T-Sensor at distance 3mm downstream.

It is easy to see the two-dimensional simulation is just an extension of the one-dimensional case. In a similar way to the one dimensional case, the concentration across the channel depends on the diffusivity and the velocity of the fluid.

5.4.1 Butterfly effect

Such as we can see in Fig. 5.60 the concentration across the z-dimension (the height) remains constant. Seem that the concentration is only a function of $C\left(\vec{x},t\right)$. This is not real. In this model has been considered the fluid's velocity as a constant in every point. The velocity profile for a pressure-driven flow in a rectangular duct device is parabolic such as it has been demonstrated before. It means that the velocity at the walls is almost 0 and maximum in the duct center. The profile follows a function as (2.12).

For channels with an aspect ratio, w/h, greater than 20, the velocity profile across w is unchanging for at least 90% of its length.

This velocity profile has an important effect in the diffusion inside the T-Sensor. Because the velocity is lower at the walls in the points closed to them the molecules move slower. It results that there is more time to diffuse in the w-direction. That means a molecule near to the top or bottom walls will diffuse more distance to the w-direction than another molecule situated in the center of the device. This effect is called "Butterfly Effect".

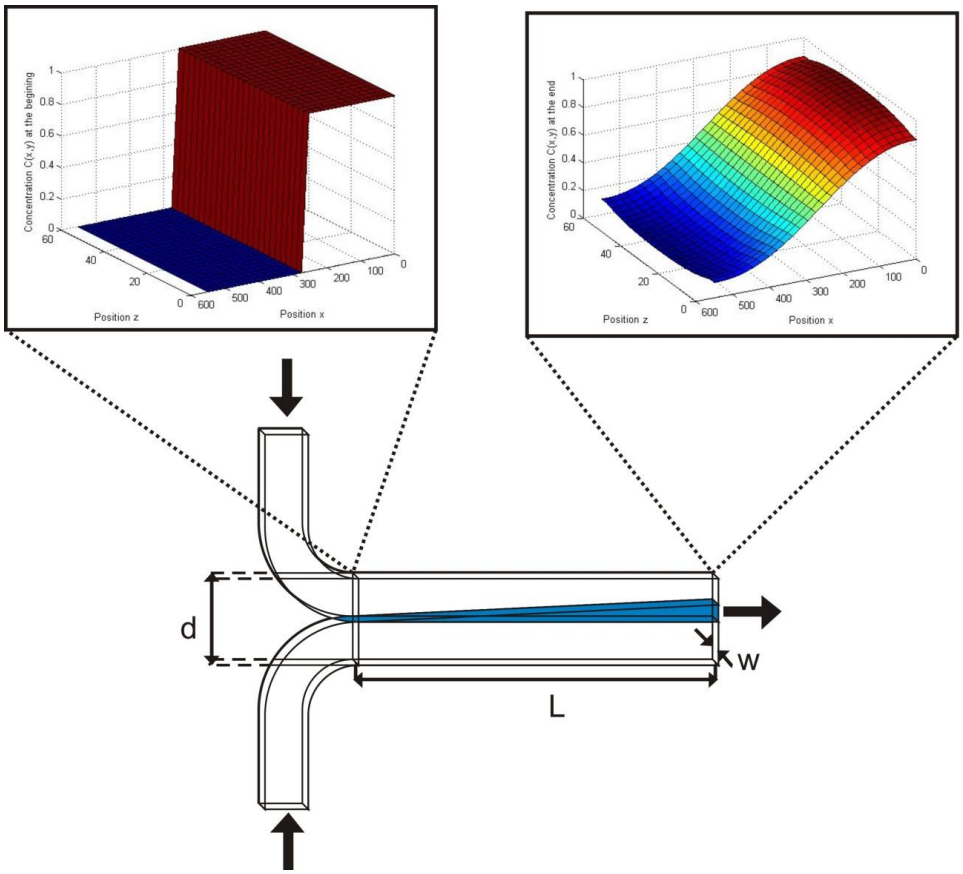

Fig. 5.61 Concentration profile across the w-dimension in a T-Sensor at distances 0cm and 3cm downstream.

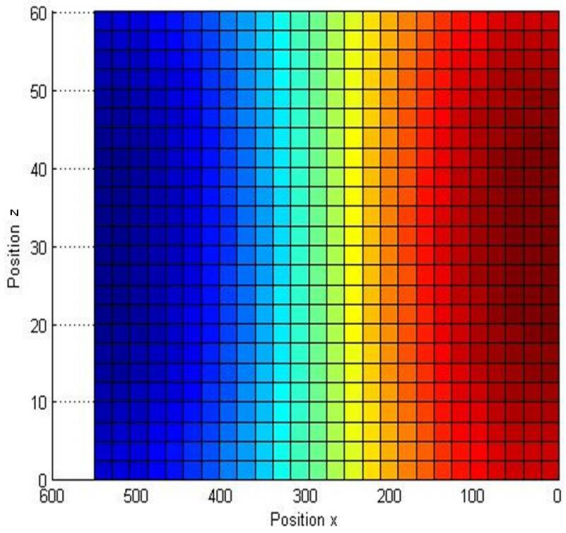

Fig. 5.62 X-Z view of the concentration in a T-Sensor at distance 3mm downstream. Using a parabolic velocity profile appears the "Butterfly Effect".

More diffusion occurs near the top (z=60μm) and bottom (z=0μm) surfaces, where the velocity is slower. This causes a shape like a butterfly in the interdiffusion zone and should occur when the mean interdiffusion distance across w is significantly less than the height, h.

5.4.2 Stability in finite difference 2-D

We will study the stability using the same way as it was done above. Extending the stability theorem for finite difference presented in the equation (5.120) to this new case the coefficients are [28]:

$$A = 2 \cdot \frac{D \cdot dt}{dx^2}$$
$$C = 2 \cdot \frac{D \cdot dt}{dy^2} \qquad (5.136)$$
$$B = 1 - 2 \cdot \frac{D \cdot dt}{dx^2} - 2 \cdot \frac{D \cdot dt}{dy^2}$$

A and C are always positive and is easy to see that $A + B + C \leq 1$ in any case. So the only condition for the stability is B must be positive:

$$B = 1 - 2 \cdot \frac{D \cdot dt}{dx^2} - 2 \cdot \frac{D \cdot dt}{dy^2} \geq 0$$

$$D \cdot dt \cdot \frac{dx^2 + dy^2}{dx^2 \cdot dy^2} \leq \frac{1}{2} \rightarrow dt \leq \frac{1}{2D} \cdot \frac{dx^2 \cdot dy^2}{dx^2 + dy^2} \qquad (5.137)$$

In the case $dx = dy$ the equation (5.137) becomes:

$$dt \leq \frac{dx^2}{4D} \qquad (5.138)$$

Comparing this result with the one obtained in one-dimension case we can estimate that in general, being N the number of dimensions the stability condition for a T-Sensor situation is:

$$dt \leq \frac{dx^2}{2D \cdot N} \qquad (5.139)$$

This result shows us that the processing time increases quickly since the number of dimensions grow.

5.5 Results and discussions

The use of finite differences has allowed us the programming of a one-dimensional and a two-dimensional simulator of the microfluidic device T-Sensor. With them we can predict the behavior of the molecules moving by diffusion and the relations with diffusivities and velocities.

The most important issue using the two-dimensional simulator is the processing time.

As it has said before, the computation increases quickly when the number of dimensions grow. The extra information obtained using this model, the diffusion across the h-dimension, does not worth the extra calculation time. The next table shows the differences between the processing time in one and two dimensions for a T-Sensor with the same features:

Longitude	***Processing time 1-D***	***Processing time 2-D***
30 um	*≈0.04 s*	*≈14 s*
300 um	*≈0.05 s*	*≈2 min*
30000 um	*≈0.06 s*	*≈25 min*

Table 5.13 Processing time for one and two dimension simulators

Such as it can see in Table 5.13 the temporal differences between the one or two dimensional simulations are very significant. In this case the biggest device had a longitude of 3cm, and the simulation in two dimensions took about 25 minutes.

When we need fine simulations of devices with dimensions of some cm the simulation may take several hours. This is the main reason for choosing the one-dimensional simulator as the best simulator for our proposals.

Once the simulator has been programmed, it is necessary a validation of is operation, in order to know whether or not the simulations reflect the real behavior of the diffusion.

5.5.1 Simulator validation with theoretical results

In order to determinate if this simulator works properly it will compare the results obtained in the simulations with some other simulations already published.

The first paper used is: "*E.Kamholz, P. Yager; Theoretical Analysis of Molecular Diffusion in Pressure-Driven Laminar Flow in Microfluidic Channels*".

The device used in this paper has the following features:

w *(width)*	*2405 µm*
h *(height)*	*10 µm*
L *(Longitude)*	*5500 µm*
D *(Diffusion Constant)*	*65 µm2/s*
Q1 *(Flow Rate)*	*1000 nL/s*
Q2 *(Flow Rate)*	*500 nL/s*
Q3 *(Flow Rate)*	*250 nL/s*

Table 5.14 T-Sensor features

In this simulation the authors wanted to see the concentration profile across the diffusion dimension at the end of the channel for three different flow rates.

In this situation is expected more diffusion for the minimum flow rate because of its slower velocity downstream. This is because the molecules move slower downstream and then they have more time to diffuse in the w-dimension. A simulation of this device was made using the 1-D T-Sensor simulator and the difference are shown below:

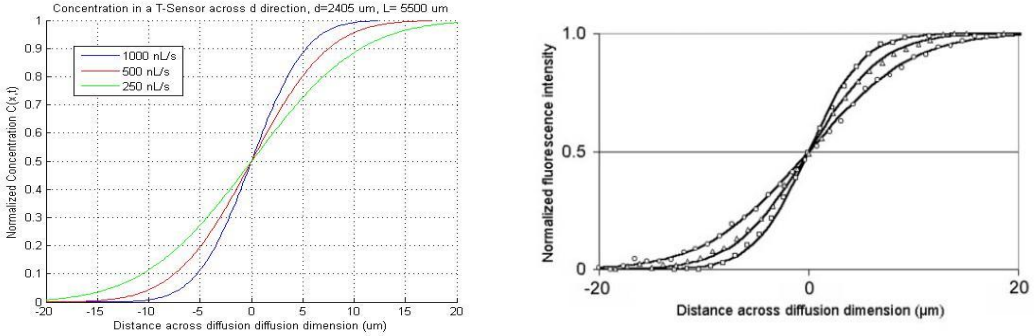

Fig. 5.63 On the left simulation using the 1-D T-Sensor simulator. On the right the results observed in the E. Kamholz, P. Yager paper [27].

And doing an overlap of these two images:

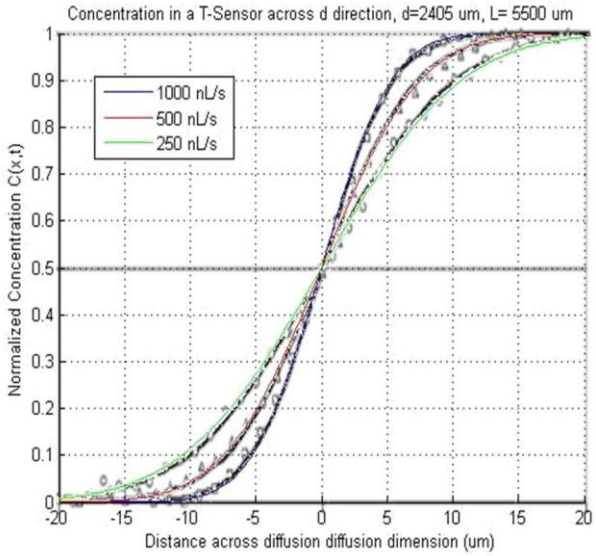

Fig. 5.64 Overlap of the obtained results using the 1-D simulator and the observed results in the paper E. Kamholz, P. Yager [27].

The results are very similar. The differences may be due because of the number of points used in the mesh.

The second paper used is: "*E. Kamholz, P. Yager: Molecular diffusive laws in pressure-driven microfluidic channels: deviation from one-dimensional Einstein approximations*".

In this case the device used is:

***w** (width)*	*2405 μm*
***h** (height)*	*10 μm*
***L** (Longitude)*	*2000 μm*
***D** (Diffusion Constant)*	*340 μm2/s*
***Q** (Flow Rate)*	*42 nL/s*
***V** (Velocity)*	*1700 μm/s*

Table 5.15 T-Sensor features

In this simulation the objective was to see the distance traveled by the molecules across the w-dimension at different points downstream in the device. For do that the authors considered the fluid had diffused until one point if the concentration was 30% of the initial bulk concentration.

The results using the 1-D T-Sensor simulator for this device and the comparison with the previous paper are shown below:

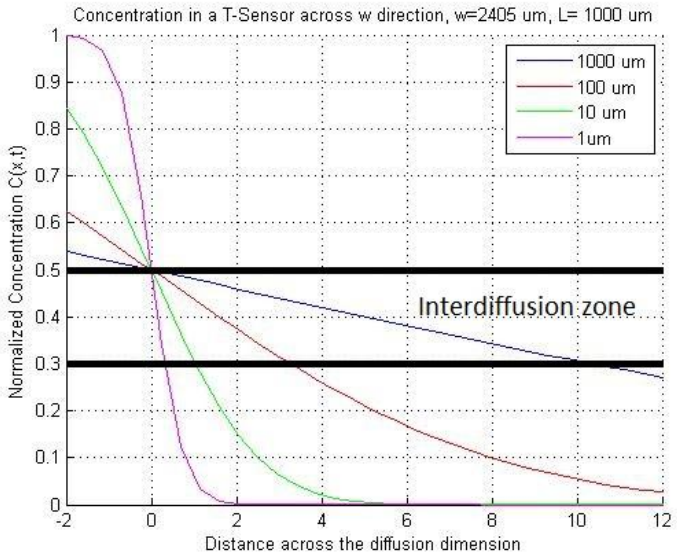

Fig. 5.65 Simulation using the 1-D T-Sensor simulator for the device presented in Table 5.15

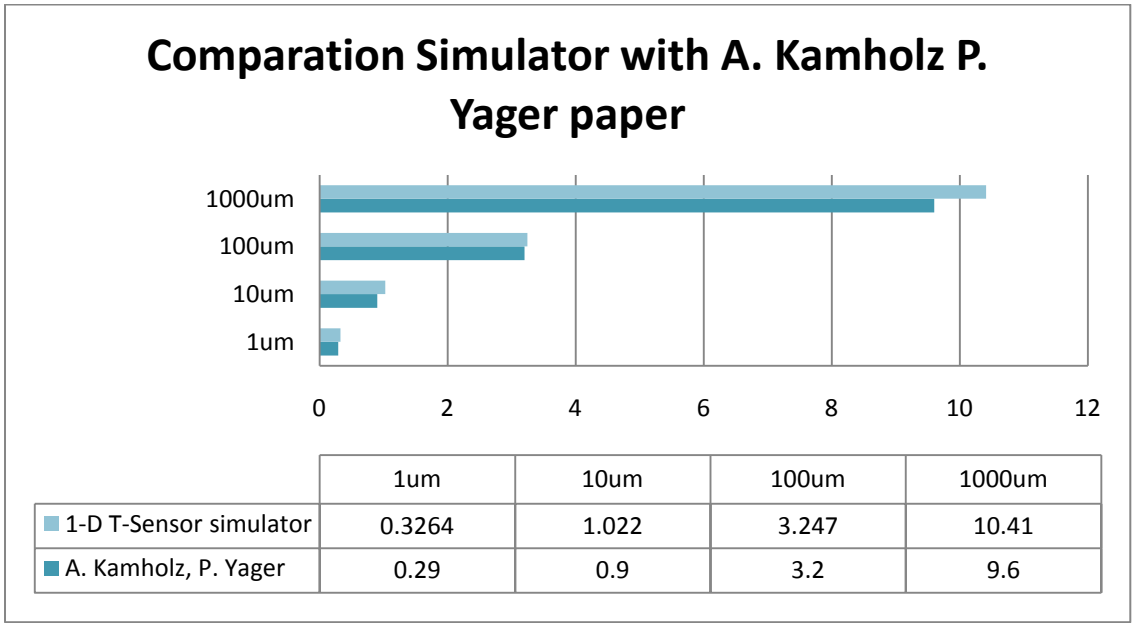

	1um	10um	100um	1000um
1-D T-Sensor simulator	0.3264	1.022	3.247	10.41
A. Kamholz, P. Yager	0.29	0.9	3.2	9.6

Fig. 5.66 Comparison between the E.Kamholz, P. Yager paper end the simulation using the 1-D T-Sensor simulator [29].

Again the results are very similar to each other. The error between them is probably because the number of points used to build the mesh is not the same.

The results here presented shows that the one dimensional simulator agrees with simulations realized by other scientists. Their results have been published in important journals that give credibility to their work. Is for this reason that we can state our simulations are reliable.

However, an experimental validation would provide even more reliability to this simulator

5.5.2 Simulator validation with experimental results

Using the results of the characterization of the T-Sensor presented in Fig. 4.52, is possible to simulate the theoretic behavior for the same system and figure out which is the diffusion coefficient that fits better to the experimental profiles.

The value of diffusivity for the molecule fluorescein is well known, and many documents report it. If this parameter coincides with the one find by simulation, we will be able to state that the simulator predicts faithfully the diffusion of particles in a T-Sensor.

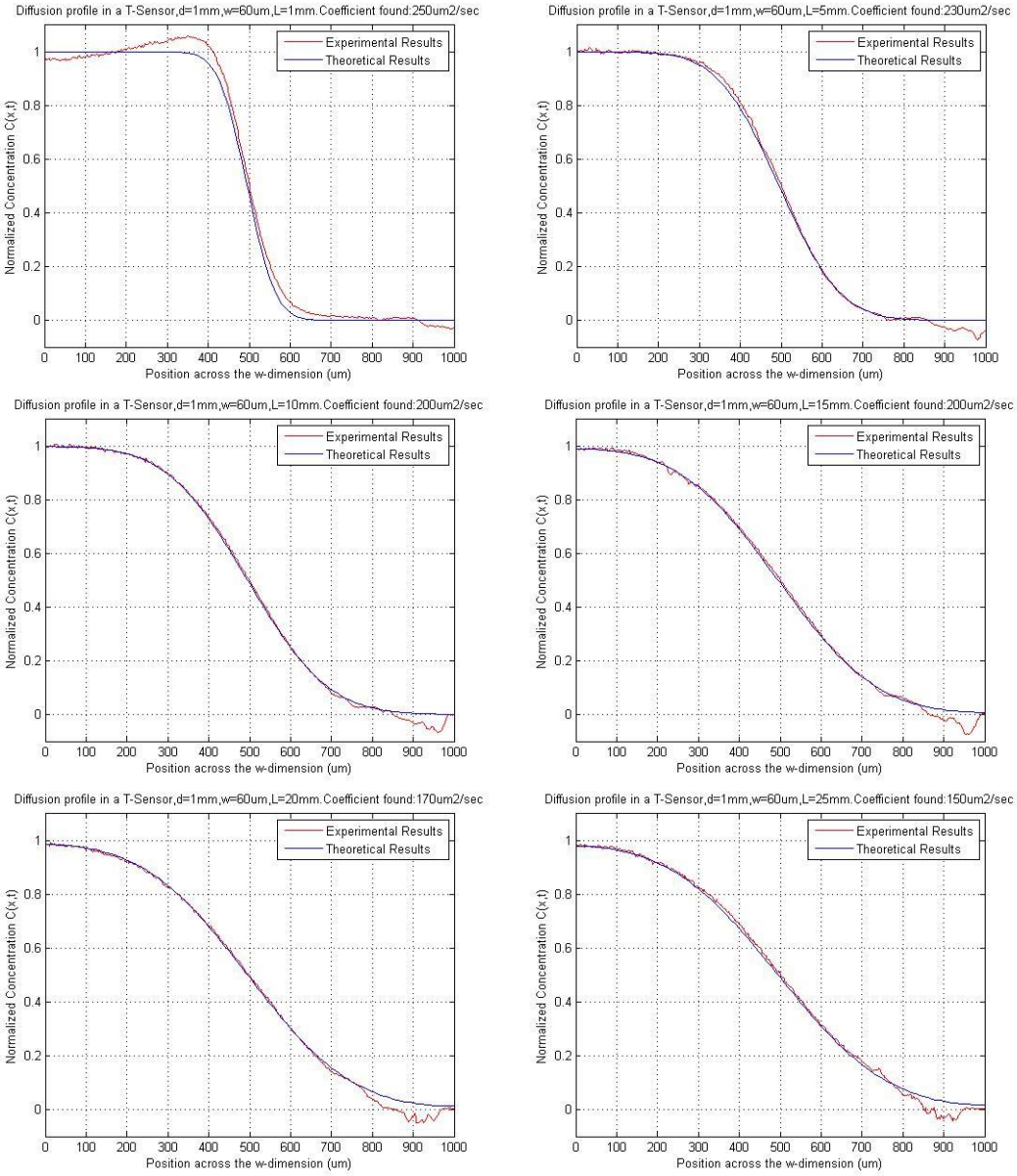

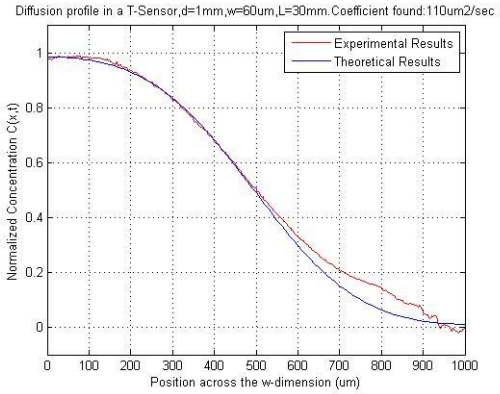

Fig. 5.67 Comparison between the theoretic concentration profile and the profile found experimentally. In each image we have found the diffusion coefficient which best approximates to the theoretical curve.

A simulation for the device studied in the characterization of the T-Sensor (chapter 4) was made at different points downstream according to the data got from the pictures. For each image the diffusivity whose value fit better to the concentration profile was stored, and at the end the mean average of those values was calculated in order to fin the mean value of the diffusion coefficient.

The results for the best diffusion coefficients in each image are the following:

Distance downstream (mm)	***Diffusion Coefficient (μ2/s)***
1	*250*
5	*230*
10	*200*
15	*200*
20	*170*
25	*150*
30	*110*

Table 5.16 Diffusion Coefficient at different points downstream for the Fluorescein Disodium. Flow rate 20nL/s, width 1 mm, height 120 μm and longitude 3 cm.

The mean value for the Diffusion coefficient is:

$$\overline{D} = 187 \mu m^2 / s$$

The next table shows the common values found for other publications of the diffusion coefficient for the molecule Fluorescein:

Paper	*Temperature*	*Diffusion Coefficient (μ2/s)*
Rapid Diffusion of Fluorescent Tracers into Staphylococcus epidermidis Biofilms Visualized by Time Lapse Microscopy [30]	*21.5°C*	*490 μ2/s*
Measurements of local diffusion coefficients in biofilms by microinjection and confocal microscopy. Biotechnol [31]	*21.5°C*	*From 500 to 600 μ2/s*
Introduction to microfluidics by Patrick Tabeling [16]	*20°C*	*300 μ2/s*

Table 5.17 Values of the diffusion coefficient found in other publications for the molecule Fluorescein.

According with the Table 5.17, the value that we have found is significantly low.

Probably this difference is because of the temperature. The diffusion coefficient changes very quickly with the temperature. At 21.5°C the diffusion coefficient is very similar, around 500 μ2/s, but when the temperature is to 20°C the diffusivity decreases to 300 μ2/s. Our experiment was done in a room whose temperature was 17°C. Temperature may be a reasonable explanation for the value of diffusivity found with the experiment.

Following the comparison for the experimental results with the theoretic results using the mean value of the diffusion coefficient are presented:

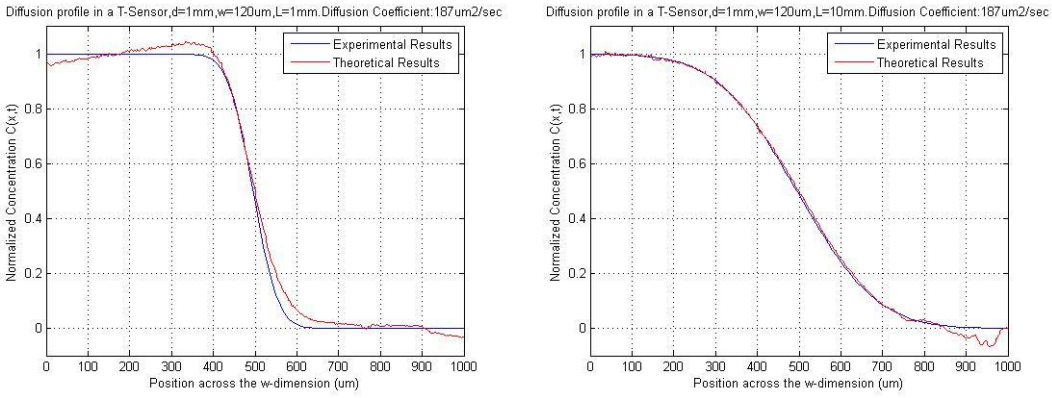

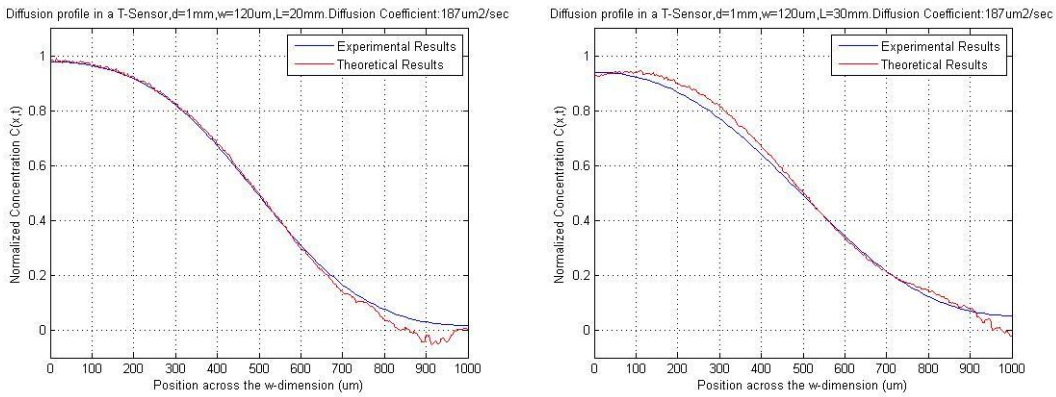

Fig. 5.68 Comparison between the theoretic concentration profile and the profile found experimentally. The diffusion coefficient is 187μm²/s for all the simulations.

The simulations using the mean value of the diffusivity fit perfectly to the experimental results.

Finally after theoretical validations (by comparison of previous reported results in papers) and experimental validations (comparing the simulations with experimental results) we are able to state the reliability of this programmed simulator.

The programming of this simulator have provides a strong background in processes based on diffusion of particles. Following the same procedure we are able to find new simulators that adapted to specific situations are able to describe real phenomena mathematically.

6 SIMULATION OF MOLECULAR COMMUNICATION SYSTEMS

In this section the molecular communication simulator is programmed using as a model the T-Sensor simulator done in previous chapters. The concept of signals with variable concentration is presented, achieving the possibility of study the diffusion of this type of signals in a T-Sensor. A simulator that includes this possibility is also programmed.

6.1 Introduction

Molecular communications are often based on diffusion processes. The aim of this work is to achieve a method that provides a criterion for which discriminates when the information is more convenient to module it using AM or FM.

In order to do that, we can base on real phenomena of this type of communication such as those that occur in biological communications. Cells are able to encode the information using amplitude or frequency modulation using as a signal carries waves of calcium ions [13, 14]. Our objective is to determine under what conditions cell decides to module using one method or the other.

Previously it was purposed a mathematical model for this phenomenon that explained the development of this type of communications. It also provided a decision threshold to decide when each type of encoding was more convenient. But that model had stability issues, and it was not valid to describe the diffusion process across the whole system due to these stability issues in the mathematical solution.

Our objective is to program a simulator of molecular communication which provides an approximated result of the diffusion of particles in a cellular environment, thereby avoiding any stability issue. The T-Sensor is based on the same diffusion processes and a simulator for this device has been developed and validated before. It is simple to extend that simulator to make it work in conditions as the required in molecular communications, simply two considerations have to be taken into account:

- The new geometry of the system and its new boundary conditions.
- The fact that the modulations of molecular signals is done by means of the transmission of signals with concentration of molecules variable with the time.

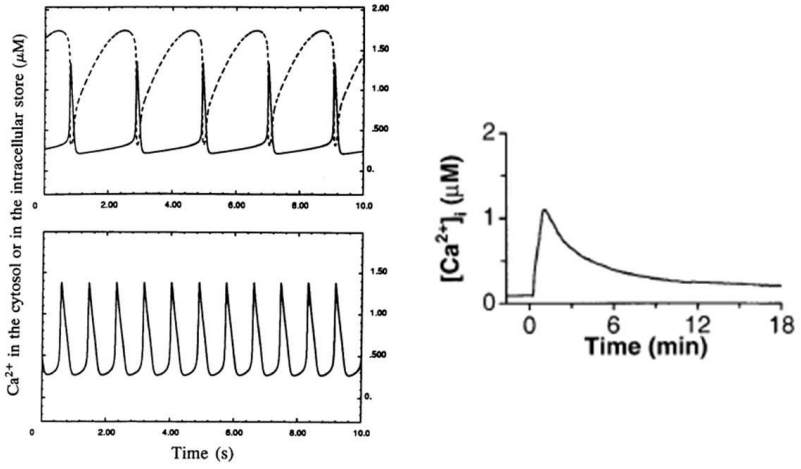

Fig. 6.69 Molecular information modulated by cell in frequency [32] (on the left) and in amplitude [33] (on the right).

Until now in the T-Sensor we always have considered that the concentration of particles of the infused fluid by one inlet was always constant

Then, the design of a molecular communications simulator passes to get first simulations of the diffusion process for input signals with variable concentration. To achieve that, firstly the T-Sensor simulator will be modified in order to achieve such behavior and then the molecular communication will be programmed using the same technique.

6.2 T-Sensor Simulation: Entrance with Variable Concentration

The T-Sensor simulator such as it has been programmed previously, does not have into account the possibility of including input signals with variable concentration of particles.

Assuming a hypothetical case, a T-Sensor is being filled for one of its channels with water and the other is being filled with a fluid that has a variable concentration of particles depending on the time.

In this case the changes of concentration at the beginning would be transported along the main channel, and the concentration at all points of the device would be constantly changing.

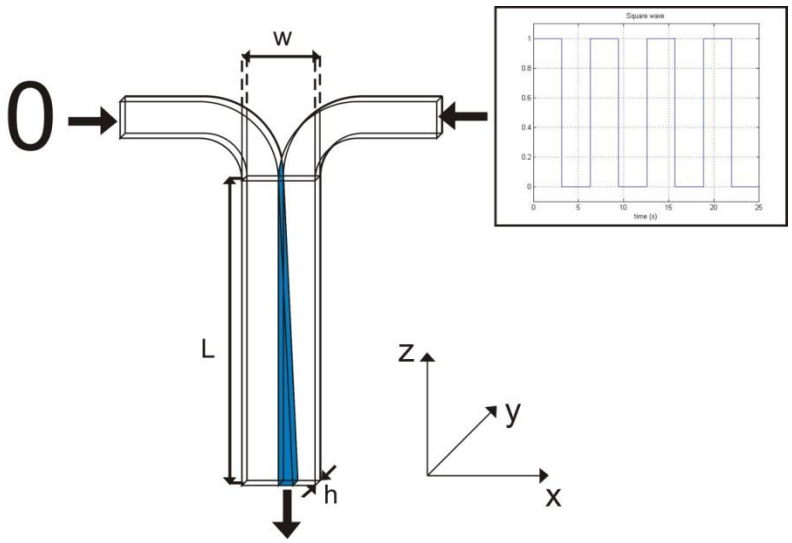

Fig. 6.70 Schematic of T-Sensor with variable concentration entrance.

The simulation process for this specifications change, in this case, comparing with the simple T-Sensor simulator. There, the system arrives to the steady state so the cross-sectional concentration profiles at different points never change during the time. In this new scenario that is not true.

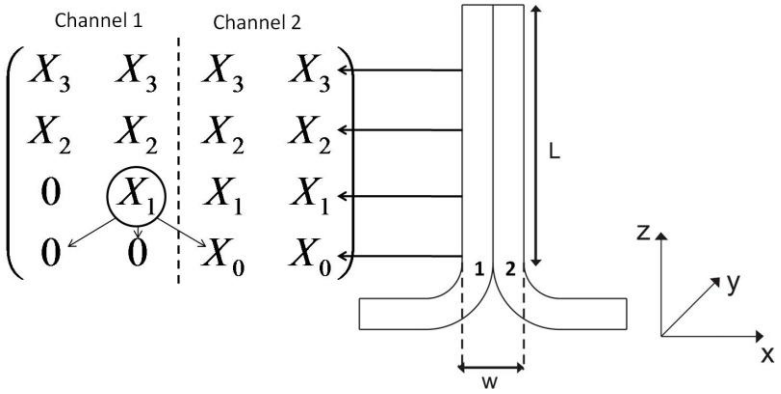

Fig. 6.71 Method for the calculus of the concentration in a T-Sensor.

The finite differences method states that the concentration along the main channel is calculated in a finite number of points. The concentration of those points depends on its previous value and the value of its neighbors. Following this algorithm it is possible to calculate the concentration everywhere in the device.

When the concentration at the beginning is unchanging, once a values has been calculated it always remains equal. This is because the T-Sensor works under steady state situation. When the input signal has a variable concentration, the changes are transported along the device so the concentration values have to be recalculated every time.

The continuous input signal has to be discretized into a finite number of equidistant points if we want to use it in a finite difference simulator.

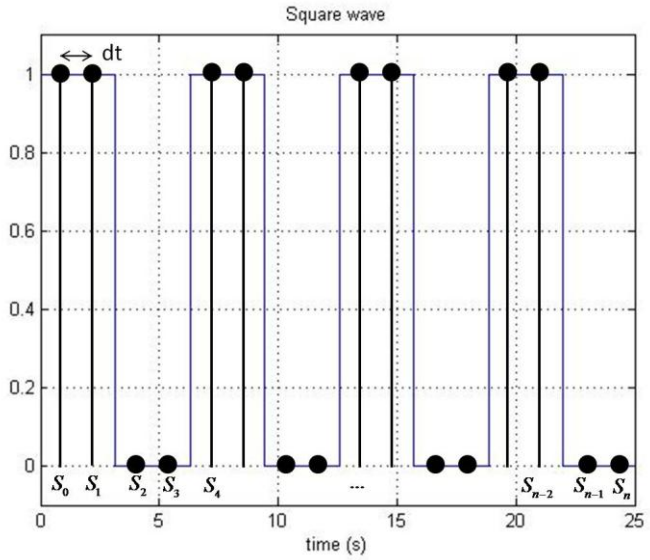

Fig. 6.72 Normalized input signal. Samples are taken every dt.

As we can see in the image, every dt the input signal changes its value. That means all the points in the T-Sensor must be recalculated again. For $t = 0$, the initial condition

says the concentration at the beginning of the channel is the initial concentration and 0 in the rest of the device.

$t = 0$:

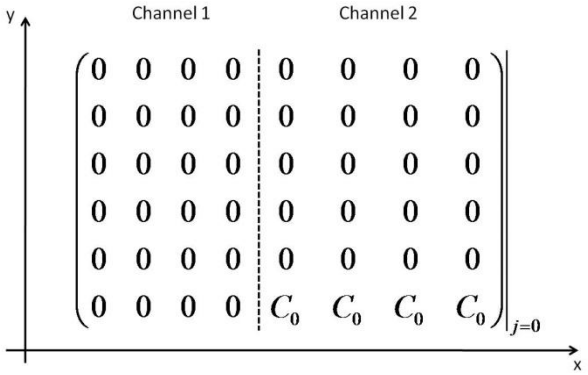

The matrix shows that the concentration in one channel is C_0 at the beginning, and the rest of the device does not have any particle yet. In the next instant $t = 0 + dt$, the particles are transported along the channel, and they diffuse across the w-direction.

$t = 0 + dt$:

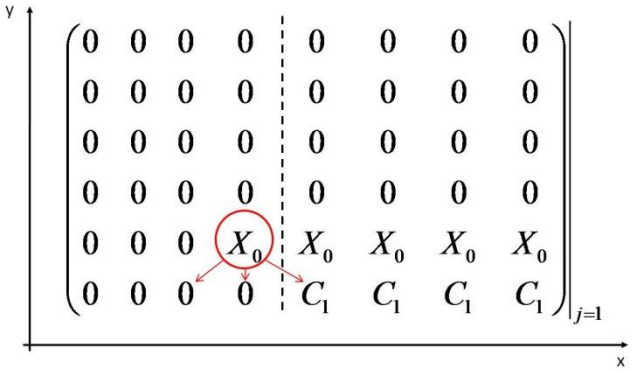

Fig. 6.73 Concentration matrix after the first instant.

As we can see in the matrix, the concentration in the second row is not zero. That is the consequence of the transportation of molecules. At the same time those particles have diffused to the left.

The concentration varies every instant:

$$\left.\begin{pmatrix} 0 & 0 & 0 & 0 & 0 & 0 & 0 & 0 \\ 0 & 0 & 0 & 0 & 0 & 0 & 0 & 0 \\ 0 & 0 & 0 & 0 & 0 & 0 & 0 & 0 \\ 0 & 0 & X_0 & X_0 & X_0 & X_0 & X_0 & X_0 \\ 0 & 0 & 0 & X_1 & X_1 & X_1 & X_1 & X_1 \\ 0 & 0 & 0 & 0 & C_2 & C_2 & C_2 & C_2 \end{pmatrix}\right|_{j=2} \rightarrow \left.\begin{pmatrix} 0 & 0 & 0 & 0 & 0 & 0 & 0 & 0 \\ 0 & 0 & 0 & 0 & 0 & 0 & 0 & 0 \\ 0 & X_0 & X_0 & X_0 & X_0 & X_0 & X_0 & X_0 \\ 0 & 0 & X_0 & X_1 & X_1 & X_1 & X_1 & X_1 \\ 0 & 0 & 0 & X_2 & X_2 & X_2 & X_2 & X_2 \\ 0 & 0 & 0 & 0 & C_3 & C_3 & C_3 & C_3 \end{pmatrix}\right|_{j=3}$$

$$\left.\left(\begin{array}{ccc:ccccc} 0 & 0 & 0 & 0 & 0 & 0 & 0 & 0 \\ X_0 & X_0 & X_0 & X_0 & X_0 & X_0 & X_0 & X_0 \\ 0 & X_1 & X_1 & X_1 & X_1 & X_1 & X_1 & X_1 \\ 0 & 0 & X_2 & X_2 & X_2 & X_2 & X_2 & X_2 \\ 0 & 0 & 0 & X_3 & X_3 & X_3 & X_3 & X_3 \\ 0 & 0 & 0 & 0 & C_4 & C_4 & C_4 & C_4 \end{array}\right)\right|_{j=4} \rightarrow \left.\left(\begin{array}{ccc:ccccc} X_0 & X_0 & X_0 & X_0 & X_0 & X_0 & X_0 & X_0 \\ X_1 & X_1 & X_1 & X_1 & X_1 & X_1 & X_1 & X_1 \\ 0 & X_2 & X_2 & X_2 & X_2 & X_2 & X_2 & X_2 \\ 0 & 0 & X_3 & X_3 & X_3 & X_3 & X_3 & X_3 \\ 0 & 0 & 0 & X_4 & X_4 & X_4 & X_4 & X_4 \\ 0 & 0 & 0 & 0 & C_5 & C_5 & C_5 & C_5 \end{array}\right)\right|_{j=5}$$

The values indicated with X_i are calculated in a loop that takes into account previous values. In order to not lose information, the computation of the values has to be done from further positions downstream to the beginning. That means the values of a new matrix must be calculated starting up and then descending row by row. Otherwise we would remove values that we would need to calculate others.

In the **Appendix D** a Matlab code which is able to do this computation is presented.

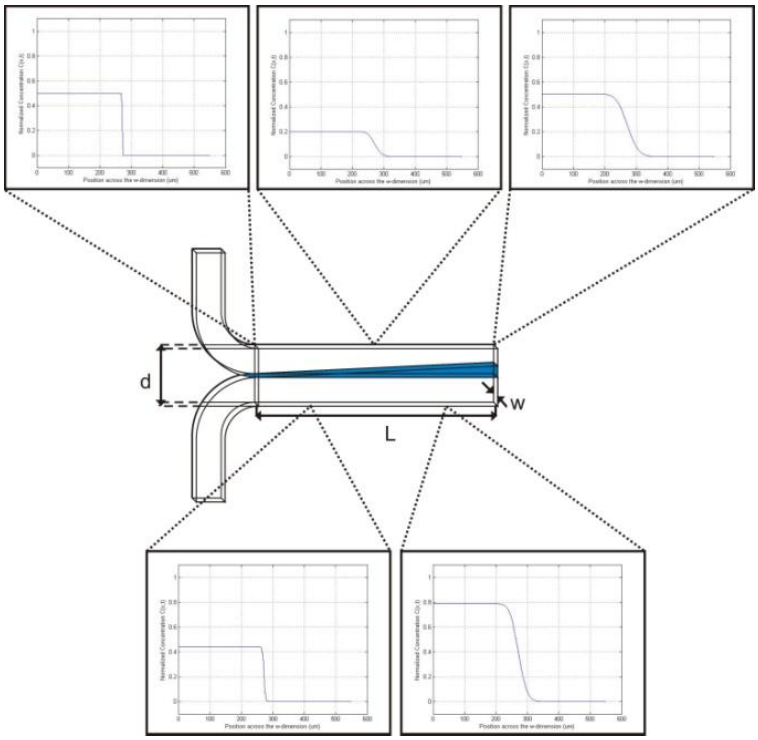

Fig. 6.74 Concentration profile across the w-dimension in some points downstream when the entrance is a wave whose concentration varies in sinusoidal way.

The images expose the behavior of this device. As we can see in the figure Fig. 6.74 different points downstream have very different concentration profiles. That shows the transportation of changes from the source along the channel. The concentration profiles at the beginning and at the end of the channel are similar, but it is possible to how the diffusion process occurs along the device.

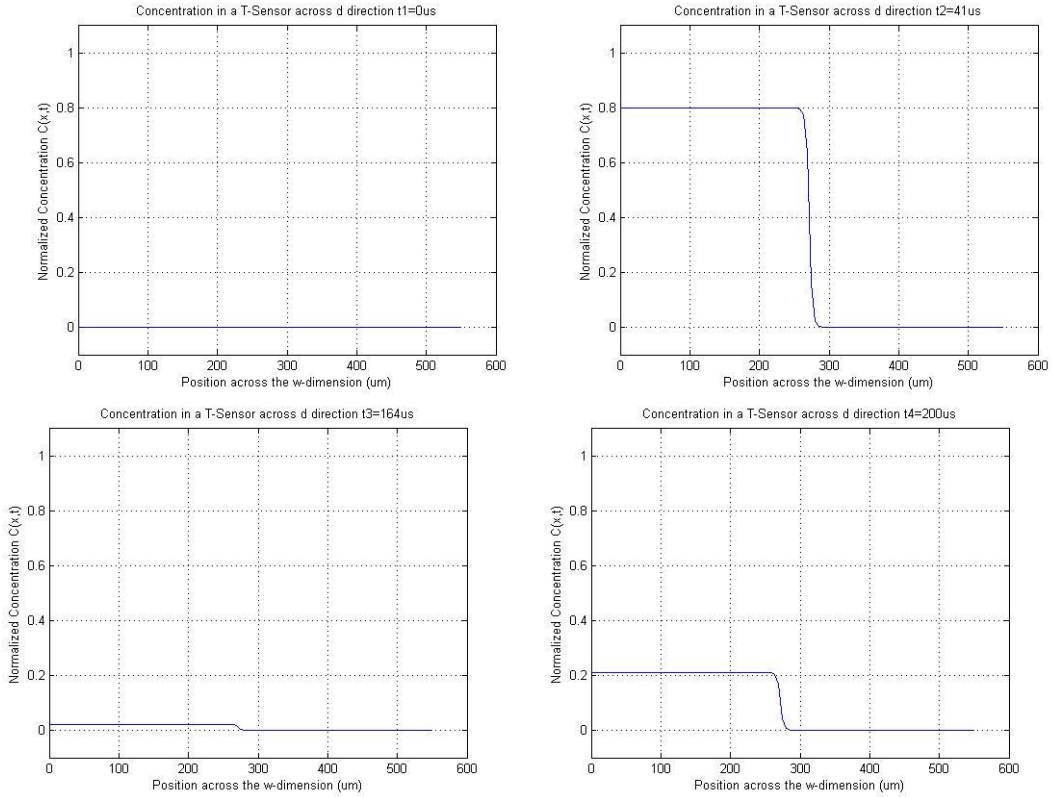

Fig. 6.75 Concentration profile across the w-dimension at 500μm downstream when the entrance is a wave whose concentration varies in sinusoidal way. On the top-left image, concentration at the beginning t=0μs. On the top-right image concentration after 41μs. On the bottom-left image concentration after 164μs. On the bottom-right image the simulation shows the concentration at the end of the simulation, 200μs

In the image Fig. 6.75 it is shown how changes the concentration profile in a specific point during the time. How the concentration grows and decreases shows up that the input signal has a profile also varying between low and high concentrations. In this case this is a sinusoidal signal.

Once the simulation of diffusion in a system with changing concentration has been done, we are able to use this same method in a simulator that predicts the behavior in molecular communication systems.

6.3 Cell Communications simulation

Cell communications environment is a completely different scenario, but the molecules that one cell release to the media diffuse around it according the diffusion equation. Therefore the change of the simulator capabilities to predict the behavior of cell communication is easy coming from the T-sensor simulator.

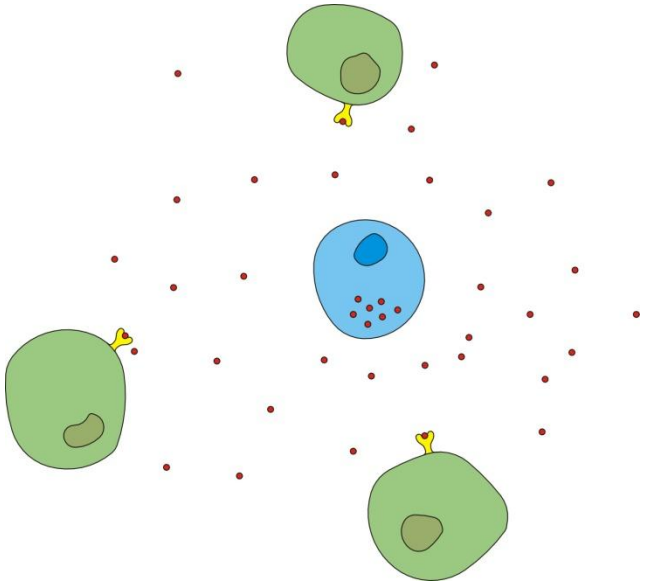

Fig. 6.76 The source which can be a cell or an external source is situated in one point and it emits the concentration wave to the media. The target cell receives this information.

The most important difference between this simulator and the T-Sensor simulator is how the molecules can diffuse. Cells release molecules to the medium and them diffuse in any direction around it, on the other hand in a T-Sensor the molecules only diffuse from one channel to the other.

Modulation processes in molecular communication are based on signals with variable concentration. That forces molecular communication simulator to handle with theses kind of signals. The same technique used in the T-Sensor with variable entrance will be applied in this case.

In the **Appendix E** a simulator able to predict the behavior of molecular communications based of diffusion processes is programmed using MATLAB.

As it has been said before, molecular waves modulated in FM encode the information in their frequency. For this reason it is important to know how the simulator reacts to periodic signals.

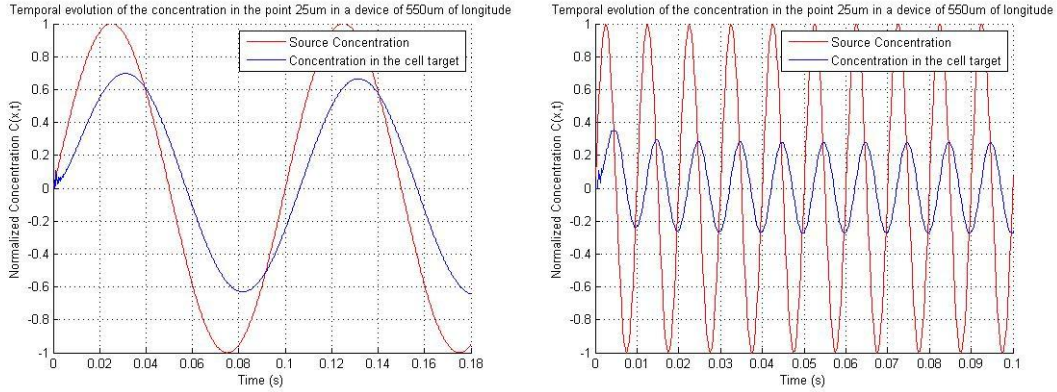

Fig. 6.77 Simulations in a cell communications environment. On the left the input signal is a sinus with a frequency F=10Hz. On the right the input signal is a sinus with a frequency F=100Hz.

Such as the images above show us, the system acts like a low pass band filter. For low frequencies (the image on the left) the output signal cross the system practically unchanged while for high frequencies (the image on the right) the output signals is attenuated. Physically that states for signals which varies slowly it is easier for the system to diffuse all of these changes. Or with other words, the changes of signals that vary slowly are easier to detect than the changes of signals that varies quickly.

The band can be modified changing the diffusivity or changing the distance between the source and the sink.

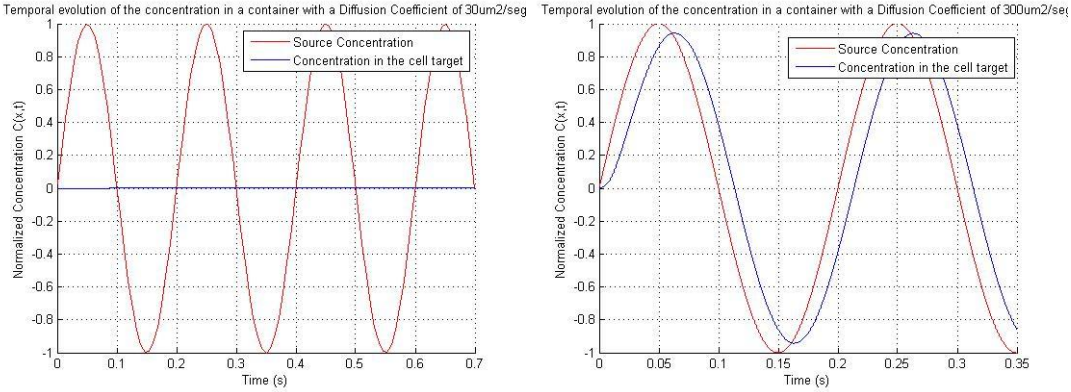

Fig. 6.78 Simulations in a cell communications environment. he input frequency signal is F=5Hz. On the left the response of the system for a low value of diffusivity (Dn=30μm²/s, H=20μm), on the right the response for a low value of the cuvette's size (L=3μm, Dn=30μm²/s).

As it was found out in the Chapter 4, molecular communication systems based on diffusion processes are modeled by low pass band filters. The corner frequency in these systems is approximated by the equation (3.79), and it depends on the diffusivity and the distance between transmitter and receiver. Exactly the same behavior has been found by simulations.

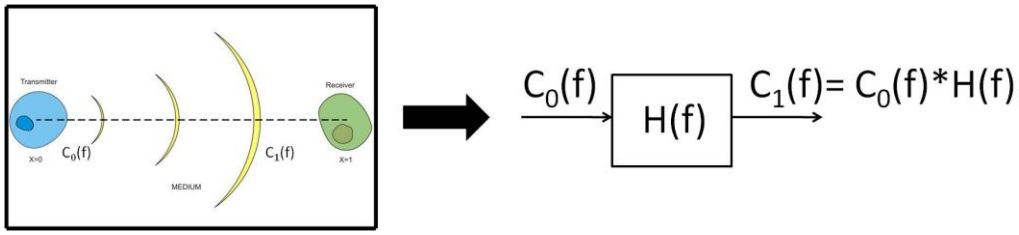

Fig. 6.79 Molecular communications can be considered using their mathematical model.

A low pass filter has a characteristic behavior when the input signal is a square wave. Because this signal is composed by infinite harmonics plus a dc component (which is the men value of the signal) as the pass band increases, more components can pass through the filter, so the output signal is more similar to the input signal.

Cells module the information in FM by sending spikes of particles concentration. We can assume that square waves are a simplification of that process.

The mathematical expression of a square signal with frequency $f = 2\pi T$ using Fourier series is:

$$f(t) = \frac{1}{2} + \sum_{n=1}^{\infty} \frac{2}{n\pi} \cdot \sin\left(\frac{2\pi}{T} nt\right) \quad (6.140)$$

Using this kind of signal as an input, we expect the system will be able to transport the wave through the media for large values of diffusivity or for short distances between the transmitter and the receiver. Both cases yield a filter with high bandwidth. Otherwise the filter bandwidth narrows being the signals susceptible to be attenuated.

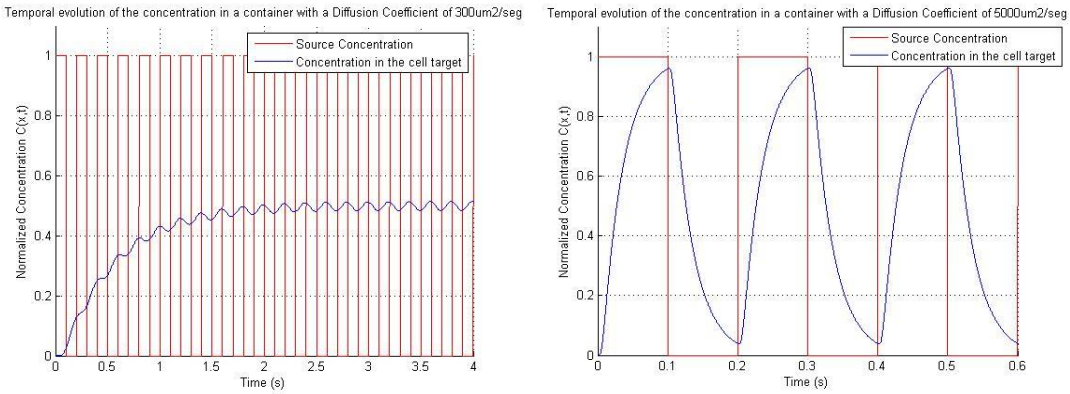

Fig. 6.80 Simulations in a cell communications environment. On the left the input signal is a square wave with a frequency F=5Hz and the diffusion coefficient is 300μm2/s. On the right the input signal is a square wave of the same frequency and the diffusion coefficient is 5000μm2/s. The simulations have been done in cuvette with a size of H=20μm.

As we can see in Fig. 6.80 the media is able to transport the changes from the source when the diffusion coefficient is high. In the image on the top the system is filtering the high frequency components and only the mean term survives, for this reason the graph tends to 0.5. In the case on the bottom the band of the filter is higher so some of the high frequency components pass through the filter. For this reason is easier to see the changes coming from the input signal.

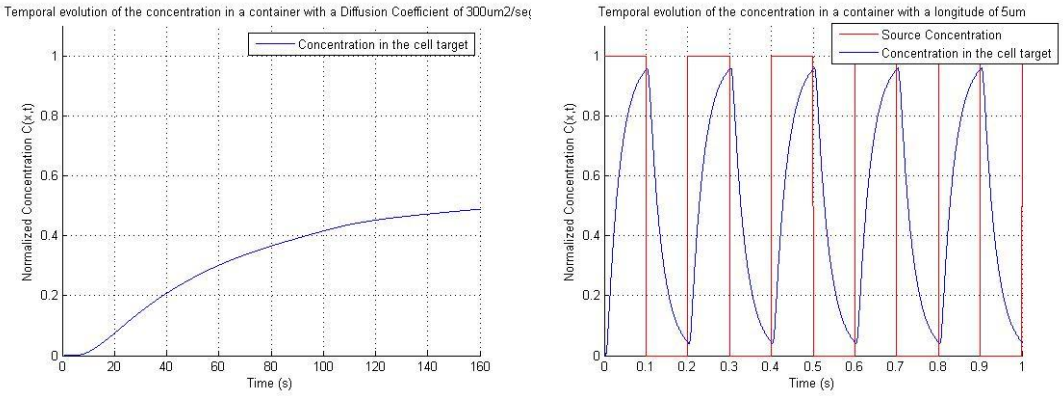

Fig. 6.81 Simulations in a cell communications environment. On the left the input signal is a square wave with a frequency F=5Hz and a size of H=550µm. On the right the input signal is a square wave with the same frequency and a size of H=5µm. The simulations have been done considering a diffusivity of 300µm2/s.

In the image above the variation of the input signal can be detected when the size of the container, or for short distance between transmitter and receiver. That provokes a high bandwidth allowing multiple harmonics to cross the filter. On the other hand, when the distance is large, the bandwidth gets narrower, and only the mean average is able to cross the system.

This system could be modeled using an electronic comparation, as a first order low pass band filter.

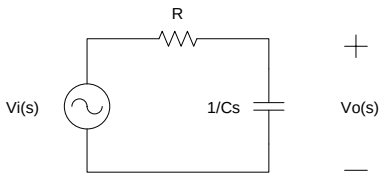

Fig. 6.82 First order Low Pass Band Filter (LPBF)

The output voltage is:

$$V_o(s) = V_i(s) \cdot \frac{1/C \cdot s}{R + 1/C \cdot s} = V_i(s) \cdot \frac{1/RC}{s + 1/RC} = V_i(s) \cdot \frac{1}{1 + \frac{s}{1/RC}} \qquad (6.141)$$

The corner frequency in the system (6.141) is $\omega_c = 1/RC$. Until this frequency, a periodic signal is considered inside the band. Up to this frequency the signal is considered out of band. The inverse of the corner frequency is called the charge time constant capacitor charging $\tau = 1/\omega_c = RC$.

According with this we can say that the cell communication system acts in a similar way to an electronic filter. And the frequency corner has to depend on the coefficient diffusion and the distance between the transmisor and the receptor.

$$\omega_c = \left(\frac{\pi}{2}\right)^2 \frac{D}{H^2}$$

As it happens in the capacitor which is charged and discharged of electronic energy, the medium is "charged" and "discharged" of molecules.

6.4 Results and discussions

As it has been seen, the capabilities of simulating systems with inputs signals with variable concentration require a more complexity in the calculation of the values in each point. These must be continuously recalculated whenever the input concentration varies. This requires obviously a higher computational cost to the system that is translated in a higher simulation times.

At each iteration we must calculate the values of concentration that appears with the symbol X_i. The simulator calculates the all the values in a row, but only calculates the rows that are different of zero. Thus, the computational depends on the number of rows that the system must calculate. Considering NUM the number of rows that we have to calculate in each matrix the number of rows solved in the previous example is:

$$NUM = 0+1+2+3+4+5 = 15$$

In the first matrix there was not any row to calculate, the values of initial concentration are provided by the input signal. The second matrix had one unknown row; the third had two and so on.

At the end of the entire simulation 15 rows are calculated.

In general for numt iterations the NUM is:

$$NUM = \sum_{j=0}^{numt-1} j = \left[(numt-1)+1\right] \cdot \frac{(numt-1)}{2} = numt \cdot \frac{(numt-1)}{2} \qquad (6.142)$$

For non variable entrance, the rows remain always constant once they have been calculated. For this reason the rows that must be calculated are the number of rows in a matrix, except the first which is provided by the initial conditions.

NUM for the non variable case is:

$$NUM = (numt - 1) \tag{6.143}$$

The computational cost is proportional to NUM so, the increment of the computational cost for use variable entrance is:

$$C = \frac{NUM_{\text{var}ible}}{NUM_{non\_\text{var}ible}} = \frac{\frac{(numt-1)}{2} \cdot numt}{(numt-1)} = \frac{numt}{2} \tag{6.144}$$

This means in a program with numt=2000 iterations, the computational cost in the non variable entrance case would be proportional to 1999. In the variable entrance case the computational cost would be proportional to 1999000. One thousand times higher. Although the computational time augment is significantly big, that is not a problem for the simulations that we do.

Cell communications simulator solved any stability issues that the analytical solution had. The behavior of molecules in cell communications environments moving by diffusion can be predicted even when the concentration at the source is changing during the time.

The simulations behave as the mathematical solution stated. The molecular communication system is mathematically modeled by a low pass band filter and its bandwidth depends on the diffusivity and the size of the container where the cells are placed.

The simulations react in the same way that the real solution to square molecular waves, detecting the changes in the signal transmitted for large values of diffusivity or small containers.

Large values of the diffusion equation indicate that the molecules can move easily in the medium so they do it fast. Therefore, the changes of concentration forced by the transmitter are quickly propagated by the medium.

Small containers can be filled of molecules quicker than the big containers, so all changes of the concentration forced by the transmitter can be detected by the receiver easily.

Using this simulator we state cells encode the information using FM when the carrier frequency can pass through the filter, which implies that frequency is lower than the corner frequency of the filter.

6.4.1 Comparison with theoretical results

Theoretically is has been demonstrated that the frequency corner in a molecular communications system is given approximately by (3.79).

In a first-order low pass filter, the cutoff frequency is the one which halved the power of the input signal to the system output when the input signal is sinusoidal.

We can achieve the cutoff frequency by simulation changing the input frequency until reach the one that yields an output with half power. For a sinusoidal input signal, if the frequency the cutoff frequency, after crossing the system the output amplitude will be $A_o = A_i \cdot 1/\sqrt{2}$

Three different systems will be evaluated in order to determine whether or not the approximation found out in the Chapter 4 agrees with the simulations. The theoretical cutoff frequency will be calculated for each case and a sinusoidal signal with that frequency and unit amplitude will be generated. After that, the systems will be simulated using as an input signals those sinusoidal signals and we will compare the output amplitude with the expected amplitude $A_o = 1/\sqrt{2} \approx 0.707$

$$\omega_c \approx \left(\frac{\pi}{2}\right)^2 \cdot \frac{D}{H^2}$$

$$f_c \approx \left(\frac{\pi}{2}\right)^2 \cdot \frac{D}{H^2} \cdot \frac{1}{2\pi} = \frac{\pi}{8} \cdot \frac{D}{H^2}$$

The features of the first system are:

Dn=5000μm2/s
H=20μm
Fc=4.9Hz (using the approximation)

Table 6.18Features for the first system.

The simulation result is:

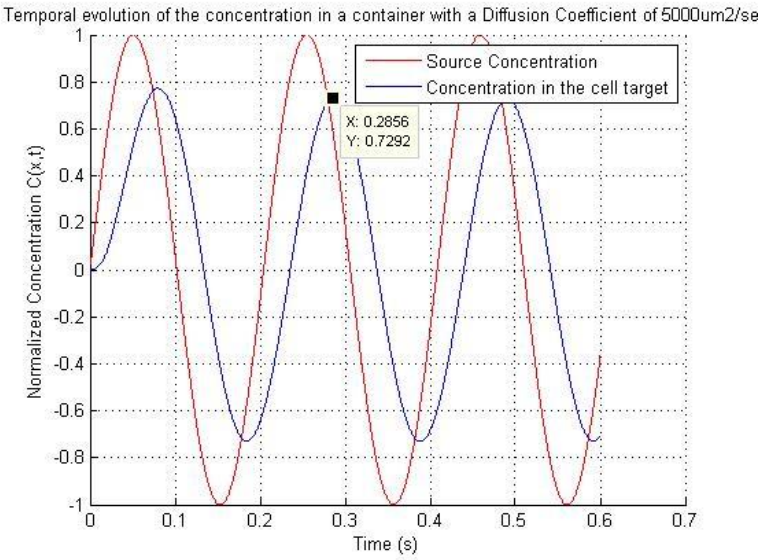

Fig. 6.83 Input and output sinusoidal waves with frequency F=Fcutoff.

We were expecting an output sigma with an amplitude of $A_o = 0.707$. The simulation shows for sinusoidal wave with a frequency equal to the cutoff frequency an output amplitude of $A_o = 0.7292$. The simulation agrees with the theoretic results. The difference may be due especially to two factors, firstly the cutoff frequency used is an approximation of the real one, and secondly the simulation has been made using a numerical method that always provides an approximation of the real solution.

The features of the second system are:

Dn=300μm2/s
H=5μm
Fc=4.71Hz (using the approximation)

Table 6.19Features for the second system.

The simulation result is:

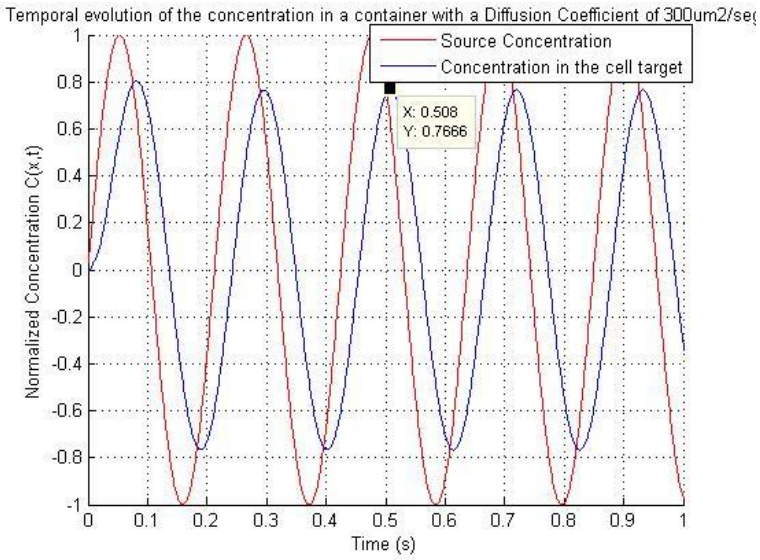

Fig. 6.84 Input and output sinusoidal waves with frequency F=Fcutoff.

In this second case the output amplitude is $A_o = 0.7666$. It is also very similar to the expected result.

The features of the second system are:

Dn=300μm2/s
H=20μm
Fc=0.295Hz (using the approximation)

Table 6.20Features for the second system.

The simulation result is:

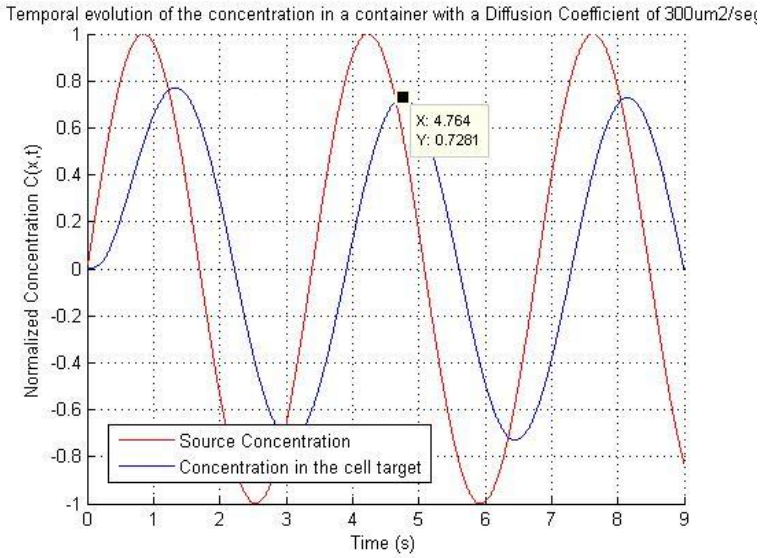

Fig. 6.85 Input and output sinusoidal waves with frequency F=Fcutoff.

One more time the simulation agrees with the theoretical results.

The values of the corner frequency were obtained by simulation searching what values gave the exact output amplitude $A_0 = 0.707$.

The next table shows the comparison of the theoretical and simulated values of the cutoff frequency:

System	***Theoretic Frequency (Hz)***	***Simulated Frequency (Hz)***
1	*4.9*	*5.22*
2	*4.71*	*5.1*
3	*0.295*	*0.315*

Table 6.21 Comparison of the theoretical and simulated values of the corner frequency in the three systems

The results here presented demonstrate the value of the frequency corner can be calculated either by using the molecular communication simulator or using the analytical solution. This cutoff frequency can be used as the threshold that determines if the information must be encoded amplitude or frequency modulation.

A simple formula for this parameter is given by the equation (3.79) which has been obtained by the resolution of the diffusion equation in a cellular environment. That solution provides practical information of how molecular communication systems work, but it is not useful to achieve a prediction of the concentration in the whole system. In these cases the simulator here presented provides a stable solution that approximates the reality with veracity.

7 CONCLUSIONS

Communication at nanometric scale is one of the challenges in the near future and molecular communication is considered the most promising option for this matter.

In this project it has been modeled a molecular communication system base on diffusion processes of particles. One of the contributions of this work is obtaining a parameter that allows us to decide if the information should be encoded using amplitude or frequency modulation.

To achieve this goal, it started from the Fick's second law, and it was particularized to a specific case of molecular communications. The transmitter sent a variable concentration wave with a square shape to the receptor, and applying the needed boundary conditions the system was solved finding an analytical solution. This model describes the behavior of the molecular communication systems according to their physical parameters, the diffusivity and the distance between transmitter and receiver.

The model that was obtained presented in Chapter 3 by the equations (3.58) and (3.71), shows a system that behaves as a first order low pass band filter whose cutoff frequency is approximately described by the equation (3.79). The pass band of this filter depends on the diffusion coefficient of the diffusing molecule and the dimensions of the container of the fluidic medium.

In Chapter 3 is demonstrated that this model presents instabilities under certain conditions, so even providing a qualitative explanation of the behavior of such systems, it is useless to describe the communication process in the whole system. To solve this issue it was decided to program a simulator that provided an approximate numerical solution of this process. The combination of the analytical model and the simulator becomes a powerful tool to describe and understand molecular communication systems.

Before programming this simulator a microfluidic device called T-SENSOR, whose operating principle is based on the same process of diffusion of particles, was fabricated. With this system the diffusion process was studied in a practical way, and experimental results were got in order to validate the simulator programmed using numerical methods. The device was fabricated using a new process known as "Scotch Tape Patterned Method" that presents the same features as the methods based on lithography being much more inexpensive and simple. It was found that this method is useful until sizes that can be treated with bench top tools, around 300 μm.

In order to determine whether or not numerical methods based on finite differences achieved a reliable approximation of particles diffusion processes, such as molecular communication systems, firstly a T-SENSOR simulator was programmed. We obtained 1-dimensional and 2-dimensional simulators, providing more information about the diffusion the second one. But the longer computation time made us to decide that the 1-dimensional simulator was more useful for our purposes. This simulator was validated with theoretical and experimental results that we got in the experiments performed with the microfluidic device.

Once the diffusion of particles was studied using the T-SENSOR simulator, the possibility to add the capability of simulating systems with variable concentration input signals was studied. This is what happens in cellular communications, and the T-SENSOR simulator did not reflect this possibility. This new capability adds a strong computational workload to the simulator, but it does not affect to the simulations done in this work. So, the T-SENSOR simulator was extended to a simulator with variable concentration signals and the behavior under this situation was studied. A continuous change of concentration was observed in these systems, being transported all changes from the beginning of the channel to the outlet.

The molecular communications simulator was programmed from the T-SENSOR simulator with variable concentration inputs. With this simulator the instability issues that the analytical solution are solved, besides exposing the system to all types of inputs with variable concentration is possible without having the recalculate the model for each entrance.

Using this simulator the value of the cutoff frequency found in Chapter 3 was proven, and it was established this parameter as a decision criterion to choose the type of modulation. Assuming that the information is encoded using FM when is possible, due to the advantages that this modulation presents over AM, the cutoff frequency establishes a decision threshold of the kind of modulation. As long as the frequency of the carrier signal is able to cross the filter without being filtered the information will be modulated using FM, otherwise it will be modulated using AM. This, we state that the decision of the way of modulation is determined by the physical parameter of diffusivity and the dimensions of the container of the fluidic medium.

With this decision threshold can be understood why ions of calcium are used as information carriers in FM modulation in cell communications. Information (changes in the concentration of molecules secreted by the cell) can be modulated using FM for large values of the diffusion coefficient, which result in a larger cutoff frequency. The diffusion coefficient is a function of the size of the carrier molecule and therefore, one would expect larger cutoff frequencies for smaller molecules, such as Ca^{2+}.

Information can also be modulated using FM when diffusion occurs in small containers, which yields higher cutoff frequencies. This may be the reason why FM modulation of Ca^{2+} has been found in intracellular communications. A common size of a cell is around 10 μm, subtracting the volume of the nucleolus and the organelles; the size of this container is a few microns which agree with the simulations presented in Chapter 6.

At the beginning, the aim of this work was to achieve a mathematical model that described the behavior of molecular communications based on diffusion processes, as well as establishing a threshold able to differentiate when the encoding should be done using amplitude or frequency modulation. At the end we can conclude that the analytical model with the simulator based on numerical methods provide a sturdy model of the

behavior of these communications. In the same way, it has succeeded providing a criterion that depends on the physical parameters that allow us to understand different events in nature, such as the reason of using ions of calcium as molecular carriers of information and the reason why the FM modulation usually occurs in intra-cell communications.

APPENDIX A

1-D T-Sensor Simulator

This code simulates the behavior of a T-Sensor of 550um width and 3cm longitude for a diffusion coefficient of 340u2/s.

Constants Definition

```
numx=61;%number of grid points in x

numt=2000;%number of iterations and t points in the grid

t(1)=0;

Dn=340;%Diffusion Coefficient


C=zeros(numx,numt);%we inicialize de matrix to 0

% The device width is 550um

dx=550/(numx-1);

dt1=0.045;

% The time simalated is T=numt*dt, so in this case is T=90sec. Because an

% steady state system the knoledge of the time is exactily de the same thant the
knlowledge of the position: V=x/T

x=0:dx:550;


stability1=(Dn*dt1)/(dx^2)
```

```
stability1 =


    0.1821
```

Initial Conditions

The initial condition force maximum concentration at the beginning in one channel and minimum in the other. We are going to browse the matrix through the first column, putting the values of the uniform distribution.

```
for i=1:fix(numx/2)

    C(i,1)=1;

end
```

Main loop

Now we can calculate the coefficients of the matrix C in the time t(j+1), using the results in the time t(j).

```
for j=1:numt
    t(j+1)=t(j)+dt1;
    for i=2:numx-1
        C(i,j+1)=C(i,j)+(C(i+1,j)-2*C(i,j)+C(i-1,j))*(Dn)*(dt1/(dx)^2);
    end
    % Boundary Conditions, no flux at the walls
    C(1,j+1)=C(2,j+1);
    C(numx,j+1)=C(numx-1,j+1);


end


L=3; %The device's longitude is 3cm
Velocity=(L*10000)/(numt*dt1);
```

Plotting results

We are going to plot the concentration profile at 3 different points downstream, for L=0cm, L=0.5cm and L=3cm.

```
figure(1)
plot(x,C(:,1));
title(['Diffusion profile in a T-Sensor, d=550um, L=0cm, Mean
Velocity=',num2str(Velocity),'um/sec. Diffusion Coefficient:',num2str(Dn),'um2/sec']);
xlabel('Normalized Concentration');
ylabel('Position across the w-dimension (um)');
grid;
axis([0 550 -0.1 1.1]);
figure(2)
plot(x,C(:,250));
title(['Diffusion profile in a T-Sensor, d=550um, L=0.5cm, Mean
Velocity=',num2str(Velocity),'um/sec. Diffusion Coefficient:',num2str(Dn),'um2/sec']);
xlabel('Normalized Concentration');
ylabel('Position across the w-dimension (um)');
grid;
axis([0 550 -0.1 1.1]);
figure(3)
```

```
plot(x,C(:,2000));

title(['Diffusion profile in a T-Sensor, d=550um, L=3cm, Mean
Velocity=',num2str(Velocity),'um/sec. Diffusion Coefficient:',num2str(Dn),'um2/sec']);

xlabel('Normalized Concentration');

ylabel('Position across the w-dimension (um)');

grid;

axis([0 550 -0.1 1.1]);
```

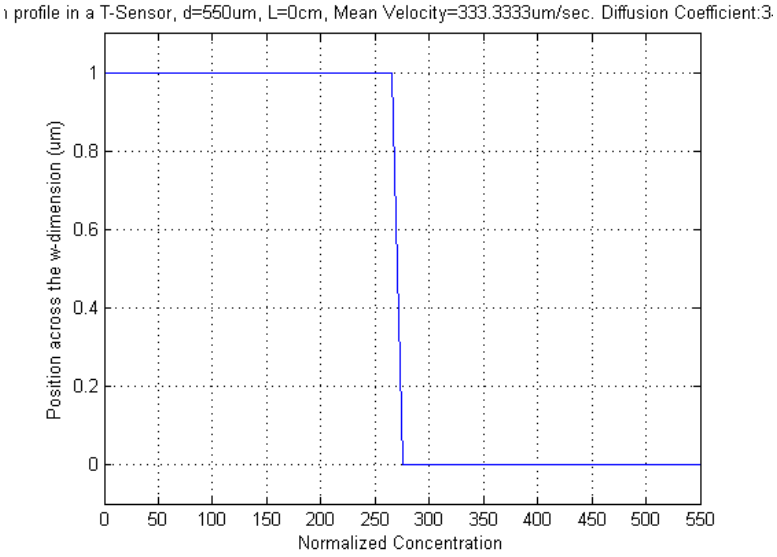

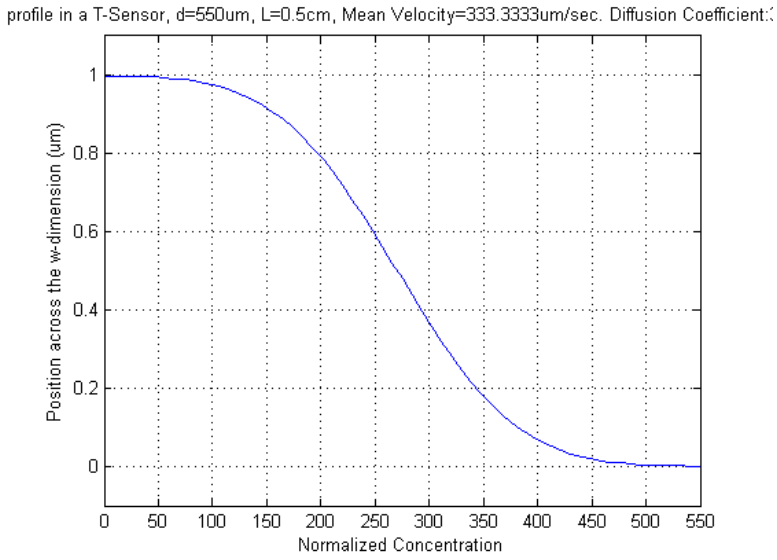

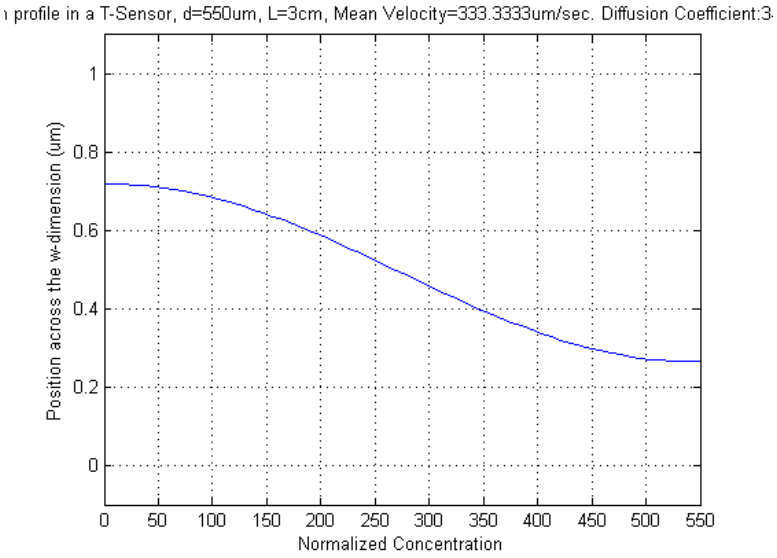
ı profile in a T-Sensor, d=550um, L=3cm, Mean Velocity=333.3333um/sec. Diffusion Coefficient:3
Position across the w-dimension (um)
Normalized Concentration
0
0.2
0.4
0.6
0.8
1
0
50
100
150
200
250
300
350
400
450
500
550

APPENDIX B

2-D T-Sensor Simulator

This code simulates the behavior of a T-Sensor device of any size. This is the function which is called from the user interface. In that interface introduces the information of width, height, and longitude and also the diffusion coefficient. Because the number of points to calculate, the system's memory may not be big enough, so this code have to storage the information in the hard disk in order to avoid this problem.

```
function out = funcion_tsensor(d,w,L,Dn,Vmax,numx,numy,dz)

tic

% d  length in the x-dimension

% w length in the y-dimension

% L length in the z-dimension

% Dn micrometer per second

% Vmax micrometer/sec

% dz distance between z points

% numx number of x points in the grid

% numy number of y points in the grid
```

Constants declaration

```
numiter=7000; %number of iterations

dx=d/(numx-1); %distance between x points

dy=w/(numy-1); %distance between y points

b=dy/dx; %proportionality constant


Vz=zeros(numy);


numz=fix(L/dz); %number of z points in the grid


a=numz/numiter;

num_matrix=fix(a);%number of matrix of size (numx x numy x numiter) we have to
calculate

r=numz-(num_matrix*numiter);%number of residual points to calculate


x=0:dx:d; %vector with x positions
```

```
y=0:dy:w; %vector whit y position


C=zeros(numx,numy,numiter);% Inizialize concentration matrix to 0

Cinitial=zeros(numx,numy);%initial concentration matrix

counter=0;
```

```
Input argument "d" is undefined.


Error in ==> funcion_tsensor at 25

dx=d/(numx-1); %distance between x points
```

Initial Conditions

The initial condition forces maximum concentration in one channel and minimum concentration in the other channel.

```
for i=1:fix(numx/2)%Inicial condition: Concentration max. in all analite microchannel

    for j=1:numy

        for k=1:numz

            C(i,j,1)=1;

        end

    end

end


Cinitial=C(:,:,1);%in the first iteration C and Cinitial are equal


for j=1:numy+1 %parabolic profile velocity in a laminar flow

    Vz(j)=400+Vmax*(1-(((j-1)*dy-w/2)^2/(w/2)^2));%el perfil parabolic sobre pedestal
es una patillada perque no es faci inestable el sistema!!!!

end;
```

Main Loop

This part calculates the concentration in each point of the grid. Is an extension for the 2 dimensional case. The intention is to calculate the points for a grid numx x numy x numz in a matrix, and if the system is bigger, keep this information in the hard disk and reuse the same matrix for save the memory of the system.

```
for q=1:num_matrix+1
```

```
    if q ~= num_matrix+1


        C(:,:,1)=Cinitial; % the initial condition for each matrix depends on the state
in the previous matrix.


        % we can calculate the concentration in the point k+1 using the information

        % in the k point

        for k=1:numiter

            for i=2:numx-1

                for j=2:numy-1

                    C(i,j,k+1)=C(i,j,k)+((C(i+1,j,k)+C(i-1,j,k))+C(i,j+1,k)*b^2+C(i,j-
1,k)*b^2-(2+2*b^2)*C(i,j,k))*(dz/dy^2)*(Dn/Vz(j));

                end


            % Boundary conditions, no flux in the walls. We have to be

            % careful, because in this case we have four walls, top, bottom

            %, left and right walls.

                C(i,1,k+1)=C(i,2,k+1);

                C(i,numy,k+1)=C(i,numy-1,k+1);

            end

            % no flux in the walls boundary condition

            for j=1:numy

                C(1,j,k+1)=C(2,j,k+1);

                C(numx,j,k+1)=C(numx-1,j,k+1);

            end


        Cinitial=C(:,:,numiter); % we use the last iteraton as the initial value in the
next iteration


        counter=counter+1;

        l_distance(counter,C,k,numz);% function which save the matrix with the results
each 10% of the L size

        end


    else % the residual r points, less than numiter

       if r~=0

        C(:,:,1)=Cinitial;


        % we can calculate the concentration in the point k+1 using the information
```

```
        % in the k
        for k=1:r
            for i=2:numx-1
                for j=2:numy-1
                    C(i,j,k+1)=C(i,j,k)+((C(i+1,j,k)+C(i-1,j,k))+C(i,j+1,k)*b^2+C(i,j-
1,k)*b^2-(2+2*b^2)*C(i,j,k))*(dz/dy^2)*(Dn/Vz(j));
                end
                % no flux in the walls boundary condition
                C(i,1,k+1)=C(i,2,k+1);
                C(i,numy,k+1)=C(i,numy-1,k+1);
            end
            % no flux in the walls boundary condition
            for j=1:numy
                C(1,j,k+1)=C(2,j,k+1);
                C(numx,j,k+1)=C(numx-1,j,k+1);
            end

        counter=counter+1;
        l_distance(counter,C,k,numz);

        end
       else
       end
    end
end
```

Plotting Results

```
mean_distance=fix((3*numx)/4);
width=(numy-1)/2;
plot_results(x,y,mean_distance,width);% we plot the found results

out=1;

toc
```

l_distance Function

This function save a matrix with the concentration points in 10 regions of the L size

```
function correct_distance = l_distance(counter,C,k,numz)


if counter == 1
    A=C(:,:,k);
    save concentration0.txt A -ascii;
elseif counter == fix(0.1*numz)
    A=C(:,:,k);
    save concentration10.txt A -ascii;
elseif counter == fix(0.2*numz)
    A=C(:,:,k);
    save concentration20.txt A -ascii;
elseif counter == fix(0.3*numz)
    A=C(:,:,k);
    save concentration30.txt A -ascii;
elseif counter == fix(0.4*numz)
    A=C(:,:,k);
    save concentration40.txt A -ascii;
elseif counter == fix(0.5*numz)
    A=C(:,:,k);
    save concentration50.txt A -ascii;
elseif counter == fix(0.6*numz)
    A=C(:,:,k);
    save concentration60.txt A -ascii;
elseif counter == fix(0.7*numz)
    A=C(:,:,k);
    save concentration70.txt A -ascii;
elseif counter == fix(0.8*numz)
    A=C(:,:,k);
    save concentration80.txt A -ascii;
elseif counter == fix(0.9*numz)
    A=C(:,:,k);
```

```
        save concentration90.txt A -ascii;
    elseif counter == numz
        A=C(:,:,k);
        save concentration100.txt A -ascii;

    end
    correct_distance=1;
```

```
Input argument "counter" is undefined.

Error in ==> l_distance at 6
if counter == 1
```

Plot function

This function plot the results stored in the hard disk.

```
function correct_plot = plot_results(x,y,distance,width)
aa=load('concentration0.txt');
a=load('concentration10.txt');
b=load('concentration20.txt');
c=load('concentration30.txt');
d=load('concentration40.txt');
e=load('concentration50.txt');
f=load('concentration60.txt');
g=load('concentration70.txt');
h=load('concentration80.txt');
i=load('concentration90.txt');
j=load('concentration100.txt');

figure(2)
surf(y,x,aa);
xlabel('Position y');
ylabel('Position x');
zlabel('Concentration C(x,y) at the begining');

figure(1)
surf(y,x,a);
```

```
xlabel('Position y');
ylabel('Position x');
zlabel('Concentration C(x,y) at the end');


% figure(3)
% surf(y,x,b);
% xlabel('Position y');
% ylabel('Position x');
% zlabel('Concentration C(x,y) in 20% of L');
%
% figure(4)
% surf(y,x,e);
% xlabel('Position y');
% ylabel('Position x');
% zlabel('Concentration C(x,y) in 50% of L');
%
% figure(5)
% surf(y,x,h);
% xlabel('Position y');
% ylabel('Position x');
% zlabel('Concentration C(x,y) in 80% of L');
%
% figure(6)
% surf(y,x,j);
% xlabel('Position y');
% ylabel('Position x');
% zlabel('Concentration C(x,y) in 100% of L');
%
% figure(7)
% title('Diffusion in d dimension');
% hold on
% plot(x,a(:,width),'b');
% plot(x,b(:,width),'r');
% plot(x,c(:,width),'r');
% plot(x,d(:,width),'r');
% plot(x,e(:,width),'r');
% plot(x,f(:,width),'r');
```

```
% plot(x,g(:,width),'r');
% plot(x,h(:,width),'r');
% plot(x,i(:,width),'r');
% plot(x,j(:,width),'b');
% xlabel('Position x');
% ylabel('Concentration C(x)');
```

correct_plot=1;

APPENDIX C

Image processing

This code pretends to extract the concentration profile from a .jpg image and compare this profile with the theoretical in order to find what the best diffusion coefficient is

Get image

```
[name,path]=uigetfile('*.jpg','Select the input JPG file');
fullname=strcat(path,name)
image2=imread(fullname);
image=rgb2gray(image2);
image=double(image);
[row,col]=size(image);
```

```
fullname =

D:\Lab\Probes imatges\Tratamiento de las imagenes del microscopio\20nlsec\15mm.jpg
```

Diffusion coefficient

```
%The key is to change this value until find the theretical caoncentration
%which most agree with the experimental results
Dn=200;
```

Obtaining the concentration information from the image

I take 10 random columns from the image and I extract the light intensity from each pixel. Then I average the 10 different curves.

```
pixel=1:1:row;
pixel=pixel';
for i=1:10
    x1(i)=random('unid',col);
```

```
end
X=zeros(row,10);
for i=1:10
    X(:,i)=image(:,x1(i));
end

A=zeros(row,1);
for j=1:row
    for i=1:10
        A(j)=A(j)+X(j,i);
    end
end
A=A/10;
```

The calculus of the max and min average for normalize the curve

In order to normalize the concentration profile, the maximum and the minimum values are obtained averaging the first points, where the curve has a maximum value and the lasts points where the concentration is minimum.

```
%Firstly a manual way to do that for any imatge it is shown.

% plot(pixel,A);
%
% msgbox('Insert in the prompt in the pixels at max concetration','Max
concentration','help');
% start1=input('First Pixel: ');
% start2=input('Second Pixel: ');
% msgbox('Insert in the prompt in the pixels at min concetration','Min
Concentration','help');
% eend1=input('First pixel: ');
% eend2=input('Second pixel: ');

% But for the images used in this work all of those point have been found
% and they are the following

% 1mm
```

```
% start1=240;
% start2=300;
% eend1=685;
% eend2=1040;
% position=1;
% limit=236;

% %5mm
% start1=193;
% start2=313;
% eend1=701;
% eend2=1040;
% position=5;
% limit=260;

% %10mm
% start1=208;
% start2=252;
% eend1=712;
% eend2=1040;
% position=10;
% limit=268;

%15mm
start1=215;
start2=261;
eend1=721;
eend2=1040;
position=15;
limit=266;

% %20mm
% start1=197;
% start2=256;
% eend1=729;
% eend2=1040;
% position=20;
```

```
% limit=271;


%25mm
% start1=241;
% start2=248;
% eend1=741;
% eend2=1040;
% position=25;
% limit=262;


% %30mm
% start1=280;
% start2=310;
% eend1=745;
% eend2=1040;
% position=30;
% limit=247;


% minavg=mean(A(eend1:eend2));
% B=A-(minavg);
% maxavg=mean(B(start1:start2));
% B=B/maxavg;
% plot(pixel,B);
```

Theoretical profile

"tensor" is the function which calculates the theoretical concentration curve. It returns the maximum and the minimum concentration value because they are needed to normalize the concentration profile coming from the image.

```
[inipoint endpoint]=tsensor(Dn,position);


% This is true only in the cases when the concentration at the walls are 1
% or 0. As the boundary conditions permit this no happen always, sometime a
% correction in the normalization is required. The values at the walls can
% be found using the simulator.
```

```
minavg=mean(A(eend1:eend2));
B=A-(minavg)+endpoint;
maxavg=mean(B(start1:start2));
B=(B/maxavg)*inipoint;
```

```
stability1 =

    0.0900
```

```
Warning: Ignoring extra legend entries.
```

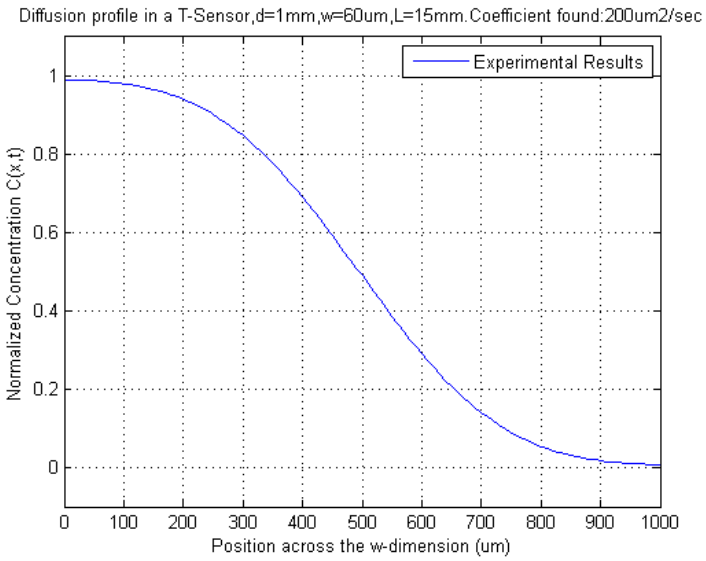

Putting the curve in the center of the graphic

In order to discriminate the channel edges, the method decide is to center the curve at the mean point. As the concentration at 500um has to be C=0.5, we center the profile at this point. For do that limit tell us how many pixels there are between the center and one of the walls. There are two possible results for limit, one for each wall, and sometime does not agree. In this case the minimum value is chosen

```
[valueCenter,posCenter]=min(abs(B-0.5));
Con=B((posCenter-limit):(posCenter+limit));
```

Plotting the normalize concentration curve

```
[sizeC,u]=size(Con);
y=0:1000/(sizeC-1):1000; %Vector with spatial information
y=y';

plot(y,Con,'r');
axis([0 1000 -0.1 1.1]);
grid on
hold on
```

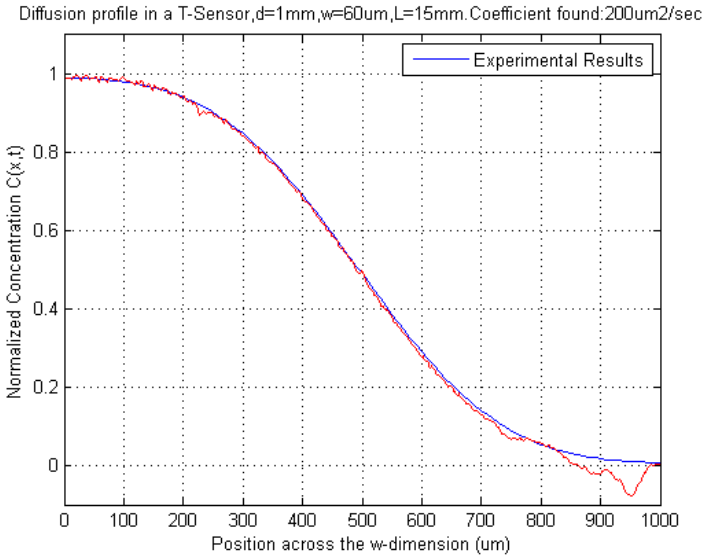

APPENDIX D

1-D T-Sensor Simulator, Variable entrance

This code is able to determine the behavior of a T-Sensor when the input flux has a variable concentration.

```
%tic
```

Constants declaration

```
numx=101;%number of grid points in x
numt=500;%number of iterations
Dn=455;
C=zeros(numx,numt);%we inicialize de matrix to 0
dx=550/(numx-1);
dt1=4.1e-4;
x=0:dx:550; %vector of x values
stability1=(Dn*dt1)/(dx^2)
```

```
stability1 =

    0.0062
```

Initial Conditions

In this case the initial condition is maxim concentration at the beginning in one channel and minimum in the order channel, but only the first iteration. Then at the beginning the concentration changes according with the variable VecCon.

```
% we are going to browse the matrix throght the first column, putting the values of the
uniform distribution
C(1:fix(numx/2),1)=1;

%Concetration at the begining in each instant: Sinusioidal variation

W=0:2*pi/numt:2*pi;
VecCon=(0.5*sin(W))+0.5;
```

Main Loop

```
%Now we can calculate the coefficients of the matrix C in the time t(j+1), using the
results in the time t(j)


for j=1:numt
    for k=(j+1):-1:1
        if k~=1 %Is not the beginig
            for i=2:numx-1
                C(i,k)=C(i,k-1)+(C(i+1,k-1)-2*C(i,k-1)+C(i-1,k-1))*(Dn)*(dt1/(dx)^2);
            end
            C(1,k)=C(2,k);
            C(numx,k)=C(numx-1,k);
        else
            for i=1:fix(numx/2)
                C(i,1)=VecCon(j+1);
            end
        end
    end

end
```

Plotting

```
figure(1)
hold on;
plot(x,C(:,1));
plot(x,C(:,10));
plot(x,C(:,100));
plot(x,C(:,200));
plot(x,C(:,300));
plot(x,C(:,400));
plot(x,C(:,500));
xlabel('Position across the w-dimension (um)');
ylabel('Normalized Concentration C(x,t)');
title('Concentration in a T-Sensor across d direction,W=550um,L=5000um,D=455um2/s');
grid on;
%toc
```

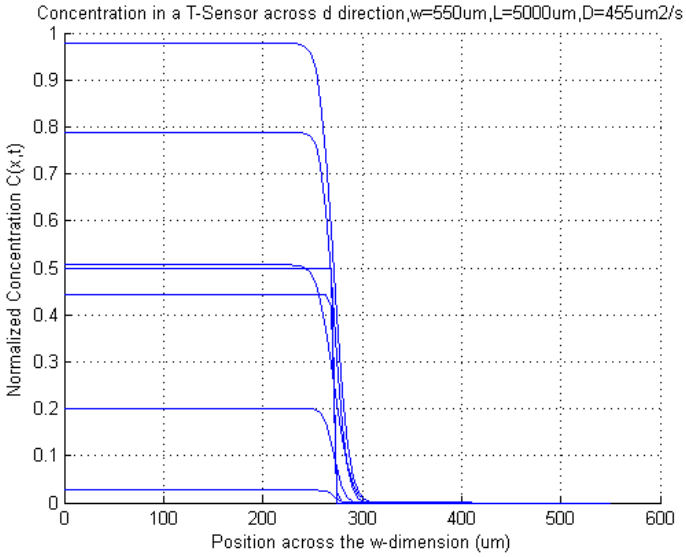
Concentration in a T-Sensor across d direction,w=550um,L=5000um,D=455um2/s
Normalized Concentration C(x,t)
Position across the w-dimension (um)
0
0.1
0.2
0.3
0.4
0.5
0.6
0.7
0.8
0.9
1
0
100
200
300
400
500
600

APPENDIX E

Cell system

This code pretends to simulate the behavior of cell communications system. The idea is that in one pint there is a source which can be a cell or an external source that is infusing molecules in the media. This system calculates the concentration in the sink point where the target cell is placed.

Constants definition

```
numx=51;%number of grid points in x
numt=1000;%number of iterations
F=0.5; % frequency of the input signal
Dn=100;
C=zeros(numx,numt);%we inicialize de matrix to 0
dx=550/(numx-1);
dt1=0.5;
x=0:dx:550; %vector of x values
t=0:dt1:numt*dt1;
stability1=(Dn*dt1)/(dx^2)
```

```
stability1 =

    0.4132
```

Initial condition

In this case the initial condition is that the source has maximum concentration at the beginning. But only in the first iteration, after that the concentration at the sources follows the value stored in VeCon.

```
posIniCell=2; % source position in the mesh

posDetectionCell=5; % sink position in the mesh


C(posIniCell,1)=1;


%Concetration at the begining in each instant

VecCon=0.5*square(2*pi*F*t)+0.5; %square case

% VecCon=sin(2*pi*F*t); %sinusioidal case
```

Main loop

```
%Now we can calculate the coefficients of the matrix C in the time t(j+1), using the
results in the time t(j)


for j=1:numt

    for k=(j+1):-1:1

        if k~=1 %Is not the beginig

              for i=posIniCell-1:-1:2

                   C(i,k)=C(i,k-1)+(C(i+1,k-1)-2*C(i,k-1)+C(i-1,k-
1))*(Dn)*(dt1/(dx)^2);

              end

              for i=posIniCell+1:numx-1

                   C(i,k)=C(i,k-1)+(C(i+1,k-1)-2*C(i,k-1)+C(i-1,k-
1))*(Dn)*(dt1/(dx)^2);

              end

              %Boundary conditions

              C(numx,k)=C(numx-1,k);

        else

              C(posIniCell,j+1)=VecCon(j+1);

        end

    end

end


Ctarget=C(posDetectionCell,:);

positionSource=posIniCell*dx;

positionTarget=posDetectionCell*dx;
```

Plotting

```
figure(1)

hold on;

plot(x,C(:,1),'r');

plot(x,C(:,10));

plot(x,C(:,100));


xlabel('Position x');

ylabel('Normalizated Concentration C(x,t)');

title(['Molecule diffusion for a cell situated in the position
',num2str(positionSource),'um']);

grid on;


figure(2)

ax(1)=subplot(2,1,1);

plot(t,VecCon);

grid

xlim([0 t(numt)]);

ylim([0 1.2]);

ylabel('Normalizated Concentration C(x,t)');

xlabel('Time (s)');

title('Variable concentration from the source');


ax(2)=subplot(2,1,2);

plot(t,Ctarget);

grid

ylabel('Normalizated Concentration C(x,t)');

xlabel('Time (s)');

title(['Temporal evolution of the concentration in the point
',num2str(positionTarget),'um in a device of 550um of longitude']);


linkaxes(ax,'xy');


% figure(3)

% hold on

% grid on
```

```
% plot(t,VecCon,'r');

% plot(t,Ctarget);

% % axis([0 0.1 0 1]);

% ylabel('Normalized Concentration C(x,t)');

% xlabel('Time (s)');

% title(['Temporal evolution of the concentration in the point
',num2str(positionTarget),'um in a device of 550um of longitude']);

% legend('Source Concentration','Concentration in the cell target')
```

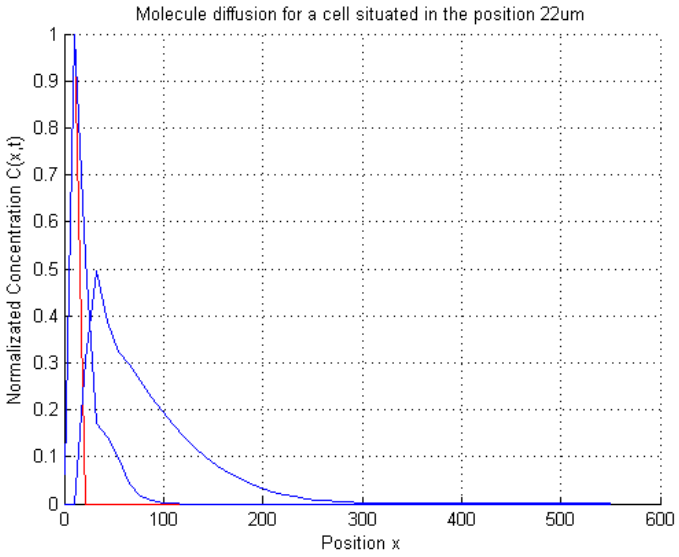

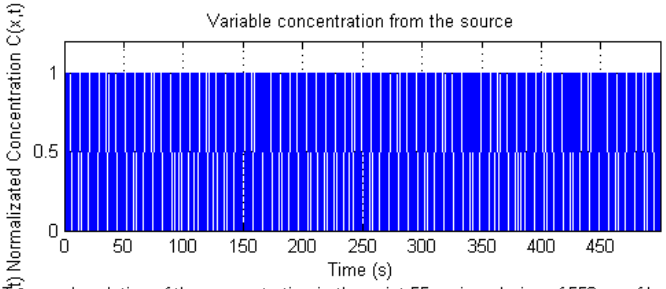

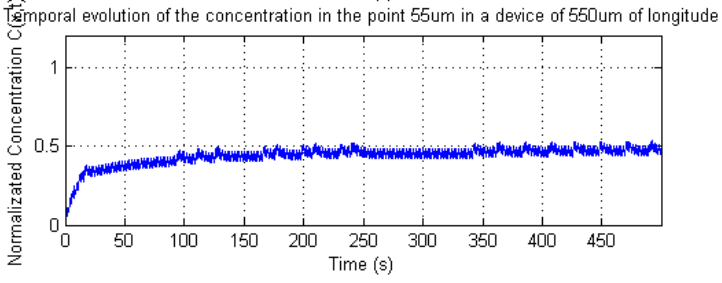

APPENDIX F

Solution for the diffusion equation

This code has programmed the solution for the diffusion equation. In this script the idea is to call the functions "gasificacion.m" and "degasificacion.m" alternately. Each call is one half-period in the periodic square wave at the beginning.

```
position=0.5; %position from the domain 0<X<1 where we are calculating the result
P=0.05; %periode
F=1/P; %frequency
DC=0.5; %duty cicle
cicles=100; %number of cicles simulated
```

Main Loop

```
concentration=gasificacion(position,0,P*DC); %calcul of the first half period

%the solution is calculated in each half period, cicles is the number of
%cicles that is being calculated
for i=1:cicles
    [row col]=size(concentration);

    %the initial condition in the next half period depends on the last
    %value in the period before, this value is keep in concentration(col)
    aux=degasificacion(position,concentration(col),P*DC);

    %the concentration array is made concatenating the different half
    %periods
    concentration=horzcat(concentration,aux);

    [row col]=size(concentration);

    %the initial condition in the next half period depends on the last
```

```
    %value in the period before, this value is keep in concentration(col)
    aux=gasificacion(position,concentration(col),P*DC);

    %the concentration array is made concatenating the different half
    %periods
    concentration=horzcat(concentration,aux);
end

[row col]=size(concentration);
```

Plotting Results

```
simTime=P*(cicles+DC);%The total time is cicle periodes plus una half periode(P*DC)

T=0:simTime/(col-1):simTime;
figure
plot(T,concentration);
xlabel('time (s)');
ylabel('Normalized concentration');
title(['Concentration at X=',num2str(position),' for a square concentration wave from
the source']);
% axis([0 0.5 0 1]);
grid on
```

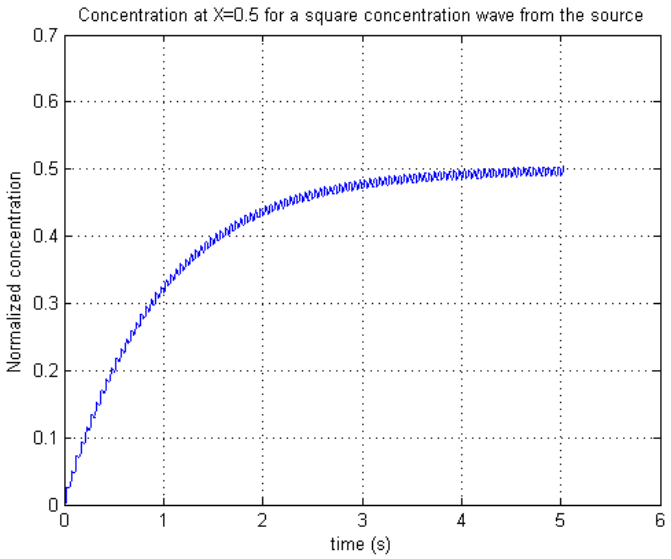

Gasificacion Function

This function calculates the concentration using the charge equation

```
function [concentration] = gasificacion(position,IC,halfP)
T=0:0.001:halfP;
sum=0;

X=position;
for n=1:1:10000
Wn=((2*n)-1)*(pi/2);
Bn=(2*(1-IC))/Wn;
sum=Bn*(sin(Wn*X))*(exp(-Wn^2*T))+sum;
end

concentration=1-sum;
```

Degasificacion Function

This function calculets the concentration using the discharge equation

```
function [concentration] = degasificacion(position,IC,halfP)
T=0:0.001:halfP;
sum=0;

X=position;
for n=1:1:10000
Wn=((2*n)-1)*(pi/2);
Bn=(2*IC)/Wn;
sum=Bn*(sin(Wn*X))*(exp(-Wn^2*T))+sum;
end

concentration=sum;
```

```
Input argument "halfP" is undefined.


Error in ==> degasificacion at 4
T=0:0.001:halfP;
```

8 REFERENCES

[1] P. Carmeliet and R. K. Jain, "Angiogenesis in cancer and other diseases," *Nature,* vol. 407, pp. 249-257, 2000.

[2] M. J. Berridge, "The AM and FM of calcium signaling," *Nature,* vol. 386, pp. 759-760, 1997.

[3] B. Alberts*, et al.*, *Molecular Biology of the Cell*, 2002.

[4] A. R. Asthagiri and D. A. Lauffenburger, "Bioengineering models of cell signaling," *Annual Review of Biomedical Engineering,* vol. 2, pp. 31-53, 2000.

[5] R. Weiss*, et al.*, "Genetic circuit building blocks for cellular computation, communications, and signal processing," *Natural Computing,* vol. 2, pp. 47-84, 2003.

[6] S. F. Bush, *Nanoscale Communication Networks*, 2010.

[7] I. F. Akyildiz*, et al.*, "Nanonetworks: A new communication paradigm," *Computer Networks,* vol. 52, pp. 2260-2279, 2008.

[8] R. A. Freitas, *Nanomedicine, Volume I: Basic Capabilities*, 1999.

[9] S. Hiyama*, et al.*, "Molecular Communication," in *Proceedings of the 2005 NSTI Nanotechnology Conference*, 2005, pp. 391 - 394.

[10] M. Moore*, et al.*, "A design of a molecular communication system for nanomachines using molecular motors," *Fourth Annual IEEE International Conference on Pervasive Computing and Communications Workshops, Proceedings,* pp. 554-559, 2006.

[11] T. Nakano*, et al.*, "Molecular communication for nanomachines using intercellular calcium signaling," in *Nanotechnology, 2005. 5th IEEE Conference on*, 2005, pp. 478-481 vol. 2.

[12] Y. Moritani*, et al.*, "Molecular communication for health care applications," in *Pervasive Computing and Communications Workshops, 2006. PerCom Workshops 2006. Fourth Annual IEEE International Conference on*, 2006, pp. 5 pp.-553.

[13] E. Carafoli, "Calcium signaling: A tale for all seasons," *Proceedings of the National Academy of Sciences of the United States of America,* vol. 99, pp. 1115-1122, February 5, 2002 2002.

[14] W. D. Kepseu and P. Woafo, "Intercellular waves propagation in an array of cells coupled through paracrine signaling: A computer simulation study," *Physical Review E,* vol. 73, 2006.

[15] C. Bustamante*, et al.*, "Mechanical processes in biochemestry," *Annual Review of Biochemistry,* vol. 73, pp. 705-748, 2004.

[16] P. Tabeling, *Introduction to Microfluidics*, 2003.

[17] G. M. Whitesides, "The origins and the future of microfluidics," *Nature,* vol. 442, pp. 368-373, 2006.

[18] J. P. Abraham*, et al.*, "Heat transfer in all pipe flow regimes: laminar, transitional/intermittent, and turbulent," *International Journal of Heat and Mass Transfer,* vol. 52, pp. 557-563, 2009.

[19] C. Noakes and A. Sleigh, *An Introduction to Fluid Mechanics*, 2009.

[20] A. P. Wong*, et al.*, "Partitioning microfluidic channels with hydrogel to construct tunable 3-D cellular microenvironments," *Biomaterials,* vol. 29, pp. 1853-1861, 2008.

[21] J. Philibert, "One and a Half Century of Diffusion: Fick, Einstein, Before and Beyond," *Diffusion Fundamentals,* vol. 4, pp. 1-19, 2006.

[22] R. B. Bird*, et al.*, *Transport Phenomena*, 2001.

[23] Z. Zhenrong*, et al.*, "Roughness characterization of well-polished surfaces by measurements of light scattering distribution," *Optica Applicata,* vol. 40, pp. 811-818, 2010.

[24] K. Ogata, *Modern Control Engineering*, 1996.

[25] A. E. Kamholz*, et al.*, "Quantitative analysis of molecular interaction in a microfluidic channel: The T-sensor," *Analytical Chemistry,* vol. 71, pp. 5340-5347, 1999.

[26] A. B. Shrirao and R. Perez-Castillejos, "Simple fabrication of microfluidic devices by replicating Scotch-tape masters," *Lab on a Chip: Chips and Tips,* 2010.

[27] A. E. Kamholz and P. Yager, "Theoretical analysis of molecular diffusion in pressure-driven laminar flow in microfluidic channels," *Biophysical Journal,* vol. 80, pp. 155-160, 2001.

[28] B. A. Finlayson, *Nonlinear analysis in chemical engineering*, 1980

[29] A. E. Kamholz and P. Yager, "Molecular diffusive scaling laws in pressure-driven microfluidic channels: deviation from one-dimensional Einstein approximations," *Sensors and Actuators B-Chemical,* vol. 82, pp. 117-121, 2002.

[30] S. A. Rani*, et al.*, "Rapid diffusion of fluorescent tracers into Staphylococcus epidermidis biofilms visualized by time lapse microscopy," *Antimicrobial Agents and Chemotherapy,* vol. 49, pp. 728-732, 2005.

[31] D. deBeer*, et al.*, "Measurement of local diffusion coefficients in biofilms by microinjection and confocal microscopy," *Biotechnology and Bioengineering,* vol. 53, pp. 151-158, 1997.

[32] A. Goldbeter*, et al.*, "Minimal model for signal-induced Ca2+ oscillations and for their frequency encoding through protein phosphorylation," *Proceedings of the National Academy of Sciences,* vol. 87, pp. 1461-1465, February 1, 1990 1990.

[33] R. E. Dolmetsch*, et al.*, "Differential activation of transcription factors induced by Ca2+ response amplitude and duration," *Nature,* vol. 386, pp. 855-858 24 April 1997 1997.